

# The Multiphase Chemical Kinetics of Dinitrogen Pentoxide with Aerosol Particles

Inauguraldissertation  
der Philosophisch-naturwissenschaftlichen Fakultät  
der Universität Bern

vorgelegt von  
**Goran Gržinić**  
aus Kroatien/Italien

Leiter der Arbeit:  
Prof. Dr. Andreas Türler  
Departement für Chemie und Biochemie



# The Multiphase Chemical Kinetics of Dinitrogen Pentoxide with Aerosol Particles

Inauguraldissertation  
der Philosophisch-naturwissenschaftlichen Fakultät  
der Universität Bern

vorgelegt von  
**Goran Gržinić**  
aus Kroatien/Italien

Leiter der Arbeit:  
Prof. Dr. Andreas Türler  
Departement für Chemie und Biochemie

Von der Philosophisch-naturwissenschaftlichen Fakultät angenommen.

Bern, 16.12.2014

Der Dekan:

Prof. Dr. Gilberto Colangelo



*It matters not how strait the gate,  
How charged with punishments the scroll,  
I am the master of my fate,  
I am the captain of my soul*

Invictus, William Ernest Henley



## Abstract

Dinitrogen pentoxide ( $\text{N}_2\text{O}_5$ ) is an important reactive intermediate in the nighttime chemistry of nitrogen oxides ( $\text{NO}_x$ ). As one of the major  $\text{NO}_x$  sinks, it plays an important role in the regulation of the oxidative capacity of the atmosphere.

The  $^{13}\text{N}$  radioactive isotope tracer technique was used to synthesize  $^{13}\text{N}$  labeled  $\text{N}_2\text{O}_5$  for the first time, and an experimental system for the study of uptake kinetics of  $\text{N}_2\text{O}_5$  on aerosol particles was developed. A computer model of the gas phase chemistry involved was created to help optimizing the production of  $\text{N}_2\text{O}_5$ . The experimental setup was successfully tested, and routine production of  $^{13}\text{N}_2\text{O}_5$  in the ppb range was established.

The uptake of  $\text{N}_2\text{O}_5$  on citric acid aerosol was studied over an atmospherically relevant humidity range (17-70% RH). Citric acid was used as a proxy for highly oxidized organic species present in ambient organic aerosol. The results have shown that reactivity in the above mentioned humidity interval varies roughly an order of magnitude, with the uptake coefficient, the probability that a gas kinetic collision with the particle is leading to its net loss, ranging from approximately  $3 \times 10^{-4}$  to  $3 \times 10^{-3}$ . This is significantly lower than for similar organic compounds. These relatively low loss rates were attributed to the effect of viscosity, which is considerably higher in concentrated citric acid solution than in solutions of simpler organic or inorganic solutes. The humidity dependence of the uptake coefficient could be largely explained by the effects of the changing viscosity on the diffusivity and thus reactivity. It is postulated that this factor might be responsible for lower  $\text{N}_2\text{O}_5$  loss rates observed in field measurements than predictions based on earlier laboratory results.

The particular properties of the  $^{13}\text{N}$  tracer method have allowed probing the chemical mechanism of  $\text{N}_2\text{O}_5$  heterogeneous hydrolysis and obtain insight into some of the individual steps of the mechanism. Specific use was made of the fast exchange of the  $^{13}\text{N}$ -labelled nitrate deriving from the uptake of  $^{13}\text{N}$ -labelled  $\text{N}_2\text{O}_5$  into the aqueous particles with the non-labelled nitrate pool present in  $\text{NaNO}_3$  particles. This was then used to demonstrate very fast dissolution and dissociation of  $\text{N}_2\text{O}_5$  into nitronium and nitrate. In addition, a lower limit to the bulk accommodation coefficient,  $\alpha_b$ , was estimated to be 0.4, which is significantly larger than previously thought. This will

likely have a strong impact on the modeling of  $\text{N}_2\text{O}_5$  uptake on aerosol particles. Additionally, it helps explaining some situations where uptake measured in ambient aerosol is higher than expected based on previous laboratory studies for situations where organics are not dominating the aerosol composition.



## Table of Contents

<b>1. Introduction .....</b>	<b>11</b>
1.1. The troposphere .....	11
1.2. Aerosols .....	12
1.2.1. General information .....	12
1.2.2. Atmospheric impact and health effects .....	13
1.3. Dinitrogen Pentoxide .....	14
1.3.1. The NO <sub>x</sub> cycle .....	14
1.3.2. N <sub>2</sub> O <sub>5</sub> formation and role .....	17
1.3.3. Chemical mechanism .....	19
1.3.4. N <sub>2</sub> O <sub>5</sub> measurement techniques .....	21
1.4. The kinetics of gas uptake on aerosol particles .....	23
1.5. Scope of the thesis .....	27
<b>2. Production and use of <sup>13</sup>N labeled N<sub>2</sub>O<sub>5</sub> to determine gas – aerosol interaction kinetics.....</b>	<b>39</b>
2.1. Introduction .....	40
2.2. Experimental.....	43
2.2.1. General layout of the experiment .....	43
2.2.2. Production and transport of <sup>13</sup> NO .....	44
2.2.3. Production of <sup>13</sup> N <sub>2</sub> O <sub>5</sub> .....	45
2.2.4. Modeling of gas phase <sup>13</sup> N <sub>2</sub> O <sub>5</sub> production.....	46
2.2.5. Aerosol generation and characterization .....	47
2.2.6. Aerosol flow tube .....	48
2.2.7. Detection system .....	48
2.3. Results and Discussion .....	49
2.3.1. Gas phase production of <sup>13</sup> N <sub>2</sub> O <sub>5</sub> .....	49
2.3.2. Comparison with model.....	51
2.3.3. Uptake by aerosol .....	55
2.4. Conclusions and Outlook.....	59
<b>3. Humidity Dependence of N<sub>2</sub>O<sub>5</sub> Uptake on Citric Acid Aerosol .....</b>	<b>63</b>
3.1. Introduction .....	64
3.2. Experimental.....	67
3.2.1. Production of <sup>13</sup> N labeled N <sub>2</sub> O <sub>5</sub> .....	68
3.2.2. Aerosol production .....	69
3.2.3. Aerosol flow tube .....	69

---

3.2.4.	Separation and detection of $^{13}\text{N}$ labeled species.....	70
3.3.	Results and discussion.....	72
3.3.1.	Measuring the uptake coefficient of $\text{N}_2\text{O}_5$ over a wider humidity range.....	72
3.3.2.	Physical state, reaction mechanism and parameterization.....	76
3.4.	Conclusions and atmospheric impact.....	85
<b>4.</b>	<b>Uptake of <math>^{13}\text{N}</math>-labelled <math>\text{N}_2\text{O}_5</math> to Nitrate containing Aerosol.....</b>	<b>93</b>
4.1.	Introduction.....	94
4.2.	Experimental Section.....	96
4.3.	Results and Discussion.....	98
<b>5.</b>	<b>Summary and Outlook.....</b>	<b>107</b>
	<b>Acknowledgements.....</b>	<b>117</b>

## List of Figures

<b>Fig. 1.1.</b> Classification of particles according to size.....	12
<b>Fig. 1.2.</b> A simplified representation of the $\text{NO}_x + \text{NO}_3$ and VOC cycles .....	16
<b>Fig. 1.3.</b> The chemical mechanism of $\text{N}_2\text{O}_5$ uptake on aerosol particles .....	20
<b>Fig. 2.1.</b> Schematic representation of the experimental arrangement .....	44
<b>Fig. 2.2.</b> Production of gas phase $^{13}\text{N}_2\text{O}_5$ .....	50
<b>Fig. 2.3.</b> Decay plot of $\text{N}_2\text{O}_5$ vs. reactor length fitted to the measured data using the CKD method .....	52
<b>Fig. 2.4.</b> Gas phase model graphs.....	54
<b>Fig. 2.5.</b> $\text{N}_2\text{O}_5$ interacting with citric acid aerosol (295 K, 26% RH) .....	56
<b>Fig. 2.6.</b> $\text{N}_2\text{O}_5$ interacting with ammonium sulphate particles at different aerosol S/V ratios (295 K, 52% RH) .....	58
<b>Fig. 3.1.</b> Exemplary traces of inverted detector signals for an experiment .....	73
<b>Fig. 3.2.</b> Normalized particle-phase $\text{N}_2\text{O}_5$ concentration vs. aerosol surface/volume ratio graph for the experiment from Fig 2.....	74
<b>Fig. 3.3.</b> Uptake coefficients obtained in this study at various RH values.....	75
<b>Fig. 3.4.</b> Diffusivity of $\text{N}_2\text{O}_5$ in citric acid solutions as calculated according to four parameterization methods .....	80
<b>Fig. 3.5.</b> Parameterization of $\text{N}_2\text{O}_5$ uptake on citric acid aerosol based on diffusivities estimated by the four parameterization methods .....	82
<b>Fig. 4.1.</b> Schematic of the modified experimental setup used in this study .....	97
<b>Fig. 4.2.</b> Normalized particle-phase $\text{N}_2\text{O}_5$ concentration vs. time graph for the experiments performed at 50% RH (a) and 70% RH (b).....	100
<b>Fig. 4.3.</b> The chemical mechanism of $^{13}\text{N}$ labeled $\text{N}_2\text{O}_5$ hydrolysis.....	102
<b>Fig. 5.1.</b> Normalized $\gamma$ ( $\text{N}_2\text{O}_5$ ) values for mixtures of ammonium bisulfate and organics....	110
<b>Fig. 5.2.</b> A histogram of $\text{N}_2\text{O}_5$ uptake coefficients determined using a iterative box model and determined from the NACHTT field study data set .....	112
<b>Fig. 5.3.</b> Parameterizations of $\text{N}_2\text{O}_5$ uptake on malonic acid .....	113

---

## List of Tables

<b>Tab. 3.1.</b> Reacto-diffusive lengths calculated using diffusivity values obtained via the four above mentioned parameterizations. ....	83
<b>Tab. 4.1.</b> Experimental parameters and results .....	101

## Chapter 1

### 1. Introduction

#### 1.1. The troposphere

The troposphere (from the Greek *tropos* - turn, change) is the lowest part of the atmosphere, comprising the gaseous shroud around the Earth up to a height of about 10-15 km. It is separated from the next atmospheric layer (stratosphere) by the tropopause. The troposphere contains the majority of the atmospheric mass, humidity, particulate loading and precipitations. As the name suggests, the troposphere is characterized by strong turbulences derived from thermal currents caused by the heat emitted from the surface. This gives rise to strong meteorological events which help gas mixing in this region of the atmosphere. Since the planetary surface is also the source of the majority of atmospheric emissions, the troposphere is also the compartment, where a major part of the atmospheric chemical processing of these emissions occurs.

The sources of emission can be anthropogenic, biogenic or geogenic and they can be divided into primary (emitted directly into the atmosphere) and secondary emissions (formed from reactions of primary emission components in the air), either in the form of trace gases or in the form of aerosol particles. Once in the atmosphere, they are subject to dispersion and transport due to meteorological events as well as chemical and physical transformation by reaction between them. Finally, they can be removed from the atmosphere by dry or wet deposition to the surface (Finlayson-Pitts and Pitts, 2000).

## 1.2. Aerosols

### 1.2.1. General information

Aerosols are defined as a suspension of liquid or solid particles, of diameter between  $\sim 0.002$  and  $\sim 100 \mu\text{m}$ , in a gaseous medium. They can arise from natural processes like wind erosion, sea spray or volcanic eruptions or from anthropogenic activities like combustion, mining activities etc. They are divided, similarly to other types of emissions, into primary aerosol (emitted directly) or secondary aerosol (resulting from gas to particle conversion processes in the atmosphere). According to size they can be classified into coarse ( $>2.5 \mu\text{m}$ ) and fine ( $<2.5 \mu\text{m}$ ) particles. The latter are further split into nuclei mode ( $<0.1 \mu\text{m}$ ) and accumulation mode ( $0.1 > x \leq 2.5 \mu\text{m}$ ).

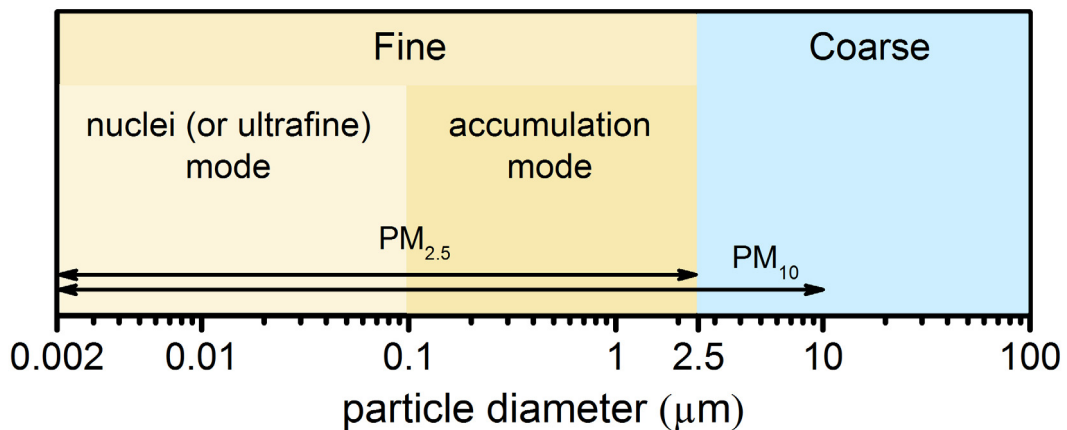


**Fig. 1.1.** Classification of particles according to size: PM<sub>2.5</sub>, PM<sub>10</sub> stand for Particulate Matter with diameter up to 2.5 and 10  $\mu\text{m}$  respectively

Particles belonging to the nuclei mode, because of their small size, represent a few percent in mass of the total aerosol particles in the atmosphere. They are formed from condensation or nucleation of hot vapors during combustion or other industrial processes and nucleation of atmospheric trace gases. Accumulation mode particles are generally formed from coagulation of smaller particles or condensation of vapors onto existing particles. They account for the majority of the total aerosol number and surface area concentration, and a major fraction of the overall mass. Coarse mode

particles derive from mechanical processes, both anthropogenic and natural in origin, and are primarily constituted by wind-blown dust, sea spray particles and volcanic dust. Particle removal mechanisms are most efficient in the two opposite sides of the particle size spectrum. Nuclei mode particles are removed primarily by coagulation with other particles, thus contributing to the growth of accumulation mode particles, while coarse mode particles have large sedimentation velocities and deposit out of the atmosphere reasonably quickly. The accumulation mode particles are thus the predominant species among atmospheric aerosol and can persist in the atmosphere up to a few weeks and be transported over long distances (Finlayson-Pitts and Pitts, 2000; Seinfeld and Pandis, 1998).

### **1.2.2. Atmospheric impact and health effects**

The atmospheric implications and impact of aerosols on our environment are multifold and far reaching. They interact with trace gases (like  $\text{NO}_x$ ,  $\text{SO}_x$ ) and radical species (like OH,  $\text{NO}_3$ ) present in the atmosphere and can scavenge them or facilitate their production thus altering the oxidative capacity of the atmosphere (Alexander et al., 2005; Cooper and Abbatt, 1996; Prinn, 2003; Ravishankara, 1997; Sievering et al., 1992; Thornton et al., 2008). For example,  $\text{NO}_2$  can be processed to HONO on organic aerosols (Sosedova et al., 2009). Photolysis of HONO can substantially contribute to  $\bullet\text{OH}$  production in some environments (Zhang et al., 2009). Another example of chemical processing of aerosols is the atmospheric processing of mineral dust aerosol by acidic gases (like  $\text{SO}_2$  or  $\text{HNO}_3$ ) and transformation of insoluble iron (Fe in the oxidized or  $\text{Fe}^{3+}$  form) to soluble forms (e.g.,  $\text{Fe}^{2+}$ , inorganic soluble compounds of  $\text{Fe}^{3+}$ , and organic complexes of iron) which then act as a nutrient for marine phytoplankton (Ito and Feng, 2010; Meskhidze et al., 2003; Zhu et al., 1992).

The changes in chemical composition induced by reaction with atmospheric trace gases (chemical aging) can likewise influence our climate. Organic or soot aerosol can absorb incoming solar radiation, inducing a local heating effect on the air mass they are contained in. Inorganic particles like sulfates or nitrates on the other hand scatter incoming radiation, which has a net cooling effect on the atmosphere (Chung et al., 2005; Wang et al., 2014). These aerosols need not necessarily be of anthropogenic

origin: volcanic eruptions can eject large quantities of SO<sub>2</sub> in the atmosphere, which can be converted to sulfate aerosol. One such event was the eruption of Mount Pinatubo in the Philippines in 1991, which led to a drop of the global temperature by 0.5 °C over a period of two years (Newhall and Punongbayan, 1997). Atmospheric aerosols can also act as cloud condensation nuclei (CCN), facilitating cloud formation and increasing the cloud albedo effect. At the same time, they decrease the precipitation efficiency of clouds and thus increase the amount and lifetime of clouds as well as influencing precipitation (Leaitch et al., 2010; Schwartz et al., 2002; Stevens and Feingold, 2009).

Deposited aerosol damage plant surfaces and reduce the amount of photosynthetically active radiation, thus impacting agricultural production (Gerstl and Zardecki, 1982; Vardaka et al., 1995).

Aerosols can also impact human health. They have been linked with an increase in mortality due to respiratory and cardio-vascular diseases (Brunekreef and Holgate, 2002) as well as an increase in the incidence of chronic obstructive pulmonary disease (Sunyer, 2001) and other acute respiratory effects (Dockery and Pope, 1994) like allergic inflammations (Nel et al., 1998) and asthma (Nel et al., 2001).

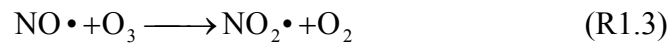
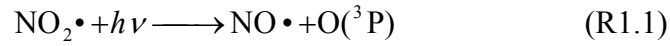
Taking these factors into consideration, a comprehensive understanding of the sources, distribution pathways and relevant properties is necessary to estimate their effects on the environment and human health.

### **1.3. Dinitrogen Pentoxide**

#### **1.3.1. The NO<sub>x</sub> cycle**

The NO<sub>x</sub> (NO<sub>x</sub>=NO•+NO<sub>2</sub>•) cycle is one of the key drivers of tropospheric chemistry. When NO• and NO<sub>2</sub>• and O<sub>2</sub> are present in sunlight, ozone is formed starting from photolysis of NO<sub>2</sub> at wavelengths <424 nm. It is a closed photochemical cycle which is governed by the following reactions:



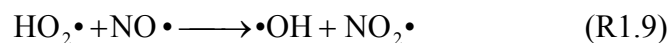
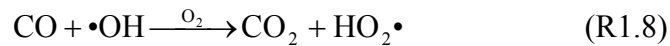
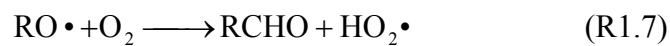
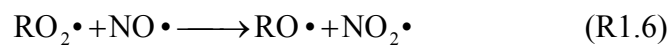
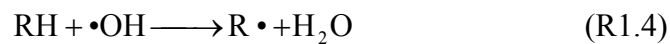


When equilibrium is established the concentrations of  $\text{NO}\bullet$ ,  $\text{NO}_2\bullet$  and  $\text{O}_3$  remain constant and are governed by the Leighton relationship (Eq. 1.1):

$$\frac{[\text{O}_3][\text{NO}]}{[\text{NO}_2]} = \frac{j_{1.1}}{k_{1.3}} \quad (\text{Eq. 1.1})$$

where  $j_{1.1}$  ( $\text{s}^{-1}$ ) and  $k_{1.3}$  ( $\text{cm}^3 \text{ molecule}^{-1} \text{ s}^{-1}$ ) are the photolysis and reaction rate constants for reactions R1.1 and R1.3 respectively. Since  $j_{1.1}$  changes with the solar zenith angle, the ratio also changes during the day as do the concentrations of  $\text{NO}\bullet$ ,  $\text{NO}_2\bullet$  and  $\text{O}_3$ .

In the presence of atmospheric  $\bullet\text{OH}$  radical however, additional reaction cycles with volatile organic compounds (VOCs) and carbon monoxide can produce  $\text{RO}_2\bullet$  and  $\text{HO}_2\bullet$  radicals which can react with  $\text{NO}\bullet$  (R1.6,1.9).



These reactions (R1.4-1.9) constitute a cycle where  $\bullet\text{OH}$  is reformed and  $\text{NO}\bullet$  is transformed into  $\text{NO}_2\bullet$ . This in turn drives tropospheric  $\text{O}_3$  production via the photochemical  $\text{NO}_x$  cycle. The  $\bullet\text{OH}$  radical acts as a cleansing agent, oxidizing VOCs present in the atmosphere, while at the same time helps the production of ozone. Its

major source is the photolysis of ozone to electronically excited atomic oxygen  $O(1D)$  followed by reaction with water vapor. In polluted atmospheres additional important sources of  $\bullet OH$  are photolysis of nitrous acid ( $HONO$ ) and hydrogen peroxide ( $H_2O_2$ ). The overall atmospheric nitrogen cycle is complex and contains several additional pathways which can contribute to the cycle for example by forming  $\bullet OH$  radicals or acting as termination steps for the various subcycles. One example of such termination steps is the reaction of  $NO_2\bullet$  with  $\bullet OH$ , which leads to production of  $HNO_3$ . This is one of the primary  $NO_x$  removal mechanisms during daytime. A simplified diagram of the nitrogen cycle can be seen in Figure 1.2. For a more detailed overview of the chemistry of the atmospheric nitrogen cycle, the seminal works on atmospheric chemistry by Finlayson-Pitts and Pitts (2000) and Seinfeld and Pandis (1998) are a recommended read.

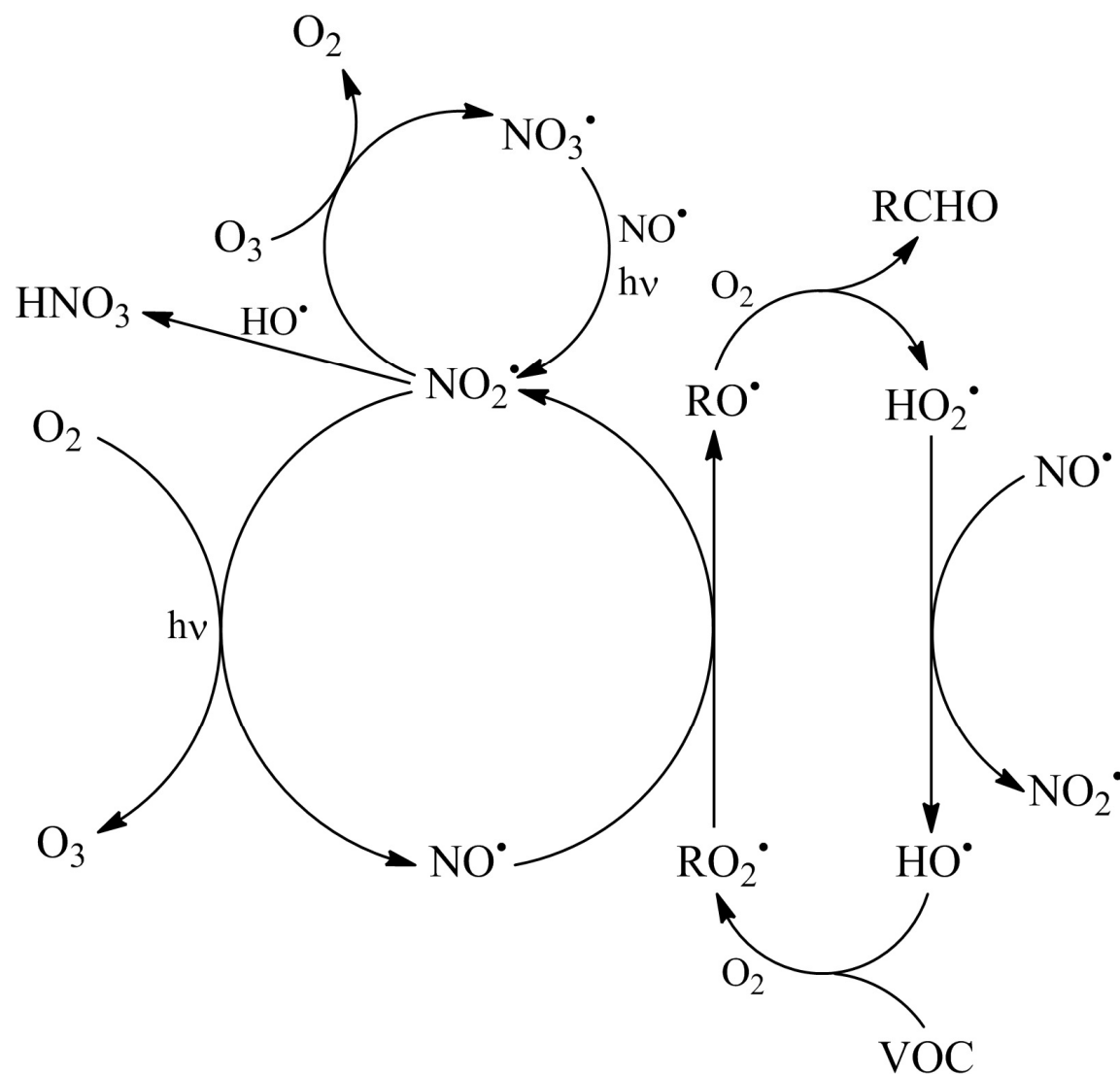
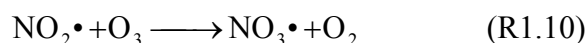


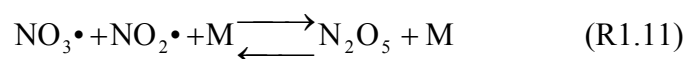
**Fig. 1.2.** A simplified representation of the  $NO_x+NO_3$  and VOC cycles

### 1.3.2. N<sub>2</sub>O<sub>5</sub> formation and role

In presence of ozone, NO<sub>2</sub>• can react further to NO<sub>3</sub>• (R1.10).



This reaction is relatively slow ( $k_{1.10} = 3.2 \times 10^{-17} \text{ cm}^3 \text{ molecule}^{-1} \text{ s}^{-1}$ ), but in presence of atmospherically relevant O<sub>3</sub> concentrations (100 ppbv) the lifetime of NO<sub>2</sub>• with respect to reaction R1.10 is down to 3.5 h. NO<sub>3</sub>• absorbs in the visible part of the spectrum of sunlight (620-670 nm) and, therefore, it photolyses rapidly during the day (lifetime ~1 s). Its relevance is thus restricted to the nighttime. NO<sub>3</sub>• plays an important role as an oxidant in nighttime atmospheric chemistry, being a major contributor to nighttime oxidation of organics (in particular alkenes and aldehydes). NO<sub>3</sub>• can furthermore react with NO<sub>2</sub>• to form N<sub>2</sub>O<sub>5</sub> (R1.11).



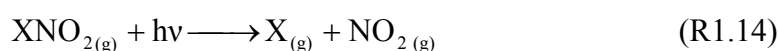
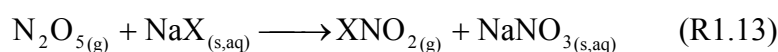
During nighttime the concentration of N<sub>2</sub>O<sub>5</sub> is controlled by the rapid equilibrium between N<sub>2</sub>O<sub>5</sub> formation and loss, which is thermally controlled. Because of the above mentioned equilibrium, N<sub>2</sub>O<sub>5</sub> can play a dual role in the tropospheric NO<sub>x</sub> chemistry. It can act as a NO<sub>x</sub> reservoir by accumulating during nighttime to be released in the early morning when photolysis of NO<sub>3</sub> depletes the accumulated N<sub>2</sub>O<sub>5</sub>. Alternatively it can act as a sink for atmospheric NO<sub>x</sub> species via hydrolysis (R1.12) (Finlayson-Pitts and Pitts, 2000).



This process provides a nighttime sink for NO<sub>x</sub>, when the other main sink, reaction of NO<sub>2</sub>• with •OH, is not active. While the hydrolysis reaction can happen in the gas

phase, as a third order reaction it is extremely slow and the most important  $\text{N}_2\text{O}_5$  sink is fast heterogeneous hydrolysis on aerosol surfaces (in presence of high aerosol concentrations) (Abbatt et al., 2012; Chang et al., 2011). The overall result is removal of atmospheric  $\text{NO}_x$  species and, therefore, a reduction of tropospheric ozone, which leads to a reduction of the oxidative capacity of the atmosphere (Dentener and Crutzen, 1993; Evans and Jacob, 2005).

Hydrolysis of  $\text{N}_2\text{O}_5$  is considered to be the major sink process; however, an additional loss pathway is interesting from the environmental standpoint.  $\text{N}_2\text{O}_5$  can react with halide salts present in marine aerosols to form the respective nitryl halides (R1.13), which can return to the gas phase and give, by photolytic dissociation, reactive halogen atoms and  $\text{NO}_2$  (R1.14) (Behnke et al., 1997; Osthoff et al., 2008).



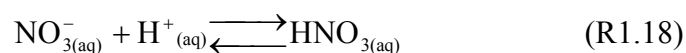
While the importance of these reactions as a source of halogen atoms has been considered uncertain or in any case restricted to marine environments, recent studies (Mielke et al., 2012; Phillips et al., 2012; Thornton et al., 2010) have shown that significant concentrations of  $\text{ClNO}_2$  can be found in continental areas as well. Marine air masses transported over long distances and local industrial emissions lead to formation of aerosol particles containing chloride, which can interact with the nighttime  $\text{NO}_x$  chemistry. This leads to  $\text{ClNO}_2$  production, and in turn to halogen atoms.

Because of the importance of  $\text{N}_2\text{O}_5$  for nighttime tropospheric chemistry and overall  $\text{NO}_x$  and  $\text{O}_3$  levels, its uptake on aerosols has been a very important topic of investigation. The uptake is characterized by the uptake coefficient  $\gamma$ , defined as the ratio between the net flux of molecules from the gas phase to the aerosol particles and the gas-kinetic collision flux of the molecules to the surface of the particles. A more detailed overview of the kinetics of  $\text{N}_2\text{O}_5$  uptake on aerosol particles will be given in subchapter 1.4.

Over the last two decades, laboratory studies have been conducted over a wide range of inorganic and organic aerosols, including nitrates (Mentel et al., 1999; Wahner et al., 1998), sulfates (Davis et al., 2008; Hallquist et al., 2003; Hu and Abbatt, 1997), NaCl/sea salt aerosol (George et al., 1994; Stewart et al., 2004; Thornton and Abbatt, 2005), mineral dust (Karagulian et al., 2006; Wagner et al., 2008), soot (Karagulian and Rossi, 2007) and organic aerosols (Bertram et al., 2009; Gaston et al., 2014; Griffiths et al., 2009; Rudich et al., 2007; Thornton et al., 2003).

### 1.3.3. Chemical mechanism

A chemical mechanism of  $\text{N}_2\text{O}_5$  reaction with aerosol particles has been first proposed by Mozurkewich and Calvert (1988). According to this mechanism,  $\text{N}_2\text{O}_5$  dissolves in water and dissociates to  $\text{NO}_2^+$  and  $\text{NO}_3^-$ , both of which then react with water and  $\text{H}^+$  to form  $\text{HNO}_3$  (R1.15-1.20). The nitronium ion ( $\text{NO}_2^+$ ) acts as an electrophile and is highly reactive, having a half-life in water of  $10^{-9}$  s (Behnke et al., 1997). In presence of chloride, which is a stronger nucleophile, it reacts preferentially with  $\text{Cl}^-$  (Johnson and Margerum, 1991) as the key step in (R1.13) mentioned above. It is also an important nitrating agent in organic chemistry by electrophilic aromatic substitution (Carey and Sundberg, 2007).



The mechanism has been found to be consistent with observed behavior and reactivity in a series of studies (Griffiths et al., 2009; Hallquist et al., 2003; Mentel et al., 1999). It likewise explains the reduction in reactivity found in nitrate aerosols, where an excess of nitrate leads to an increase of the reaction rate for the recombination reaction R1.17 and thereby inhibiting net uptake (Wahner et al., 1998). A simplified schematic of the chemical mechanism in an aqueous aerosol particle can be seen in Figure 1.3.

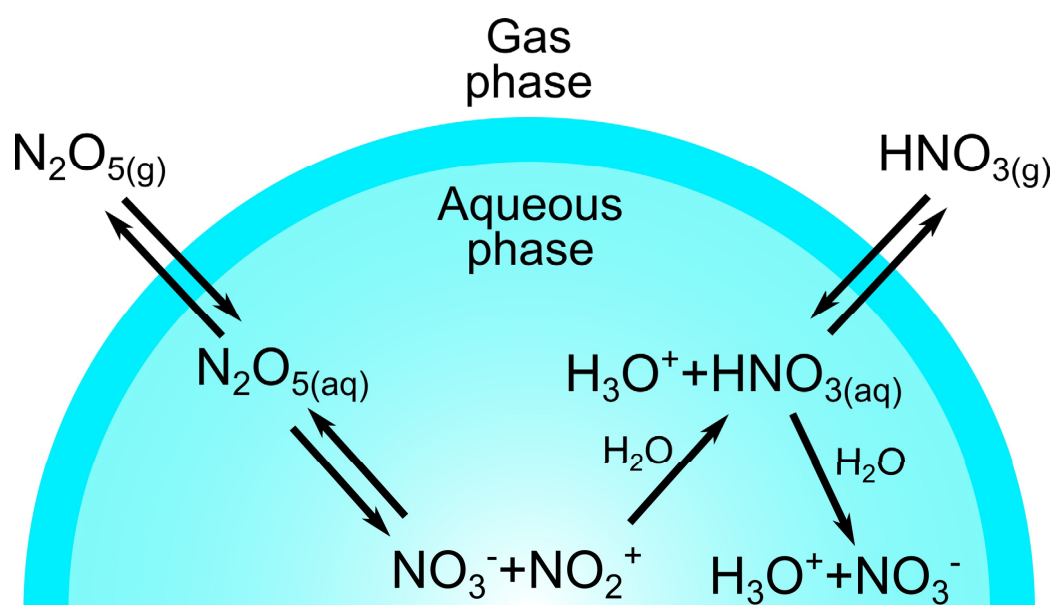


**Fig. 1.3.** The chemical mechanism of  $\text{N}_2\text{O}_5$  uptake on aerosol particles

A variation of the mechanism was proposed by Thornton et al. (2003) for dilute acidic or neutral non-halide aerosol, which involves the formation of a hydrated nitronium ion intermediate ( $\text{H}_2\text{ONO}_2^+$ ) instead of  $\text{NO}_2^+$  (R1.21), which would then react with water to give nitric acid.



A similar mechanism was suggested by Talukdar et al. (2012) for uptake of  $\text{N}_2\text{O}_5$  on HCl doped  $\text{H}_2\text{SO}_4$  liquid surfaces as well. As Robinson et al. (1997) suggest, such a mechanism would be prevalent in medium to high water activity situations. The non-

hydrated  $\text{NO}_2^+$  would exist only in strongly acidic solutions, where lack of  $\text{H}_2\text{O}$  would enable  $\text{NO}_2^+$  to exist as a stable species. We can therefore expect that the hydrated nitronium ion would be the prevalent form in most atmospheric aerosol. There is however no indication that this difference in ion structure or configuration has any impact on the kinetics of  $\text{N}_2\text{O}_5$  uptake.

#### 1.3.4. $\text{N}_2\text{O}_5$ measurement techniques

Several measurement techniques have been used over the years to measure  $\text{N}_2\text{O}_5$ , in atmospheric and/or laboratory measurements.

DOAS, or Differential Optical Absorption Spectroscopy, is often used to measure atmospheric concentrations of trace gases. The operating principle is the measurement of specific absorption bands in the UV and visible spectrum. A modern long path DOAS instrument is composed of a light source and a coaxial double Newtonian telescope transmitting a collimated beam of light to an array of quartz corner-cube reflectors positioned a few km away from the telescope (Stutz et al., 2004). This method can be used to measure  $\text{N}_2\text{O}_5$  indirectly, by measuring  $\text{NO}_3$  and  $\text{NO}_2$  concentrations in the gas column delimited by the light beam. The  $\text{N}_2\text{O}_5$  concentration is calculated based on the equilibrium in R1.11. The advantage of the technique is that measurements of  $\text{NO}_3$  and  $\text{NO}_2$  are not affected by wall loss in an instrument inlet and the technique does not require calibration (Wang et al., 2006).

Cavity Ring-Down Spectroscopy (CRDS) uses a set of high reflectivity mirrors placed in a cavity and a dye laser used to inject a laser beam into the cavity through one of the mirrors (Atkinson, 2003). The concentration of the analyte is determined by the decay of the laser intensity within the cavity, which is proportional to the species concentration ( $\text{NO}_3$ ). A second, heated inlet is used to measure the sum of  $\text{NO}_3$  and  $\text{N}_2\text{O}_5$  simultaneously by thermal conversion of  $\text{N}_2\text{O}_5$  to  $\text{NO}_3$ . The amount of  $\text{N}_2\text{O}_5$  is obtained via the difference between the two channels. The instrument is relatively compact and therefore suitable for both field and laboratory work, with very low detection limits, down to 1-5 pptv (Brown et al., 2009).

Laser-Induced Fluorescence (LIF) uses a laser to excite the species of interest to a higher electronic state, from which it may fluoresce with an efficiency determined by its fluorescence properties (Wood et al., 2003). As in the case of CRDS, this technique is used to measure  $\text{NO}_3$  concentration and indirectly  $\text{N}_2\text{O}_5$  by thermal conversion of the former, with a detection limit in the low pptv range (Griffiths et al., 2009; Wood et al., 2005).

Chemical Ionization Mass Spectrometry (CIMS) is based on a soft and selective ionization process resulting from a reaction between a reagent ion and the analyte followed by mass spectrometry of the resulting ions. The soft ionization process results in simple mass spectra with relatively little fragmentation. The reagent ion used is iodide ( $\text{I}^-$ ) which reduces possible interference by  $\text{HNO}_3$ , but it can't differentiate between  $\text{NO}_3$  or  $\text{N}_2\text{O}_5$ , ionizing both species to  $\text{NO}_3^-$  detected at 62 amu (Hanson and Ravishankara, 1991; Hu and Abbatt, 1997). Nevertheless, the method is highly sensitive (10 pptv range). Recently, a method has been developed to measure the  $\text{I}(\text{N}_2\text{O}_5)^-$  ion cluster, which allows to measure  $\text{N}_2\text{O}_5$  directly (Kercher et al., 2009).

These techniques have many advantages: they are very sensitive and relatively fast. Spectroscopic techniques usually have relatively small interferences compared to chemical methods. Additionally, the latest generation of instruments is relatively compact, enabling field measurements albeit with some restrictions. However, there are some disadvantages as well, like the fact that studies of  $\text{N}_2\text{O}_5$  uptake on aerosol particles can only be conducted by following its loss from the gas phase, with all the limitations that this implies. In this thesis we have used the short lived  $^{13}\text{N}$  radioactive tracer technique developed at the Paul Scherrer Institute (Ammann, 2001; Kalberer et al., 1996). This technique allows studying the uptake of a wide range of nitrogen oxides and related compounds on aerosol particles by labeling them with  $^{13}\text{N}$ , a short-lived isotope with a half-life of 10 min.  $^{13}\text{N}$  is a well-known positron emitter, used for example in positron emission tomography (PET) for medical purposes (Miller et al., 2008). This technique allows monitoring the gas phase concentrations of  $\text{NO}_2$ ,  $\text{NO}_3$  and  $\text{N}_2\text{O}_5$  as well as the particle phase concentrations for  $\text{N}_2\text{O}_5$  by monitoring the decay of  $^{13}\text{N}$  labeled species both in the gas and aerosol phase. The method can be used for experiments performed at very low trace gas concentrations (100 pptv) and in



presence of high relative humidity. Similar to some of the other spectroscopic techniques, it requires separation of the analyte from the aerosol particles. In contrast to spectroscopic techniques, the tracer technique lacks direct chemical selectivity, but requires selective chemical separation. Over the previous two decades the  $^{13}\text{N}$  tracer produced at the PSI PROTRAC facility has been used to study the uptake kinetics of nitrogen oxides such as  $\text{HNO}_3$  (Guimbaud et al., 2002; Vlasenko et al., 2006),  $\text{NO}_2$  (Sosedova et al., 2009),  $\text{NO}_y$  (Bartels-Rausch et al., 2002),  $\text{HNO}_4$  (Bartels-Rausch et al., 2011) on various types of aerosol or ice substrates. This study represents the first production and use of  $^{13}\text{N}$  labeled  $\text{N}_2\text{O}_5$  for kinetic experiments. Additional information about the  $^{13}\text{N}$  technique can be found in Chapter 2 which contains a detailed description of the  $^{13}\text{N}$  production facility and the  $^{13}\text{N}_2\text{O}_5$  production method.

#### 1.4. The kinetics of gas uptake on aerosol particles

As already mentioned previously, the kinetics of gas-aerosol interactions are usually described by the uptake coefficient  $\gamma$ , defined as the ratio of the net flux of molecules from the gas phase to the aerosol particles to the gas-kinetic collision flux of the molecules to the surface of the particles (Finlayson-Pits and Pits, 2000).

$$\gamma = \frac{J_{net}}{J_{coll}} \quad (\text{Eq. 1.2})$$

The gas kinetic collision flux can be defined (based on gas kinetic theory) as:

$$J_{coll} = \frac{[X]_g \omega_x}{4} \quad (\text{Eq. 1.3})$$

where  $[X]_g$  is the concentration of the gas species in question near the surface of the aerosol particle, while  $\omega_x$  is the average molecular velocity of the gaseous species. The uptake of a gas into a liquid particle involves several physical and chemical processes.

The first one is *diffusion of the gas to the interface*. The gas molecule can then either scatter or thermally accommodate at the surface. The gaseous diffusion is determined by the gas-phase diffusion coefficient ( $D_g$ ). The rate of accommodation on the surface is described by the surface accommodation coefficient, defined as the ratio of molecules adsorbed (accommodated) at the surface to the number of gas-surface collisions.

The molecule *may then enter and dissolve in the interfacial region*. The overall process is described by the bulk accommodation coefficient ( $\alpha_b$ ), which is the convolution of the surface accommodation and surface to bulk transfer. Surface to bulk transfer of a soluble molecule essentially represents its solvation.

The *diffusion of the dissolved molecule further into the bulk* of the particle is determined by the diffusion coefficient in liquid,  $D_l$ .

If there is no reaction within the liquid phase or the reaction is slow (compared to uptake and diffusion), an equilibrium is eventually established between the gas and liquid phase (*Henry's law equilibrium*), characterized by the Henry's law constant  $H$ , where  $H=[X]_b/P_x$ , with  $P_x$  being the gas-phase equilibrium pressure and  $[X]_b$  the concentration of  $X$  in solution.

*Reaction in the bulk* can happen close to the surface or over the whole bulk of the particle depending on the rate of the reaction compared to diffusion.

*Reactions at the interface* have to be considered in some cases as well. These happen by formation of interface species which can react at the surface before or without being taken up into the bulk of the particle. The two main types of surface reactions are: gas-surface reactions (Eley-Rideal), with direct reaction of gas phase species with surface species upon collision without an adsorption step, and surface layer reactions (Langmuir-Hinshelwood), where the gas phase molecules need to be adsorbed to the surface first.

The measured net uptake can be related to the above mentioned processes and these physical and chemical processes are often treated in terms of the resistor model for gas-particle interaction (Davidovits et al., 2006, 2011; Hanson et al., 1994). According to this model, the net uptake of a gas to a particle ( $\gamma_{\text{net}}$ ) can be treated, under appropriate steady state conditions, in terms of an electrical circuit with 'conductances'  $\Gamma$  associated with each process, which reflect rates normalized to the

rate of gas-surface collisions. Under these conditions the individual processes can be treated as being not coupled. The overall resistance to the uptake on a particle would then be:

$$\frac{1}{\gamma_{net}} = \frac{1}{\Gamma_g} + \frac{1}{\alpha_b} + \frac{1}{\Gamma_{sol} + \Gamma_{brxn}} \quad (\text{Eq. 1.4})$$

where  $\Gamma_g$  is the conductance for gas phase diffusion,  $\Gamma_{sol}$  for solubility and diffusion into the bulk and  $\Gamma_{brxn}$  that for reaction in the bulk. By solving the diffusion equation for the cases in question, the following normalized rates of gas phase diffusion, solubility and bulk reaction (Finlayson-Pitts and Pitts, 2000; Pöschl et al., 2007) can be obtained:

$$\Gamma_g = \frac{Kn(1 + Kn)}{0.75 + 0.28Kn} \quad (\text{Eq. 1.5})$$

$$\Gamma_{sol} = \frac{4HRT}{\omega} \sqrt{\frac{D_l}{\pi t}} \quad (\text{Eq. 1.6})$$

$$\Gamma_{brxn} = \frac{4HRT}{\omega} \sqrt{D_l k^I} \quad (\text{Eq. 1.7})$$

where  $Kn$  is the Knudsen number, defined as  $6D_g/\omega d_p$ ,  $D_g$  is the gas phase diffusion coefficient of the reacting species,  $d_p$  is the particle diameter,  $\omega$  is the average molecular velocity,  $H$  is the Henry's Law constant,  $R$  is the gas constant,  $T$  is the absolute temperature,  $D_l$  is the diffusion coefficient in the liquid phase,  $t$  is the gas-liquid interaction time and  $k^I$  is the pseudo first order rate constant for loss within the liquid phase.

Obviously, this presents various possibilities for combinations of fast and slow gas transport, solubility and bulk reaction. Considering all this possibilities would be

outside the scope of this thesis and for a more thorough elaboration of the various cases please refer to (Davidovits et al., 2006; Finlayson-Pitts and Pitts, 2000; Hanson et al., 1994). The situation can be simplified by making some assumptions regarding the system. The first assumption is that gas-phase diffusion constraints can be neglected, which is a reasonable assumption for small particles (<500 nm) and moderate uptake coefficients (<0.05). At such high end values, and taken into consideration a  $N_2O_5$  gas-phase diffusion coefficient of  $10^{-5} \text{ m}^2/\text{s}$  (Anttila et al., 2006), the term  $1 / \Gamma_g$  is equal to 1.187, which corresponds to a ~6% correction on the overall uptake coefficient. At expected uptake values of  $10^{-2}$  or lower the correction value goes below 1%. It can be likewise assumed that the reaction is faster than solubility equilibration (governed by diffusion into the bulk) ( $\Gamma_{\text{sol}} \ll \Gamma_{\text{brxn}}$ ). Such an assumption is warranted when in the presence of a well-mixed system, where characteristic times for diffusion through the bulk of submicron particles are sufficiently short. Under these circumstances, the overall uptake coefficient for uptake on a liquid surface simplifies to:

$$\frac{1}{\gamma_{\text{net}}} = \frac{1}{\alpha_b} + \frac{\omega}{4HRT\sqrt{D_l k^I}} \quad (\text{Eq. 1.8})$$

For small aerosol particles a correction factor has to be applied that takes into consideration the spherical geometry of the particle and the competition between diffusion and reaction (Hanson et al., 1994). The overall equation then becomes:

$$\frac{1}{\gamma_{\text{net}}} = \frac{1}{\alpha_b} + \frac{\omega}{4HRT\sqrt{D_l k^I}} \frac{1}{\coth q - 1/q} \quad (\text{Eq. 1.9})$$

The reacto-diffusive parameter  $q$  is defined as:

$$q = \frac{l}{r} \quad (\text{Eq. 1.10})$$

Where  $r$  is the radius of the particle,  $l$  is the reacto-diffusive length and  $k^I$  is the pseudo-first order reaction constant:

$$l = \sqrt{\frac{D_l}{k^I}} \quad (\text{Eq. 1.11})$$

The reacto-diffusive length is the characteristic distance a particle will diffuse towards the bulk before reacting. When  $q > 1$ , the reacto-diffusive length becomes larger than the radius and the reaction occurs throughout the volume of the particle. In this case the reaction is no longer limited by diffusion and the process is volume limited:

$$\frac{1}{\gamma_{net}} = \frac{1}{\alpha_b} + \frac{\omega}{4HRTk^I} \frac{S_p}{V_p} \cong \frac{\omega}{4HRTk^I} \frac{S_p}{V_p} \quad (\text{Eq. 1.12})$$

where  $S_p/V_p$  is the ratio between particle surface area and particle volume. In such situations the second term of the equation is much greater than  $1/\alpha_b$ , and the equation can be approximated as in Eq. 1.12. If, on the other hand,  $q \ll 1$  then  $l$  is small compared to the particle radius and the mechanism is dominated by reaction near the surface, with the kinetics as given in Eq. 1.9.

## 1.5. Scope of the thesis

The scope of the thesis was to give a detailed look at some aspects of  $\text{N}_2\text{O}_5$  reactivity, which still present open questions.  $\text{N}_2\text{O}_5$  is a fairly significant trace gas and uncertainties with regards to kinetic data can lead to significant limitations in predictive power of large-scale atmospheric model parameterizations. There are several challenges that influence the connection between laboratory results and atmospheric behavior of aerosols with respect to trace gas uptake in general and  $\text{N}_2\text{O}_5$  in particular.

Results obtained from lab studies may not be representative in terms of the degree of internal mixing present in atmospheric aerosol because of a wide range of aging processes present in the field, which could bring about significant changes in composition with increased photochemical age (De Gouw and Jimenez, 2009; George et al., 2008; Takegawa et al., 2006; Volkamer et al., 2006).

The physical state has a strong influence on the reactivity of  $\text{N}_2\text{O}_5$  with aerosols (Gross et al., 2009; Mozurkewich and Calvert, 1988; Thornton et al., 2003) and predictions based on lab studies cannot easily replicate field results (Brown et al., 2009) nor can unequivocal physical states of aerosols be predicted easily because of a wide range of parameters that influence them, potentially requiring advanced methods to describe the changes that can happen with aerosol aging (Shiraiwa et al., 2011; Zaveri et al., 2010). Besides liquid and solid particles, new insights into organic aerosol physical state show that these aerosols often have viscosities intermediate between conventional liquids and solids, with important impacts on reactivity (Abramson et al., 2013; Renbaum-Wolff et al., 2013; Vaden et al., 2011). Recent measurements suggest that viscosity, and therefore diffusivity, may play an important role in  $\text{N}_2\text{O}_5$  reactivity (Gaston et al., 2014).

Finally, the role of organics and surface composition has to be taken into account, because of the large presence of organic aerosols in the environment (De Gouw and Jimenez, 2009; Kanakidou et al., 2005; Zhang et al., 2007) as well as the complex internal mixing that organic aerosols exhibit (Carlton et al., 2009; Flores et al., 2014; Hatch et al., 2011; Walser et al., 2008). Composition effects may play a central role in the reactivity of atmospheric organic aerosols (Rudich et al., 2007). The large range of uptake coefficients for  $\text{N}_2\text{O}_5$  measured in the lab on a restricted number of organic species (Griffiths et al., 2009; Iannone et al., 2011; Xiao and Bertram, 2011) has shown that predicting the reactivity of field aerosol will be a non-trivial pursuit. Additionally, organic films that form on non-organic aerosol can reduce reactivity by a significant amount (Anttila et al., 2006).

Measurements of  $\text{N}_2\text{O}_5$  reactivity in the field (Brown et al., 2009) and on ambient aerosol particles (Bertram et al., 2009; Riedel et al., 2012) have shown that uptake is

strongly influenced by chemical composition. Furthermore, the measurements have shown that the observed reactivity values are more variable and up to a factor of ten lower than predictions by large scale model parameterizations. Therefore, the reactivity of  $\text{N}_2\text{O}_5$  with complex atmospheric aerosol, which is often composed of mixtures of inorganic and organic components, is still relatively difficult to predict.

These factors represent some of the major open issues still present in atmospheric chemistry, and this work will try to address some of them. The discrepancies that exist between field measurements and predictions based on laboratory studies have been attributed by Brown et al. (2009) and Bertram et al. (2009) to organic aerosol. Riedel et al. (2012) attribute it to nitrate loading. The effect of organics on reactivity has been until recently studied primarily with an emphasis on the impact of surface active organic species on the mass transfer of  $\text{N}_2\text{O}_5$ . However, other factors, like high viscosity in secondary organic material, have not been addressed thus far and have only recently come to attention. The first goal of this work is to expand the knowledge of the impact that high viscosity has on reactivity and contribute to the developing discussion on the topic. The underlying issue that links these, and indeed most studies of  $\text{N}_2\text{O}_5$  is that the detailed mechanism has been lumped together because of the difficulty of investigating the specific reactions. The overall uptake has been presented as a net bimolecular reaction of an assumed hydrated  $\text{N}_2\text{O}_5$  species with water or some other electrophile, and the various parameters like the Henry's Law constant or the apparent/effective rate constants have been adjusted to fit the measurements. However, the exact details of the mechanism, like reaction order, bulk accommodation, reaction rates of the various reactions like  $\text{N}_2\text{O}_5$  dissociation and recombination have not been investigated. The second goal of this work is therefore to shed some light on these aspects of  $\text{N}_2\text{O}_5$  uptake, in particular bulk accommodation. As an additional goal the instrumental development related to  $^{13}\text{N}_2\text{O}_5$  production is a necessary step in the above mentioned investigations.

The related research work is presented as follows:

The first step was to prepare an experimental setup for the measurements and devise and optimize a  $^{13}\text{N}_2\text{O}_5$  production method. Chapter 2 shows the work on this problem,

with an in depth look into  $^{13}\text{N}$  isotope production,  $\text{N}_2\text{O}_5$  gas phase kinetics modeling and instrumental build-up.

Chapter 3 deals with uptake of  $\text{N}_2\text{O}_5$  on citric acid over a wider relative humidity (RH) range. The motivation for this study was to investigate reactivity on an organic aerosol which could act as a proxy for highly oxidized organic species present in secondary organic aerosol (SOA) in the atmosphere. Additionally, citric acid presents viscosities which are expected to be more compatible with real-world organic aerosol values than aerosol matrices used in other studies available to date (Griffiths et al., 2009; Iannone et al., 2011; Thornton et al., 2003).

Chapter 4 covers the investigation into  $\text{N}_2\text{O}_5$  uptake on nitrate aerosol and the nitrate effect, which refers to the apparent reduction of  $\text{N}_2\text{O}_5$  reactivity on nitrate aerosol when compared to other inorganic aerosols like sulfates. Of particular interest was to observe if the unique properties of the  $^{13}\text{N}$  radioactive tracer could be leveraged to give an insight into specific processes like bulk accommodation.

Chapter 5 contains a summary of the experimental work and results, with an outlook on future avenues of research.



## References

- Abbatt, J. P. D., Lee, A. K. Y., and Thornton, J. A.: Quantifying trace gas uptake to tropospheric aerosol: recent advances and remaining challenges, *Chemical Society Reviews*, 41, 6555-6581, 2012.
- Abramson, E., Imre, D., Beranek, J., Wilson, J., and Zelenyuk, A.: Experimental determination of chemical diffusion within secondary organic aerosol particles, *Physical Chemistry Chemical Physics*, 15, 2983-2991, 2013.
- Alexander, B., Park, R. J., Jacob, D. J., Li, Q. B., Yantosca, R. M., Savarino, J., Lee, C. C. W., and Thieme, M. H.: Sulfate formation in sea-salt aerosols: Constraints from oxygen isotopes, *Journal of Geophysical Research: Atmospheres*, 110, D10307, 2005.
- Ammann, M.: Using  $^{13}\text{N}$  as tracer in heterogeneous atmospheric chemistry experiments, *Radiochim. Acta*, 89, 831-838, 2001.
- Anttila, T., Kiendler-Scharr, A., Tillmann, R., and Mentel, T. F.: On the reactive uptake of gaseous compounds by organic-coated aqueous aerosols: Theoretical analysis and application to the heterogeneous hydrolysis of  $\text{N}_2\text{O}_5$ , *Journal of Physical Chemistry A*, 110, 10435-10443, 2006.
- Atkinson, D. B.: Solving chemical problems of environmental importance using cavity ring-down spectroscopy, *Analyst*, 128, 117-125, 2003.
- Bartels-Rausch, T., Eichler, B., Zimmermann, P., Gaggeler, H. W., and Ammann, M.: The adsorption of nitrogen oxides on crystalline ice, *Atmos. Chem. Phys.*, 2, 235-247, 2002.
- Bartels-Rausch, T., Ulrich, T., Huthwelker, T., and Ammann, M.: A novel synthesis of the N-13 labeled atmospheric trace gas peroxyxynitric acid, *Radiochimica Acta*, 99, 285-292, 2011.
- Behnke, W., George, C., Scheer, V., and Zetzsch, C.: Production and decay of  $\text{ClNO}_2$ , from the reaction of gaseous  $\text{N}_2\text{O}_5$  with  $\text{NaCl}$  solution: Bulk and aerosol experiments, *Journal of Geophysical Research-Atmospheres*, 102, 3795-3804, 1997.
- Bertram, T. H., Thornton, J. A., Riedel, T. P., Middlebrook, A. M., Bahreini, R., Bates, T. S., Quinn, P. K., and Coffman, D. J.: Direct observations of  $\text{N}_2\text{O}_5$  reactivity on ambient aerosol particles, *Geophysical Research Letters*, 36, 5, 2009.
- Brown, S. S., Dube, W. P., Fuchs, H., Ryerson, T. B., Wollny, A. G., Brock, C. A., Bahreini, R., Middlebrook, A. M., Neuman, J. A., Atlas, E., Roberts, J. M., Osthoff, H. D., Trainer, M., Fehsenfeld, F. C., and Ravishankara, A. R.: Reactive uptake coefficients for  $\text{N}_2\text{O}_5$  determined from aircraft measurements during the Second Texas Air Quality Study: Comparison to current model parameterizations, *Journal of Geophysical Research-Atmospheres*, 114, 2009.

Brunekreef, B. and Holgate, S. T.: Air pollution and health, *The Lancet*, 360, 1233-1242, 2002.

Carey, F. A. and Sundberg, R. J.: *Advanced Organic Chemistry: Part A: Structure and Mechanisms*, Springer, 2007.

Carlton, A. G., Wiedinmyer, C., and Kroll, J. H.: A review of Secondary Organic Aerosol (SOA) formation from isoprene, *Atmos. Chem. Phys.*, 9, 4987-5005, 2009.

Chang, W. L., Bhave, P. V., Brown, S. S., Riemer, N., Stutz, J., and Dabdub, D.: Heterogeneous Atmospheric Chemistry, Ambient Measurements, and Model Calculations of N(2)O(5): A Review, *Aerosol Sci. Technol.*, 45, 665-695, 2011.

Chung, C. E., Ramanathan, V., Kim, D., and Podgorny, I. A.: Global anthropogenic aerosol direct forcing derived from satellite and ground-based observations, *Journal of Geophysical Research: Atmospheres*, 110, D24207, 2005.

Cooper, P. L. and Abbatt, J. P. D.: Heterogeneous Interactions of OH and HO<sub>2</sub> Radicals with Surfaces Characteristic of Atmospheric Particulate Matter, *The Journal of Physical Chemistry*, 100, 2249-2254, 1996.

Davidovits, P., Kolb, C. E., Williams, L. R., Jayne, J. T., and Worsnop, D. R.: Mass Accommodation and Chemical Reactions at Gas-Liquid Interfaces, *Chemical Reviews*, 106, 1323-1354, 2006.

Davidovits, P., Kolb, C. E., Williams, L. R., Jayne, J. T., and Worsnop, D. R.: Update 1 of: Mass Accommodation and Chemical Reactions at Gas-Liquid Interfaces, *Chemical Reviews*, 111, 2011.

Davis, J. M., Bhave, P. V., and Foley, K. M.: Parameterization of N<sub>2</sub>O<sub>5</sub> reaction probabilities on the surface of particles containing ammonium, sulfate, and nitrate, *Atmos. Chem. Phys.*, 8, 5295-5311, 2008.

De Gouw, J. and Jimenez, J. L.: Organic Aerosols in the Earth's Atmosphere, *Environmental Science & Technology*, 43, 7614-7618, 2009.

Dentener, F. J. and Crutzen, P. J.: Reaction of N<sub>2</sub>O<sub>5</sub> on tropospheric aerosols: Impact on the global distributions of NO<sub>x</sub>, O<sub>3</sub>, and OH, *Journal of Geophysical Research: Atmospheres*, 98, 7149-7163, 1993.

Dockery, D. W. and Pope, C. A.: Acute Respiratory Effects of Particulate Air Pollution, *Annual Review of Public Health*, 15, 107-132, 1994.

Evans, M. J. and Jacob, D. J.: Impact of new laboratory studies of N<sub>2</sub>O<sub>5</sub> hydrolysis on global model budgets of tropospheric nitrogen oxides, ozone, and OH, *Geophysical Research Letters*, 32, 2005.

Finlayson-Pitts, B. J. and Pitts, J. N., Jr.: *Chemistry of the upper and lower atmosphere*, Academic Press, San Diego, CA, 2000.

Flores, J. M., Zhao, D. F., Segev, L., Schlag, P., Kiendler-Scharr, A., Fuchs, H., Watne, Å. K., Bluvshstein, N., Mentel, T. F., Hallquist, M., and Rudich, Y.: Evolution

of the complex refractive index in the UV spectral region in ageing secondary organic aerosol, *Atmos. Chem. Phys.*, 14, 5793-5806, 2014.

Gaston, C. J., Thornton, J. A., and Ng, N. L.: Reactive uptake of N<sub>2</sub>O<sub>5</sub> to internally mixed inorganic and organic particles: the role of organic carbon oxidation state and inferred organic phase separations, *Atmos. Chem. Phys.*, 14, 5693-5707, 2014.

George, C., Ponche, J. L., Mirabel, P., Behnke, W., Scheer, V., and Zetzsch, C.: Study of the Uptake of N<sub>2</sub>O<sub>5</sub> by Water and NaCl Solutions, *J. Phys. Chem.*, 98, 8780-8784, 1994.

George, I. J., Slowik, J., and Abbatt, J. P. D.: Chemical aging of ambient organic aerosol from heterogeneous reaction with hydroxyl radicals, *Geophysical Research Letters*, 35, L13811, 2008.

Gerstl, S. A. W. and Zardecki, A.: Effects of aerosols on photosynthesis, *Nature*, 300, 436-437, 1982.

Griffiths, P. T., Badger, C. L., Cox, R. A., Folkers, M., Henk, H. H., and Mentel, T. F.: Reactive Uptake of N<sub>2</sub>O<sub>5</sub> by Aerosols Containing Dicarboxylic Acids. Effect of Particle Phase, Composition, and Nitrate Content, *Journal of Physical Chemistry A*, 113, 5082-5090, 2009.

Gross, S., Iannone, R., Xiao, S., and Bertram, A. K.: Reactive uptake studies of NO<sub>3</sub> and N<sub>2</sub>O<sub>5</sub> on alkenoic acid, alkanolate, and polyalcohol substrates to probe nighttime aerosol chemistry, *Physical Chemistry Chemical Physics*, 11, 7792-7803, 2009.

Guimbaud, C., Arens, F., Gutzwiller, L., Gaggeler, H. W., and Ammann, M.: Uptake of HNO<sub>3</sub> to deliquescent sea-salt particles: a study using the short-lived radioactive isotope tracer N-13, *Atmospheric Chemistry and Physics*, 2, 249-257, 2002.

Hallquist, M., Stewart, D. J., Stephenson, S. K., and Cox, R. A.: Hydrolysis of N<sub>2</sub>O<sub>5</sub> on sub-micron sulfate aerosols, *Physical Chemistry Chemical Physics*, 5, 3453-3463, 2003.

Hanson, D. R. and Ravishankara, A. R.: The reaction probabilities of ClONO<sub>2</sub> and N<sub>2</sub>O<sub>5</sub> on 40 to 75% sulfuric acid solutions, *Journal of Geophysical Research: Atmospheres*, 96, 17307-17314, 1991.

Hanson, D. R., Ravishankara, A. R., and Solomon, S.: Heterogeneous reactions in sulfuric acid aerosols: A framework for model calculations, *Journal of Geophysical Research: Atmospheres*, 99, 3615-3629, 1994.

Hatch, L. E., Creamean, J. M., Ault, A. P., Surratt, J. D., Chan, M. N., Seinfeld, J. H., Edgerton, E. S., Su, Y., and Prather, K. A.: Measurements of Isoprene-Derived Organosulfates in Ambient Aerosols by Aerosol Time-of-Flight Mass Spectrometry—Part 2: Temporal Variability and Formation Mechanisms, *Environmental Science & Technology*, 45, 8648-8655, 2011.

Hu, J. H. and Abbatt, J. P. D.: Reaction Probabilities for N<sub>2</sub>O<sub>5</sub> Hydrolysis on Sulfuric Acid and Ammonium Sulfate Aerosols at Room Temperature, *The Journal of Physical Chemistry A*, 101, 871-878, 1997.

Iannone, R., Xiao, S., and Bertram, A. K.: Potentially important nighttime heterogeneous chemistry: NO<sub>3</sub> with aldehydes and N<sub>2</sub>O<sub>5</sub> with alcohols, *Physical Chemistry Chemical Physics*, 13, 10214-10223, 2011.

Ito, A. and Feng, Y.: Role of dust alkalinity in acid mobilization of iron, *Atmos. Chem. Phys.*, 10, 9237-9250, 2010.

Johnson, D. W. and Margerum, D. W.: Non-metal redox kinetics: a reexamination of the mechanism of the reaction between hypochlorite and nitrite ions, *Inorganic Chemistry*, 30, 4845-4851, 1991.

Kalberer, M., Tabor, K., Ammann, M., Parrat, Y., Weingartner, E., Piguet, D., Rossler, E., Jost, D. T., Turler, A., Gaggeler, H. W., and Baltensperger, U.: Heterogeneous chemical processing of (NO<sub>2</sub>)-N-13 by monodisperse carbon aerosols at very low concentrations, *J. Phys. Chem.*, 100, 15487-15493, 1996.

Kanakidou, M., Seinfeld, J. H., Pandis, S. N., Barnes, I., Dentener, F. J., Facchini, M. C., Van Dingenen, R., Ervens, B., Nenes, A., Nielsen, C. J., Swietlicki, E., Putaud, J. P., Balkanski, Y., Fuzzi, S., Horth, J., Moortgat, G. K., Winterhalter, R., Myhre, C. E. L., Tsigaridis, K., Vignati, E., Stephanou, E. G., and Wilson, J.: Organic aerosol and global climate modelling: a review, *Atmos. Chem. Phys.*, 5, 1053-1123, 2005.

Karagulian, F. and Rossi, M. J.: Heterogeneous chemistry of the NO<sub>3</sub> free radical and N<sub>2</sub>O<sub>5</sub> on decane flame soot at ambient temperature: Reaction products and kinetics, *Journal of Physical Chemistry A*, 111, 1914-1926, 2007.

Karagulian, F., Santschi, C., and Rossi, M. J.: The heterogeneous chemical kinetics of N<sub>2</sub>O<sub>5</sub> on CaCO<sub>3</sub> and other atmospheric mineral dust surrogates, *Atmospheric Chemistry and Physics*, 6, 1373-1388, 2006.

Kercher, J. P., Riedel, T. P., and Thornton, J. A.: Chlorine activation by N<sub>2</sub>O<sub>5</sub>: simultaneous, in situ detection of ClNO<sub>2</sub> and N<sub>2</sub>O<sub>5</sub> by chemical ionization mass spectrometry, *Atmos. Meas. Tech.*, 2, 193-204, 2009.

Leaith, W. R., Lohmann, U., Russell, L. M., Garrett, T., Shantz, N. C., Toom-Saunty, D., Strapp, J. W., Hayden, K. L., Marshall, J., Wolde, M., Worsnop, D. R., and Jayne, J. T.: Cloud albedo increase from carbonaceous aerosol, *Atmos. Chem. Phys.*, 10, 7669-7684, 2010.

Mentel, T. F., Sohn, M., and Wahner, A.: Nitrate effect in the heterogeneous hydrolysis of dinitrogen pentoxide on aqueous aerosols, *Physical Chemistry Chemical Physics*, 1, 5451-5457, 1999.

Meskhidze, N., Chameides, W. L., Nenes, A., and Chen, G.: Iron mobilization in mineral dust: Can anthropogenic SO<sub>2</sub> emissions affect ocean productivity?, *Geophysical Research Letters*, 30, 2085, 2003.

Mielke, L. H., Furgeson, A., and Osthoff, H. D.: Observation of ClNO<sub>2</sub> in a Mid-Continental Urban Environment, *Environmental Science & Technology*, 45, 8889-8896, 2012.

Miller, P. W., Long, N. J., Vilar, R., and Gee, A. D.: Synthesis of C-11, F-18, O-15, and N-13 Radiolabels for Positron Emission Tomography, *Angew. Chem.-Int. Edit.*, 47, 8998-9033, 2008.

Mozurkewich, M. and Calvert, J. G.: Reaction probability of N<sub>2</sub>O<sub>5</sub> on aqueous aerosols, *Journal of Geophysical Research: Atmospheres*, 93, 15889-15896, 1988.

Nel, A. E., Diaz-Sanchez, D., and Li, N.: The role of particulate pollutants in pulmonary inflammation and asthma: evidence for the involvement of organic chemicals and oxidative stress, *Current Opinion in Pulmonary Medicine*, 7, 20-26, 2001.

Nel, A. E., Diaz-Sanchez, D., Ng, D., Hiura, T., and Saxon, A.: Enhancement of allergic inflammation by the interaction between diesel exhaust particles and the immune system, *Journal of Allergy and Clinical Immunology*, 102, 539-554, 1998.

Newhall, C. G. and Punongbayan, R. S.: *Fire and Mud: Eruptions and Lahars of Mount Pinatubo, Philippines*, University of Washington Press, Seattle, 1997.

Osthoff, H. D., Roberts, J. M., Ravishankara, A. R., Williams, E. J., Lerner, B. M., Sommariva, R., Bates, T. S., Coffman, D., Quinn, P. K., Dibb, J. E., Stark, H., Burkholder, J. B., Talukdar, R. K., Meagher, J., Fehsenfeld, F. C., and Brown, S. S.: High levels of nitryl chloride in the polluted subtropical marine boundary layer, *Nature Geoscience*, 1, 324-328, 2008.

Phillips, G. J., Tang, M. J., Thieser, J., Brickwedde, B., Schuster, G., Bohn, B., Lelieveld, J., and Crowley, J. N.: Significant concentrations of nitryl chloride observed in rural continental Europe associated with the influence of sea salt chloride and anthropogenic emissions, *Geophysical Research Letters*, 39, 5, 2012.

Pöschl, U., Rudich, Y., and Ammann, M.: Kinetic model framework for aerosol and cloud surface chemistry and gas-particle interactions &ndash; Part 1: General equations, parameters, and terminology, *Atmos. Chem. Phys.*, 7, 5989-6023, 2007.

Prinn, R. G.: The Cleansing Capacity of the Atmosphere, *Annual Review of Environment and Resources*, 28, 29-57, 2003.

Ravishankara, A. R.: Heterogeneous and Multiphase Chemistry in the Troposphere, *Science*, 276, 1058-1065, 1997.

Renbaum-Wolff, L., Grayson, J. W., Bateman, A. P., Kuwata, M., Sellier, M., Murray, B. J., Shilling, J. E., Martin, S. T., and Bertram, A. K.: Viscosity of  $\alpha$ -pinene secondary organic material and implications for particle growth and reactivity, *Proceedings of the National Academy of Sciences*, 110, 8014-8019, 2013.

Riedel, T. P., Bertram, T. H., Ryder, O. S., Liu, S., Day, D. A., Russell, L. M., Gaston, C. J., Prather, K. A., and Thornton, J. A.: Direct N<sub>2</sub>O<sub>5</sub> reactivity measurements at a polluted coastal site, *Atmos. Chem. Phys.*, 12, 2959-2968, 2012.

Robinson, G. N., Worsnop, D. R., Jayne, J. T., Kolb, C. E., and Davidovits, P.: Heterogeneous uptake of ClONO<sub>2</sub> and N<sub>2</sub>O<sub>5</sub> by sulfuric acid solutions, *Journal of Geophysical Research-Atmospheres*, 102, 3583-3601, 1997.

Rudich, Y., Donahue, N. M., and Mentel, T. F.: Aging of organic aerosol: Bridging the gap between laboratory and field studies, *Annual Review of Physical Chemistry*, 58, 321-352, 2007.

Schwartz, S. E., Harshvardhan, and Benkovitz, C. M.: Influence of anthropogenic aerosol on cloud optical depth and albedo shown by satellite measurements and chemical transport modeling, *Proceedings of the National Academy of Sciences*, 99, 1784-1789, 2002.

Seinfeld, J. H. and Pandis, S. N.: *Atmospheric Chemistry and Physics: from Air Pollution to Climate Change*, John Wiley & Sons, Inc., New York, USA, 1998.

Shiraiwa, M., Ammann, M., Koop, T., and Pöschl, U.: Gas uptake and chemical aging of semisolid organic aerosol particles, *Proceedings of the National Academy of Sciences*, 108, 11003-11008, 2011.

Sievering, H., Boatman, J., Gorman, E., Kim, Y., Anderson, L., Ennis, G., Luria, M., and Pandis, S.: Removal of sulphur from the marine boundary layer by ozone oxidation in sea-salt aerosols, *Nature*, 360, 571-573, 1992.

Sosedova, Y., Rouvière, A., Gäggeler, H. W., and Ammann, M.: Uptake of NO<sub>2</sub> to Deliquesced Dihydroxybenzoate Aerosol Particles, *The Journal of Physical Chemistry A*, 2009. 2009.

Stevens, B. and Feingold, G.: Untangling aerosol effects on clouds and precipitation in a buffered system, *Nature*, 461, 607-613, 2009.

Stewart, D. J., Griffiths, P. T., and Cox, R. A.: Reactive uptake coefficients for heterogeneous reaction of N<sub>2</sub>O<sub>5</sub> with submicron aerosols of NaCl and natural sea salt, *Atmos. Chem. Phys.*, 4, 1381-1388, 2004.

Stutz, J., Alicke, B., Ackermann, R., Geyer, A., White, A., and Williams, E.: Vertical profiles of NO<sub>3</sub>, N<sub>2</sub>O<sub>5</sub>, O<sub>3</sub>, and NO<sub>x</sub> in the nocturnal boundary layer: 1. Observations during the Texas Air Quality Study 2000, *Journal of Geophysical Research: Atmospheres*, 109, D12306, 2004.

Sunyer, J.: Urban air pollution and chronic obstructive pulmonary disease: a review, *European Respiratory Journal*, 17, 1024-1033, 2001.

Takegawa, N., Miyakawa, T., Kondo, Y., Blake, D. R., Kanaya, Y., Koike, M., Fukuda, M., Komazaki, Y., Miyazaki, Y., Shimono, A., and Takeuchi, T.: Evolution of submicron organic aerosol in polluted air exported from Tokyo, *Geophysical Research Letters*, 33, L15814, 2006.

Talukdar, R. K., Burkholder, J. B., Roberts, J. M., Portmann, R. W., and Ravishankara, A. R.: Heterogeneous Interaction of N<sub>2</sub>O<sub>5</sub> with HCl Doped H<sub>2</sub>SO<sub>4</sub> under Stratospheric Conditions: ClNO<sub>2</sub> and Cl<sub>2</sub> Yields, *The Journal of Physical Chemistry A*, 116, 6003-6014, 2012.

Thornton, J. A. and Abbatt, J. P. D.: N<sub>2</sub>O<sub>5</sub> reaction on submicron sea salt aerosol: Kinetics, products, and the effect of surface active organics, *Journal of Physical Chemistry A*, 109, 10004-10012, 2005.

Thornton, J. A., Braban, C. F., and Abbatt, J. P. D.: N<sub>2</sub>O<sub>5</sub> hydrolysis on sub-micron organic aerosols: the effect of relative humidity, particle phase, and particle size, *Physical Chemistry Chemical Physics*, 5, 4593-4603, 2003.

Thornton, J. A., Jaeglé, L., and McNeill, V. F.: Assessing known pathways for HO<sub>2</sub> loss in aqueous atmospheric aerosols: Regional and global impacts on tropospheric oxidants, *Journal of Geophysical Research: Atmospheres*, 113, D05303, 2008.

Thornton, J. A., Kercher, J. P., Riedel, T. P., Wagner, N. L., Cozic, J., Holloway, J. S., Dube, W. P., Wolfe, G. M., Quinn, P. K., Middlebrook, A. M., Alexander, B., and Brown, S. S.: A large atomic chlorine source inferred from mid-continental reactive nitrogen chemistry, *Nature*, 464, 271-274, 2010.

Vaden, T. D., Imre, D., Beránek, J., Shrivastava, M., and Zelenyuk, A.: Evaporation kinetics and phase of laboratory and ambient secondary organic aerosol, *Proceedings of the National Academy of Sciences*, 108, 2190-2195, 2011.

Vardaka, E., Cook, C. M., Lanaras, T., Sgardelis, S. P., and Pantis, J. D.: Effect of dust from a limestone quarry on the photosynthesis of *Quercus coccifera*, an evergreen Schlerophyllous shrub, *Bull. Environ. Contam. Toxicol.*, 54, 414-419, 1995.

Vlasenko, A., Sjogren, S., Weingartner, E., Stemmler, K., Gäggeler, H. W., and Ammann, M.: Effect of humidity on nitric acid uptake to mineral dust aerosol particles, *Atmospheric Chemistry and Physics*, 6, 2147-2160, 2006.

Volkamer, R., Jimenez, J. L., San Martini, F., Dzepina, K., Zhang, Q., Salcedo, D., Molina, L. T., Worsnop, D. R., and Molina, M. J.: Secondary organic aerosol formation from anthropogenic air pollution: Rapid and higher than expected, *Geophysical Research Letters*, 33, L17811, 2006.

Wagner, C., Hanisch, F., Holmes, N., de Coninck, H., Schuster, G., and Crowley, J. N.: The interaction of N<sub>2</sub>O<sub>5</sub> with mineral dust: aerosol flow tube and Knudsen reactor studies, *Atmospheric Chemistry and Physics*, 8, 91-109, 2008.

Wahner, A., Mentel, T. F., Sohn, M., and Stier, J.: Heterogeneous reaction of N<sub>2</sub>O<sub>5</sub> on sodium nitrate aerosol, *Journal of Geophysical Research-Atmospheres*, 103, 31103-31112, 1998.

Walser, M. L., Desyaterik, Y., Laskin, J., Laskin, A., and Nizkorodov, S. A.: High-resolution mass spectrometric analysis of secondary organic aerosol produced by ozonation of limonene, *Physical Chemistry Chemical Physics*, 10, 1009-1022, 2008.

Wang, Q., Jacob, D. J., Spackman, J. R., Perring, A. E., Schwarz, J. P., Moteki, N., Marais, E. A., Ge, C., Wang, J., and Barrett, S. R. H.: Global budget and radiative forcing of black carbon aerosol: Constraints from pole-to-pole (HIPPO) observations across the Pacific, *Journal of Geophysical Research: Atmospheres*, 119, 2013JD020824, 2014.

Wang, S., Ackermann, R., and Stutz, J.: Vertical profiles of O<sub>3</sub> and NO<sub>x</sub> chemistry in the polluted nocturnal boundary layer in Phoenix, AZ: I. Field observations by long-path DOAS, *Atmos. Chem. Phys.*, 6, 2671-2693, 2006.

Wood, E. C., Bertram, T. H., Wooldridge, P. J., and Cohen, R. C.: Measurements of N<sub>2</sub>O<sub>5</sub>, NO<sub>2</sub>, and O<sub>3</sub> east of the San Francisco Bay, *Atmos. Chem. Phys.*, 5, 483-491, 2005.

Wood, E. C., Wooldridge, P. J., Freese, J. H., Albrecht, T., and Cohen, R. C.: Prototype for In Situ Detection of Atmospheric NO<sub>3</sub> and N<sub>2</sub>O<sub>5</sub> via Laser-Induced Fluorescence, *Environmental Science & Technology*, 37, 5732-5738, 2003.

Xiao, S. and Bertram, A. K.: Reactive uptake kinetics of NO<sub>3</sub> on multicomponent and multiphase organic mixtures containing unsaturated and saturated organics, *Physical Chemistry Chemical Physics*, 13, 6628-6636, 2011.

Zaveri, R. A., Barnard, J. C., Easter, R. C., Riemer, N., and West, M.: Particle-resolved simulation of aerosol size, composition, mixing state, and the associated optical and cloud condensation nuclei activation properties in an evolving urban plume, *Journal of Geophysical Research: Atmospheres*, 115, D17210, 2010.

Zhang, N., Zhou, X., Shepson, P. B., Gao, H., Alaghmand, M., and Stirm, B.: Aircraft measurement of HONO vertical profiles over a forested region, *Geophysical Research Letters*, 36, L15820, 2009.

Zhang, Q., Jimenez, J. L., Canagaratna, M. R., Allan, J. D., Coe, H., Ulbrich, I., Alfarra, M. R., Takami, A., Middlebrook, A. M., Sun, Y. L., Dzepina, K., Dunlea, E., Docherty, K., DeCarlo, P. F., Salcedo, D., Onasch, T., Jayne, J. T., Miyoshi, T., Shimojo, A., Hatakeyama, S., Takegawa, N., Kondo, Y., Schneider, J., Drewnick, F., Borrmann, S., Weimer, S., Demerjian, K., Williams, P., Bower, K., Bahreini, R., Cottrell, L., Griffin, R. J., Rautiainen, J., Sun, J. Y., Zhang, Y. M., and Worsnop, D. R.: Ubiquity and dominance of oxygenated species in organic aerosols in anthropogenically-influenced Northern Hemisphere midlatitudes, *Geophysical Research Letters*, 34, L13801, 2007.

Zhu, X., Prospero, J. M., Millero, F. J., Savoie, D. L., and Brass, G. W.: The solubility of ferric ion in marine mineral aerosol solutions at ambient relative humidities, *Marine Chemistry*, 38, 91-107, 1992.



## Chapter 2

### 2. Production and use of $^{13}\text{N}$ labeled $\text{N}_2\text{O}_5$ to determine gas – aerosol interaction kinetics

Goran Gržinić<sup>1,2</sup>, Thorsten Bartels-Rausch<sup>1</sup>, Mario Birrer<sup>1</sup>, Andreas Türler<sup>1,2</sup> and Markus Ammann<sup>1</sup>

Published in *Radiochimica Acta* **102** (11):1025–1034, 2014, doi: 10.1515/ract-2014-2244

---

<sup>1</sup> Laboratory of Radiochemistry and Environmental Chemistry, Paul Scherrer Institute, 5232 Villigen, Switzerland

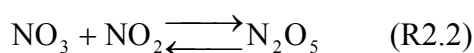
<sup>2</sup> Department of Chemistry and Biochemistry, University of Bern, 3012 Bern, Switzerland

**Summary.** Dinitrogen pentoxide has aroused significant interest in atmospheric chemistry because of its importance in the night time chemistry of nitrogen oxides to influence the tropospheric oxidation capacity. We have used an established method of  $^{13}\text{N}$  production to synthesize  $^{13}\text{N}$  labeled  $\text{N}_2\text{O}_5$  for the first time in order to study  $\text{N}_2\text{O}_5$  uptake kinetics on aerosol particles.  $^{13}\text{N}$  is produced via the  $^{16}\text{O}(\text{p}, \alpha)^{13}\text{N}$  reaction in a gas target attached to the IP2 endstation of the Injector 2 cyclotron at PSI. The  $^{13}\text{NO}$  produced in the gas target is transported to a laboratory where it is mixed, under dry conditions, with non-labeled  $\text{NO}$  and  $\text{O}_3$  in a gas reactor, giving  $^{13}\text{NNO}_5$ . The  $\text{N}_2\text{O}_5$  thus produced is fed into an aerosol flow tube together with a humidified aerosol gas flow. The gaseous species present in the resulting gas flow are selectively separated via a narrow parallel plate diffusion denuder system, while aerosol particles can be trapped on a particle filter placed at the end of the denuder system. The activity of the  $^{13}\text{N}$  labeled species trapped on the denuder plates and in the particle filter can be monitored via scintillation counters.

A system for the routine online production of  $^{13}\text{N}$  labeled  $\text{N}_2\text{O}_5$  has been assembled and used to assess the conformity of the results by kinetic modeling of gas phase  $\text{N}_2\text{O}_5$  chemistry, showing good agreement. A few exemplary experiments of uptake of labelled  $\text{N}_2\text{O}_5$  to ammonium sulfate and citric acid particles are presented that are in good agreement with results obtained with other methods reported in the literature.

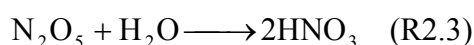
## 2.1. Introduction

During the last two decades the compound  $\text{N}_2\text{O}_5$  has been the topic of many studies in the field of atmospheric chemistry due to its significant role in the nighttime tropospheric  $\text{NO}_x$  chemistry. Its formation starts with oxidation of  $\text{NO}_2$  to  $\text{NO}_3$  radicals by ozone (R2.1) followed by a reaction with  $\text{NO}_2$  that yields  $\text{N}_2\text{O}_5$  (R2.2).



Daytime formation of  $\text{N}_2\text{O}_5$  is inefficient because of the short photolytic lifetime of  $\text{NO}_3$  ( $\sim 1$  s); however, during the night  $\text{N}_2\text{O}_5$  can reach concentrations of up to 10-15 ppb in polluted atmospheres and thus may play an important role in nighttime tropospheric chemistry (Finlayson-Pitts and Pitts, 2000). During nighttime the concentration of  $\text{N}_2\text{O}_5$  (as well as  $\text{NO}_3$  and  $\text{NO}_2$ ) is controlled by the equilibrium established between  $\text{N}_2\text{O}_5$  formation and  $\text{N}_2\text{O}_5$  loss due to thermal decomposition (R2.2).

The importance of  $\text{N}_2\text{O}_5$  stems from its role as a  $\text{NO}_3$  radical reservoir as well as being a major sink for  $\text{NO}_x$  species due to the fast heterogeneous hydrolysis reaction with water molecules (R2.3) on aerosol and ice surfaces (Chang et al., 2011; Wagner et al., 2008).



Particle phase nitric acid formed via this heterogeneous reaction may then be removed from the atmospheric cycle via wet or dry deposition. Due to the equilibrium that exists between  $\text{NO}_2$ ,  $\text{NO}_3$  and  $\text{N}_2\text{O}_5$ , removal of the latter reduces the first two which leads to a reduction of tropospheric ozone, thus lowering the oxidizing capacity of the troposphere (Dentener and Crutzen, 1993; Evans and Jacob, 2005; Finlayson-Pitts and Pitts, 2000).

Because of the impact of  $\text{N}_2\text{O}_5$  on ozone formation and the effect that removal via hydrolysis on aerosol particles has on the overall budget, uptake kinetics of  $\text{N}_2\text{O}_5$  on aerosols have been an important topic of study. The loss rate of  $\text{N}_2\text{O}_5$  to aerosol particles is determined by the available surface area and the efficiency of the gas phase-aerosol interaction process. It is characterized by the uptake coefficient  $\gamma$ , defined as the probability that a gas kinetic collision of a molecule leads to its uptake at the interface. Studies have been conducted on various types of aerosol particles such as NaCl/sea salt aerosols (Thornton and Abbatt, 2005), ammonium sulfate or nitrate particles (Badger et al., 2006; Wagner et al., 2005; Wahner et al., 1998), organic aerosols (Griffiths et al., 2009), mineral dust (Tang et al., 2012; Wagner et al.,

2008) and soot (Karagulian and Rossi, 2007). Various detection methods have been used, Cavity Ring-Down Spectroscopy (CRDS) (Brown et al., 2009) and Chemical Ionization Mass Spectrometry (CIMS) (Gross et al., 2009) have been particularly popular. CRDS is an optical method that uses a dye laser to inject a laser beam between two mirrors of high reflectivity placed in a cavity. The concentration of the analyte is determined by monitoring the decay of the laser intensity within the cavity with time, the decay rate being directly proportional to the species concentration (in this case  $\text{NO}_3$ ). Thermal conversion of  $\text{N}_2\text{O}_5$  to  $\text{NO}_3$  in a second, heated channel provides simultaneous measurements of the sum of  $\text{NO}_3$  and  $\text{N}_2\text{O}_5$ . The method provides very low detection limits (down to the 1-5 pptv range), and allows for parallel measurements of  $\text{NO}_3$  and  $\text{N}_2\text{O}_5$ . It can operate at ambient pressure and is relatively compact and thus suitable for field studies. CIMS is based on a selective ionization process resulting from a reaction between a reagent ion and the analyzed species followed by mass spectrometry of the resulting ions. Also this method is highly sensitive (10 pptv range) and the reagent ion used for  $\text{N}_2\text{O}_5$  studies ( $\text{I}^-$ ) is reasonably specific for either  $\text{NO}_3$  or  $\text{N}_2\text{O}_5$ , ionizing both species to  $\text{NO}_3^-$  detected at 62 amu. The principal drawback of the method is that it cannot differentiate between  $\text{NO}_3$  and  $\text{N}_2\text{O}_5$ , and under typical operating conditions often non negligible background noise at 62 amu appears.

While the above mentioned measurement methods have many advantages, they still present some disadvantages that are non-negligible, such as difficult operation under high relative humidity or the fact that in laboratory studies  $\text{N}_2\text{O}_5$  uptake by aerosol particles can only be derived by following its loss from the gas phase. Instead, we have used the short lived  $^{13}\text{N}$  radioactive tracer technique developed at the Paul Scherrer Institute (Ammann, 2001; Guimbaud et al., 2002). This technique has been used already to study the uptake kinetics of other nitrogen oxides such as  $\text{HNO}_3$  (Vlasenko et al., 2006) and  $\text{NO}_2$  (Sosedova et al., 2009) to aerosols and of  $\text{NO}_y$  to ice surfaces (Bartels-Rausch et al., 2002; Bartels-Rausch et al., 2011; Ulrich et al., 2012), by labeling them with  $^{13}\text{N}$ , a short-lived isotope with a half-life of 10 min.  $^{13}\text{N}$  is well known as a positron emitter and also used in positron emission tomography (PET) for medical purposes (Miller et al., 2008). In our application, we trace uptake in the particulate phase by monitoring the radioactive decay of  $^{13}\text{N}$  labeled  $\text{N}_2\text{O}_5$  absorbed

on aerosol particles while working under realistic ambient temperature and humidity conditions. In this study we will detail the method of production of  $^{13}\text{N}_2\text{O}_5$  and the experimental setup to study the uptake kinetics on aerosol particles as well as report a few exemplary measurements on aerosol particles to benchmark against other methods. To our knowledge this is the first time that  $^{13}\text{N}$  labeled  $\text{N}_2\text{O}_5$  has been produced for experimental purposes.

## 2.2. Experimental

### 2.2.1. General layout of the experiment

Using the short-lived radioactive tracer  $^{13}\text{N}$  allows for the study of heterogeneous kinetics under realistic conditions, and experiments can be performed at very low trace gas concentrations (down to a hundred pptv) and in presence of high relative humidity.  $^{13}\text{N}$  labeled NO is mixed with  $\text{O}_3$  in a first reactor to produce  $^{13}\text{N}_2\text{O}_5$ , which is then fed into an aerosol flow tube where it can be mixed with aerosols to perform heterogeneous kinetics experiments. The resulting flow is then directed into a parallel plate diffusion denuder system where the gaseous and particle phase products can be selectively separated and trapped on coated denuder plates and a particle filter, respectively. By monitoring the decay of  $^{13}\text{N}$  on each trap it is possible to derive simultaneously the concentration of the various  $^{13}\text{N}$  labeled species in the gas and particle phase. Figure 2.1 shows a schematic diagram of our experimental arrangement.

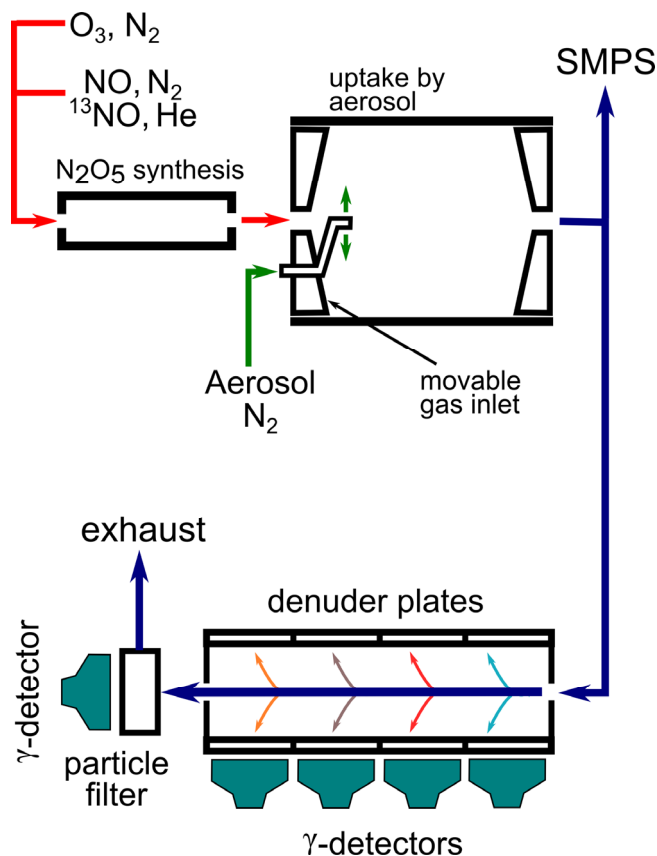


**Fig. 2.1.** Schematic representation of the experimental arrangement.  $\text{N}_2\text{O}_5$  is synthesized in the first reactor. Mixing with aerosol is achieved in an aerosol flow tube with movable inlets which allows to adjust the reaction time. The resulting gas flow is directed into the parallel plate denuder system where 4 sets of plates covered with denuder coatings (citric acid and NDA) are used to selectively separate the gas phase products. The particle phase products are trapped on the particle filter. Gamma detectors are used to monitor the activity of the products. SMPS denotes the scanning mobility particle sizer.

### 2.2.2. Production and transport of $^{13}\text{NO}$

At the Paul Scherrer Institute  $^{13}\text{NO}$  has been produced for the purpose of tracer experiments in atmospheric chemistry since about two decades. A detailed description of the method has been described earlier (Ammann, 2001). Briefly,  $^{13}\text{N}$  is produced via the  $^{16}\text{O}(\text{p}, \alpha)^{13}\text{N}$  reaction in a gas-target by irradiating  $^{16}\text{O}$  with about 11 MeV protons at around  $10 \mu\text{A}$  intensity. Developed from an earlier design (Ammann, 2001), the gas-target is a conically shaped aluminium flow reactor attached to the Isotope Production Station IP2 at a branch of the Injector II cyclotron at PSI. The primary proton beam with an energy of 72 MeV is passed through a first degrader to bring the energy down to 35 MeV. The window into the  $^{13}\text{N}$  target, consisting of two water cooled aluminium windows, is designed such that the energy of the protons at the

entry into the gas volume is further degraded down to about 11 MeV. The further degradation within the gas target depends on pressure, which was kept at 2.5 bar, and a continuous 1 l/min STP flow of 20% O<sub>2</sub> in He (all flow rates are given in volumetric flow normalized to standard temperature and pressure) is passed through the target. This pressure was also constrained by other boundary conditions of our experiments and not adjusted to optimize <sup>13</sup>N production according to the detailed structure of the excitation function for the <sup>16</sup>O(p, α)<sup>13</sup>N reaction (Qaim, 2001; Sajjad et al., 1986). Highly oxidized and reactive forms of nitrogen oxides are produced and chemically converted to <sup>13</sup>NO over a Mo converter (at ~380 °C) connected to the gas-target in order to facilitate transport. As discussed in our earlier study (Ammann, 2001), quantitative <sup>13</sup>N output is difficult to achieve, likely due to chemical losses on surfaces before the Mo converter. Non-labeled nitrogen oxide species (at around 8 ppbv) are also produced from nitrogen impurities in the carrier gas and likewise converted to NO. Only a very small fraction of the overall NO produced contain the tracer atoms (below ppt levels). Additionally, trace amounts of carbon monoxide or carbon dioxide are formed from organic impurities present in the gas feed. The resulting <sup>13</sup>NO containing gas is then continuously transported to the laboratory via a 580 m long PVDF tube (inner diameter 4 mm).

### 2.2.3. Production of <sup>13</sup>N<sub>2</sub>O<sub>5</sub>

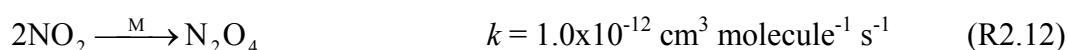
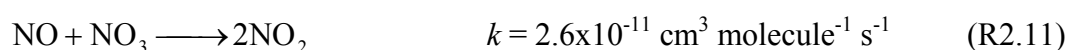
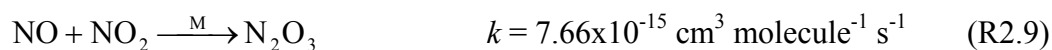
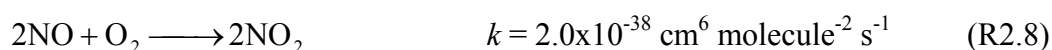
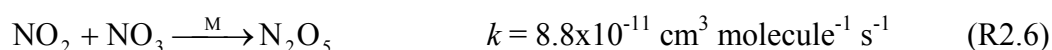
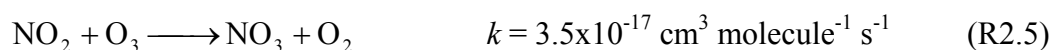
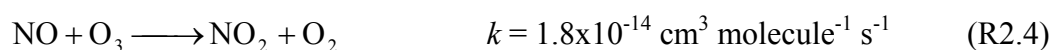
In the laboratory, selected amounts of the target gas flow (typically 50 ml/min) can be mixed with variable amounts of N<sub>2</sub> and certified amounts (1 ml/min) of non-labeled NO from a gas cylinder (10 ppm in N<sub>2</sub>) allowing to cover a wide range of NO concentrations in the ppb range. Possible traces of HONO are removed by using a Na<sub>2</sub>CO<sub>3</sub> trap.

The <sup>13</sup>NO gas flow is directed into the N<sub>2</sub>O<sub>5</sub> reactor where it is mixed with a flow (50 ml/min) containing ozone (~4 ppmv in this reactor) in order to generate <sup>13</sup>N labeled N<sub>2</sub>O<sub>5</sub> via reactions (R2.1) and (R2.2). O<sub>3</sub> is produced by passing a flow of 10 % O<sub>2</sub> in N<sub>2</sub> over a UV lamp (185 nm wavelength). The N<sub>2</sub>O<sub>5</sub> reactor is covered with a shroud in order to prevent NO<sub>3</sub> photolysis and thus loss of N<sub>2</sub>O<sub>5</sub>. Additionally, in order to minimize losses due to heterogeneous hydrolysis on the walls, N<sub>2</sub>O<sub>5</sub> production is conducted under dry conditions, and the walls of the reactor are covered with PTFE

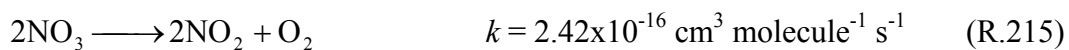
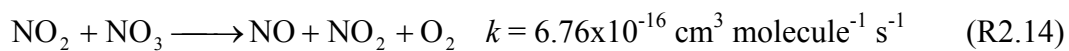
foil. The resulting gas flow (101 ml/min) is then fed into the flow tube reactor, where it is mixed with the aerosol flow (720 ml/min).

#### 2.2.4. Modeling of gas phase $^{13}\text{N}_2\text{O}_5$ production

As a support tool for the design of the experiment and to address issues such as the slow formation of  $\text{N}_2\text{O}_5$  via reactions (R2.4), (R2.1) and (R2.2) versus the radioactive decay of  $^{13}\text{N}$  with a half-life of 10 min, a modeling study of gas phase  $\text{N}_2\text{O}_5$  formation has been carried out. The kinetics was based on the recommendations of the IUPAC Task Group on Atmospheric Chemical Kinetic Data Evaluation (Atkinson et al., 2004) and the NASA Panel for Data Evaluation (Sander et al., 2011). Modeling work has been performed in Matlab using ODE (ordinary differential equation) solvers and using temperature, pressure, time, reactor geometry and starting concentrations for NO and  $\text{O}_3$  as input variables. Wall loss was also incorporated into the model. Overall 12 reactions have been included in the model (R2.4-R2.15). The rate coefficients listed beside the reactions are given at standard temperature and pressure. In the computer model pressure and temperature dependence of the rate coefficients as recommended in the above mentioned data bases has been included.







The model allowed us to analyze the influence of  $\text{O}_3$  and  $\text{NO}$  concentrations on  $\text{N}_2\text{O}_5$  production and its temperature dependence as well as estimating the  $\text{N}_2\text{O}_5/\text{NO}_3$  ratio in the gas phase. The resulting estimates and predictions were used in the experimental design phase to optimize the production of  $\text{N}_2\text{O}_5$  as well as to benchmark our  $\text{N}_2\text{O}_5$  production process to the known gas phase kinetic data.

### 2.2.5. Aerosol generation and characterization

The aerosol was produced by nebulizing a 0.07% (by weight) solution of citric acid (HQ, Fluka, >99%) or of 0.69% wt. solution of ammonium sulfate in MilliQ water by means of an ultrasonic nebulizer. Citric acid was used as a proxy for a generic organic aerosol while ammonium sulfate was chosen because of the wealth of experimental data already available in the literature. The mist droplets formed were dried by passing the flow through a Nafion membrane diffusion dryer. The sheath gas outside the Nafion membrane was humidified such that the resulting aerosol flow had the relative humidity intended for the experiment by avoiding efflorescence of the particles in experiments below the deliquescence relative humidity. In order to avoid uncontrolled losses of charged aerosol particles to the insulating walls of tubing and the aerosol flow reactor, the aerosol flow was passed through a  $^{85}\text{Kr}$  ion source, to establish an equilibrium charge distribution, followed by an electrostatic precipitator removing all charged particles. After that the aerosol flow was fed into the aerosol flow tube.

When aerosol was used in the experiments, measurement of its surface area to gas volume ratio was performed with a Scanning Mobility Particle Sizer (SMPS). This system consists of a homemade  $^{85}\text{Kr}$  source to establish charge equilibrium of the aerosol, a differential mobility analyzer (DMA, TSI 3071) and a condensation particle counter (CPC, TSI 3022). Since the aerosol water content and consequently the particle diameter and aerosol surface to volume ratio strongly depend on relative humidity, filtered carrier gas from the flow tube was used as sheath gas in the DMA in

order to keep the two flows in equilibrium. Aerosol sampling was conducted at an outlet directly behind the aerosol flow tube, where additionally other instruments such as  $\text{NO}_x$  or  $\text{O}_3$  analyzers could be connected as well.

### **2.2.6. Aerosol flow tube**

The aerosol and  $\text{N}_2\text{O}_5$  containing gas flow were mixed together in the cylindrical aerosol flow tube composed of a PFA tube with an inner diameter of 7 cm and a movable inlet and outlet that allow adjusting the length of the aerosol – gas interaction zone and thus the reaction time inside the flow tube. The gas flow is introduced via a conically shaped gas inlet along the axis of the flow tube. The aerosol flow is introduced into the flow tube via a fixed injector which protrudes from the side of the conical inlet. The injector is a 6 mm diameter Inox steel tube bent in such a way that the injector nozzles are equidistant from the reactor walls and the aerosol flow is injected perpendicularly to the gas flow. When the outlet is pushed all the way in to the minimum position inside the flow tube, the reaction time is minimum (~10 s), while pulling the outlet to the maximum position one can achieve a reaction time of 60 s. The flow tube is operated under laminar flow conditions and it is assumed that a laminar flow profile is established a few cm downstream of the aerosol injector. PFA has been chosen in an attempt to minimize  $\text{N}_2\text{O}_5$  losses to the wall. While losses are lower than with a glass tube reactor, they are still substantial when operating under humid conditions.

### **2.2.7. Detection system**

Following the aerosol flow tube, the combined gas flow was directed towards the parallel plate diffusion denuder system. A T-connector was placed between the two in order to allow connecting the SMPS system or a  $\text{NO}_x$  or  $\text{O}_3$  detector. Upon entering the denuder train the gaseous species ( $\text{N}_2\text{O}_5$  and  $\text{NO}_2$ ) are separated on different chemically selective coatings by lateral diffusion. The sub-micron aerosol particles have a small diffusivity and pass through the denuder unobstructed with almost 100% efficiency. Gaseous  $\text{N}_2\text{O}_5$  (and the small amounts of  $\text{NO}_3$  present) was collected on the first set of denuder plates coated with citric acid, prepared from a 2 wt.% solution

in 50% methanol/water. Citric acid has well documented hygroscopic properties (Peng et al., 2001) and mixes well with water, thus facilitating coating preparation. It also forms a solution down to low relative humidity and thus maintains reactivity also in experiments at low relative humidity. The citric acid coating was applied to the first and second denuder plate set; the former to capture  $\text{N}_2\text{O}_5$ , the latter to monitor the interference of  $\text{NO}_2$  on the citric acid coating. The third and fourth sets of denuder plates were coated with NDA (N-(1-naphtyl) ethylene diamine dihydrochloride) mixed with KOH (1% solution with 1% KOH and 10% water in methanol). NDA absorbs  $\text{NO}_2$  very efficiently and the basic coating assures that the nitrite product stays on the surface. Two denuder plate sets with NDA were used, because NDA is sensitive to ozone present in our system and is depleted rapidly, so the second denuder plate is used to extend the available experimental time. Fresh coatings were prepared and applied every day. After passing the denuder system, the aerosol particles were captured by a glass fiber filter.  $^{13}\text{N}$  decay results in the emission of a positron, which, upon annihilation with an electron, results in the coincident emission of two  $\gamma$ -rays in opposite directions. To each trap (the coatings and filter) a separate CsI scintillator crystal with integrated PIN diode detector was attached (Carroll and Ramsey, USA), which detects the gamma quanta emitted after decay of the  $^{13}\text{N}$  atoms. The detector signal is converted to the flux of the gaseous species into the trap using the inversion procedure reported earlier (Guimbaud et al., 2002; Kalberer et al., 1996). This flux is proportional to the concentration of the species in the gas phase. The relative counting efficiency of the various  $\gamma$ -detectors was determined by exposing in turn each of the detectors to a glass fiber filter on which a drop of a  $^{22}\text{NaI}$  solution was deposited, in a way that closely mimics the geometrical configuration at each trap. Additional information about coating preparation, traps and measurement efficiencies can be found elsewhere (Ammann, 2001; Guimbaud et al., 2002).

## 2.3. Results and Discussion

### 2.3.1. Gas phase production of $^{13}\text{N}_2\text{O}_5$

Our experiments dealing with production of  $^{13}\text{N}_2\text{O}_5$  were conducted with a 4 min residence time in the  $\text{N}_2\text{O}_5$  reactor and 1 min residence time in the aerosol flow tube

in order to simulate default operating settings also used for the aerosol experiments reported further below. These settings resulted in an NO concentration of 99 ppbv and an O<sub>3</sub> concentration of ~4 ppmv in the N<sub>2</sub>O<sub>5</sub> reactor. The resulting gas flow was fed into the flow tube, together with the flow from the aerosol gas line. The ultrasonic nebulizer connected to this gas flow line was turned off (and thus no aerosol was generated) since only gas phase kinetics were studied in this step. The humidity inside the aerosol flow tube was kept at ~27% RH (humidified aerosol gas flow). Figure 2.2 shows the resulting N<sub>2</sub>O<sub>5</sub> and NO<sub>2</sub> gas phase signals measured at the parallel plate diffusion denuder system.

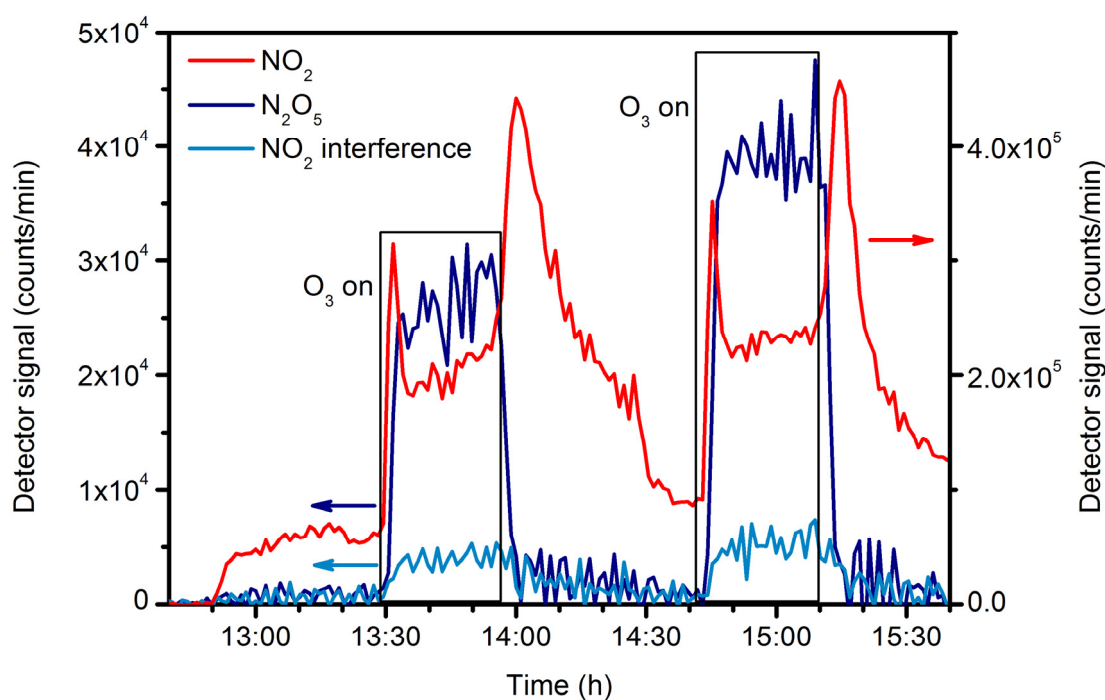


**Fig. 2.2.** Production of gas phase <sup>13</sup>N<sub>2</sub>O<sub>5</sub>: dark blue: first citric acid denuder signal (gas phase N<sub>2</sub>O<sub>5</sub>); light blue: second citric acid denuder signal (NO<sub>2</sub> interference on citric acid denuder); red: NDA denuder signal (gas phase NO<sub>2</sub>)

N<sub>2</sub>O<sub>5</sub> and NO<sub>3</sub> are absorbed on the first denuder plate set coated with citric acid. The second citric acid coated plate set, which is placed after the first, shows the NO<sub>2</sub> interference signal on the citric acid coating. Finally, the NDA coated denuder plate set gives the NO<sub>2</sub> signal. When <sup>13</sup>NO and non-labeled NO were fed into the system (12:46), the activity on all coatings increased. The signals originate from the

background of  $^{13}\text{NO}$  decaying in the gas phase while passing through the denuder system and the filter and from small amounts of  $^{13}\text{NO}_2$  and  $\text{HO}^{13}\text{NO}$  formed along the flow system that were trapped in the first citric acid coating. When  $\text{O}_3$  was turned on for the first time a marked increase of the signal on the first citric acid denuder plate set occurred due to  $\text{N}_2\text{O}_5$  (and  $\text{NO}_3$ , see below) that was formed. The signal derived from the second citric acid plate set shows a modest increase that is due to the  $\text{NO}_2$  interference on the citric acid coating. Lastly, the  $\text{NO}_2$  signal shows a significant increase due to its formation from  $\text{NO}$  and  $\text{O}_3$ . When  $\text{O}_3$  was turned off, the  $\text{N}_2\text{O}_5$  signal dropped rapidly while the other two signals did so gradually. The dynamic response of the  $\text{NO}_2$  signal in between is discussed below. The certified  $\text{NO}$  flow was then doubled to 2 ml/min (14:23, 196 ppbv in  $\text{N}_2\text{O}_5$  reactor) and  $\text{O}_3$  was turned on again. The signals have a behavior similar to the earlier ones, but with an increase in levels that can be attributed to the higher  $\text{NO}$  concentration (see model calculations below). The plotted signals also give some indication of the transient behavior of the gas phase system. In particular, peaks in the  $\text{NO}_2$  signal can be noticed shortly after  $\text{O}_3$  was turned on and off. This is due to the kinetics of the reactions involved and in particular (R2.1), (R2.2) and (R2.4). When  $\text{O}_3$  was turned on we observed the fast titration of  $\text{NO}$  to yield  $\text{NO}_2$  (R2.4). The subsequent reaction of  $\text{NO}_2$  with  $\text{O}_3$  to give  $\text{NO}_3$  (R2.1) is about 3 orders of magnitude slower than (R2.4). As  $\text{NO}_2$  was transformed into  $\text{NO}_3$  the  $\text{NO}_2$  signal diminished until it reached a steady-state level. When  $\text{O}_3$  was turned off, the faster reaction R4 consumed the remaining  $\text{O}_3$  to effectively suppress reaction (R2.1) and thus  $\text{NO}_2$  was no longer converted to  $\text{NO}_3$ . This brought about another increase of the  $\text{NO}_2$  signal before it gradually decreased as the rest of the  $\text{O}_3$  was consumed.

### 2.3.2. Comparison with model

In order to obtain a quantitative value for the  $\text{N}_2\text{O}_5$  signal measured at the parallel plate denuder system we connected a  $\text{NO}_x$  analyzer (ML 9841A) at the T connector behind the aerosol flow tube reactor. In this way we were able to measure the  $\text{NO}_2$  concentration in the system and consequently calculate the  $\text{N}_2\text{O}_5$  concentration in the gas and particle phase from the  $^{13}\text{NO}_2$  and  $^{13}\text{N}_2\text{O}_5$  signals observed on the denuder

plates and particle filter. Thus we were able to calibrate the setup and assign a concentration value to the denuder plate and particle filter signals.

The next step in the process was to evaluate the wall loss in the aerosol flow tube. The wall uptake represents the loss of gas phase  $\text{N}_2\text{O}_5$  due to hydrolysis on the walls of the flow tube. Measurements were performed by varying the flow tube length (residence time) and measuring the gas phase  $\text{N}_2\text{O}_5$  concentration in the reactor at each length. Flow tube lengths from 0 cm (10 seconds) to 20 cm (60 seconds) were evaluated, using the 10 sec position as the starting point as shown in the resulting decay plot (Figure 2.3).

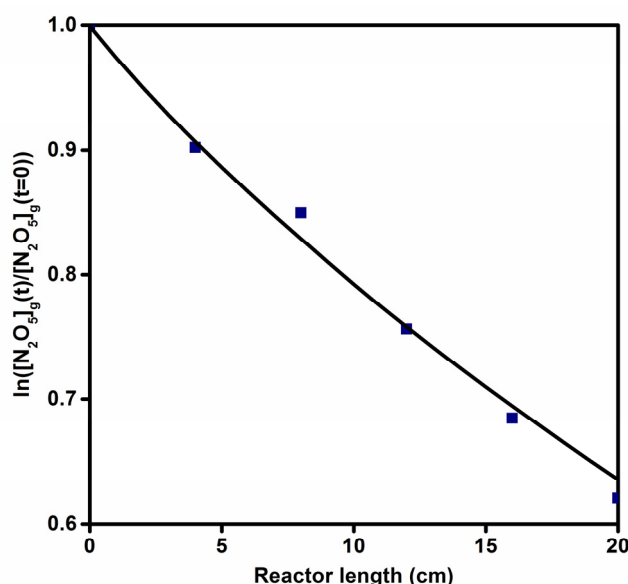


**Fig. 2.3.** Decay plot of  $\text{N}_2\text{O}_5$  vs. reactor length fitted to the measured data using the CKD method

The measured, pseudo-first order loss rate constant  $k_{\text{wall}}$  was determined to be equal to  $9.5 \times 10^{-3} \text{ s}^{-1}$ , giving an effective coefficient of uptake on the wall ( $\gamma_{\text{wall}}$ ) of  $2.8 \times 10^{-6}$ . A correction of the observed uptake rate for diffusion in the gas phase using the Cooney-Kim-Davis (CKD) method was applied (Murphy and Fahey, 1987), which yielded an uptake coefficient of  $3.7 \times 10^{-6}$ .

Finally, a data comparison of  $\text{N}_2\text{O}_5$  formation from  $\text{NO}$  and  $\text{O}_3$  with the model calculation was performed. First, a model calculation was made for the  $\text{N}_2\text{O}_5$  reactor

using the initial NO and O<sub>3</sub> concentrations therein. The resulting gas phase concentrations obtained from the model (Figure 2.4a) were then corrected for dilution by the aerosol flow into the aerosol flow tube. The model calculations were then performed again, this time for the aerosol flow tube, taking into account the experimentally measured  $k_{\text{wall}}$  (Figure 2.4b). Thus the whole experimental system can be accounted for (N<sub>2</sub>O<sub>5</sub> reactor + flow tube reactor) and modeled as a single entity. The experimental results appear in good agreement with the data obtained from model calculations, although the expected concentrations were slightly lower than the measured ones. Note that the slope was constrained by the  $k_{\text{wall}}$  measurement and thus consistency of the modeled slope with the measured slope for N<sub>2</sub>O<sub>5</sub> with time is not surprising. However, the model estimates the absolute concentration level fairly well. The difference between model and measurement is probably at least in part due to the value of  $k_{\text{wall}}$  (and  $\gamma_{\text{wall}}$  respectively) for the N<sub>2</sub>O<sub>5</sub> reactor that we used in the model calculations and that remained an adjustable parameter. It should be noted that, as mentioned in the experimental section, it is not possible to distinguish between N<sub>2</sub>O<sub>5</sub> and NO<sub>3</sub> in the gas phase since both are taken up efficiently on the denuder coating. The contribution of NO<sub>3</sub> to the overall signal depends primarily on temperature, since the decomposition of N<sub>2</sub>O<sub>5</sub> to its precursors is a thermally driven process. At STP the NO<sub>3</sub> concentration is roughly one order of magnitude lower than that of N<sub>2</sub>O<sub>5</sub>. Figure 2.4b shows this contribution.

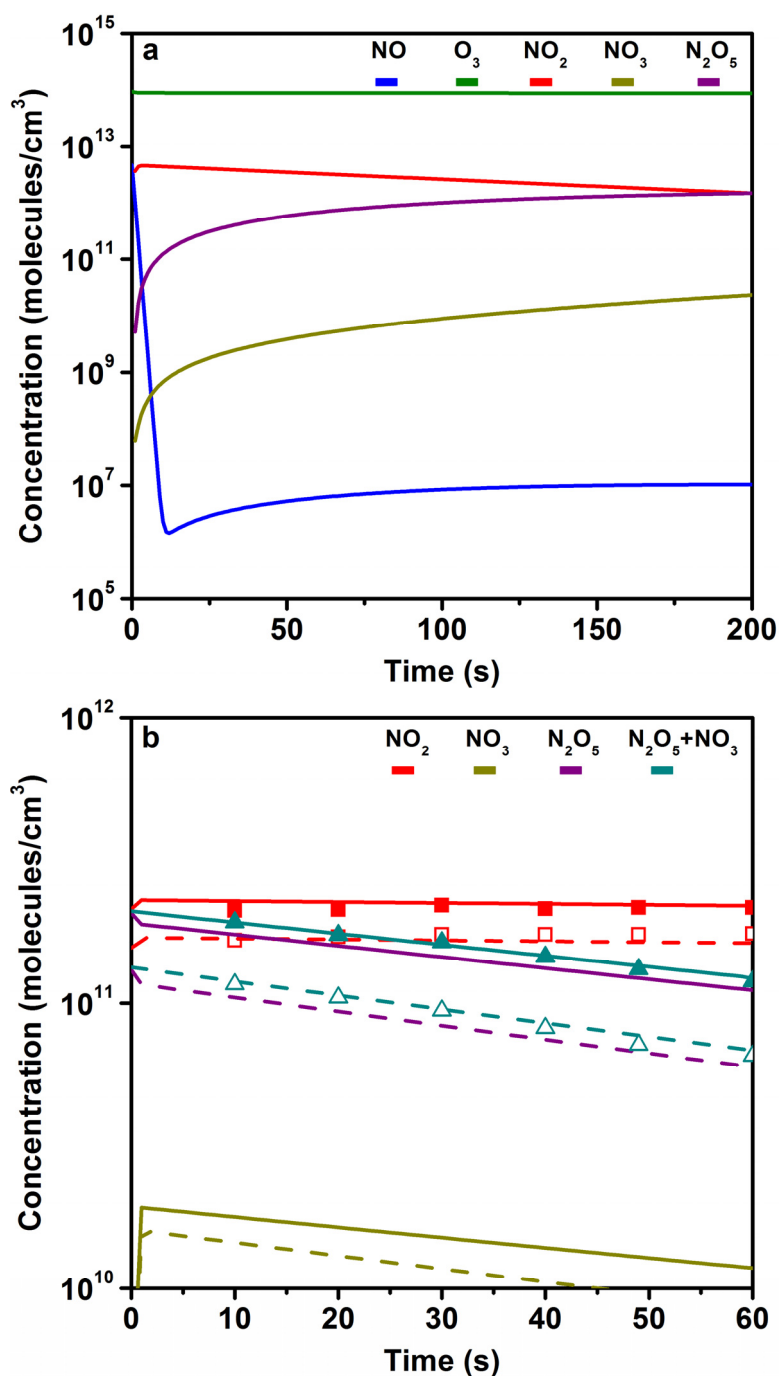


**Fig. 2.4.** Gas phase model graphs: (a) N<sub>2</sub>O<sub>5</sub> reactor with residence time of 195 sec; (b) flow tube reactor with residence time of 60 sec (calculated using the measured  $k_{\text{wall}}$ ). Full lines represent modeled values using 196 ppb initial NO concentration, dashed lines using 148 ppb initial NO concentration. The data points represent measured values using initial NO concentrations of 196 ppb (full points) and 148 ppb (open points).

The uptake coefficient on the wall for the N<sub>2</sub>O<sub>5</sub> reactor was not measured; however, taking into consideration the values obtained for the aerosol flow tube and the fact that N<sub>2</sub>O<sub>5</sub> synthesis is performed under dry conditions, a conservative value in the



range of  $1-5 \times 10^{-7}$  has been assumed by fitting the model to the experimental data. As mentioned above, this has given good results. Changing the value to  $10^{-8}$  gives  $\text{N}_2\text{O}_5$  levels slightly above those measured, while the  $\text{NO}_2$  levels show negligible changes. On the other hand, when using a value of  $10^{-6}$ , the  $\text{N}_2\text{O}_5$  level is lower by roughly a factor of two compared to measured results, while the  $\text{NO}_2$  levels decrease as well, albeit not so strongly. As far as the aerosol flow tube is concerned, increases in  $\gamma_{\text{wall}}$  and  $k_{\text{wall}}$  (for example in cases of higher humidity) bring about a strong drop in  $\text{N}_2\text{O}_5$  levels, while  $\text{NO}_2$  levels show negligible changes.

### 2.3.3. Uptake by aerosol

An exemplary measurement of  $^{13}\text{N}$  labeled  $\text{N}_2\text{O}_5$  uptake by citric acid aerosol particles at 27% relative humidity and a  $\text{N}_2\text{O}_5$  concentration of  $\sim 5$  ppbv is shown in Figure 2.5. When aerosol was fed into the system by switching on the ultrasonic nebulizer, uptake was observed by measuring an increase in activity on the particle filter. At the same time the gas phase  $\text{N}_2\text{O}_5$  signal slightly decreased, corresponding to a drop in gas phase concentration by 0.31 ppbv. However the resulting aerosol signal accounts for only 0.16 ppbv lost from the gas phase. This is the result of the complex interplay of wall loss and uptake by the particles under conditions where the apparent wall loss is larger than the loss to the particles.

By applying the principles of gas-aerosol interaction kinetics (Eq. 2.1), we can analyze the net uptake kinetics from the signal in the aerosol phase and the measured wall loss rate constant in absence of aerosol.

$$\frac{C_p^{(t)}}{C_g^{(t=0)}} = \frac{1 - e^{-(k_w + k_p)t}}{1 + \frac{k_w}{k_p}} \quad (\text{Eq. 2.1})$$

where  $C_g^{(t=0)}$  is the initial gas-phase concentration of  $\text{N}_2\text{O}_5$  at time zero,  $C_p^{(t)}$  is the concentration of  $\text{N}_2\text{O}_5$  in the particulate phase,  $k_p$  is the constant for the heterogeneous reaction between gaseous  $\text{N}_2\text{O}_5$  acid and aerosol particles and  $k_w$  describes the  $\text{N}_2\text{O}_5$

loss to the wall (Guimbaud et al., 2002). The heterogeneous rate constant  $k_p$  is related to the uptake coefficient  $\gamma$  according to Eq. 2.2:

$$\gamma = \frac{4k_p}{S_p \omega} \quad \omega = \sqrt{\frac{8RT}{\pi M}} \quad (\text{E2.2})$$

where  $S_p$  is the aerosol surface to volume ratio,  $\omega$  is the mean thermal velocity of  $\text{N}_2\text{O}_5$ ,  $R$  is the gas constant,  $T$  is the absolute temperature and  $M$  is the molar weight of  $\text{N}_2\text{O}_5$ .

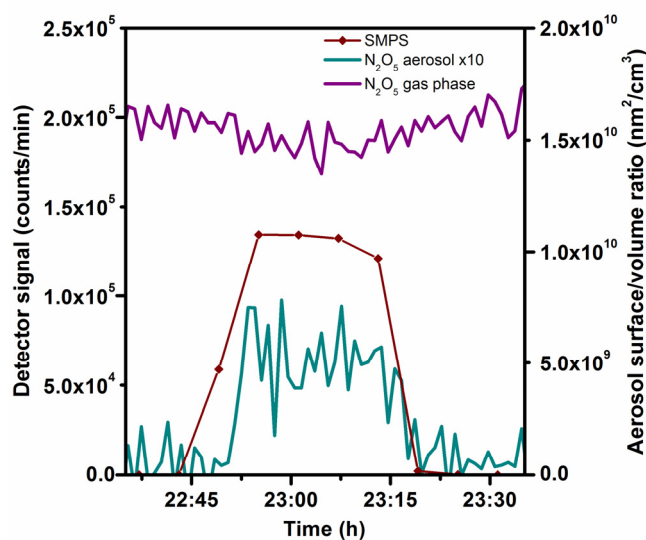


**Fig. 2.5.**  $\text{N}_2\text{O}_5$  interacting with citric acid aerosol (295 K, 26% RH): purple: first citric acid denuder signal (gas phase  $\text{N}_2\text{O}_5$ ); dark yellow: signal from particle filter multiplied by a factor of 10 (particle phase  $\text{N}_2\text{O}_5$  or nitrate); dark red: SMPS signal (aerosol surface/volume ratio)

In the experiments that were conducted, the surface to volume ratio of the aerosol was varied by changing the settings at the ultrasonic nebulizer. From the obtained experimental data the value of the uptake coefficient for citric acid at 27% RH has been estimated at  $1.4 \pm 0.4 \times 10^{-3}$ .

An experiment was also conducted using ammonium sulphate aerosol at 52% relative humidity (Figure 2.6). It becomes immediately apparent that the signal on the

particles scales with the aerosol surface area. Since this experiment has been performed at higher humidity than the one with citric acid shown above, the background signal of  $\text{N}_2\text{O}_5$  in absence of aerosol is lower due to a larger value of  $k_{\text{wall}}$ . Surprisingly, we observe a small but significant increase in the  $\text{N}_2\text{O}_5$  (g) signal in presence of aerosol. The characteristic gas – aerosol separation time in the denuder is about 30 ms per pair of coated plates. Since the time scale for diffusion of a dissolved species through the submicron particles is on the order of microseconds, there is enough time for any dissolved  $\text{N}_2\text{O}_5$  to escape and being trapped. However, we also see a corresponding increase of the signal in the second pair of denuder plates we use for assessing the  $\text{NO}_2$  interference. This indicates that there is also a slow process leading to evaporation of  $\text{N}_2\text{O}_5$ . The fate of dissolved  $\text{N}_2\text{O}_5$  is the disproportionation into  $\text{NO}_2^+$  and  $\text{NO}_3^-$ . It is therefore likely that the slow evaporation of  $\text{N}_2\text{O}_5$  out of the particles over time scales of about 100 ms or more may be limited by the kinetics of the back reaction of  $\text{NO}_2^+$  and  $\text{NO}_3^-$ . There is also the possibility that  $\text{HNO}_3$ , the product of  $\text{N}_2\text{O}_5$  uptake, is evaporating from the particles (Mentel et al., 1999; Wahner et al., 1998). In spite of its strong degree of dissociation, a small amount of undissociated  $\text{HNO}_3$  exists within the particles that remains in equilibrium with the gas phase. However, we would expect that stripping off excess  $\text{HNO}_3$  would only be limited by the time scale of diffusion through the particles, which is on the order of microseconds. The fact that the increase in signal also occurs on the second citric acid coating could thus only result from additional  $\text{HNO}_3$  formed from the reaction of  $\text{NO}_2^+$  with water after passing through the first denuder plate set, the extent of which is in turn again limited by how long  $\text{NO}_2^+$  remains available before being converted back to  $\text{N}_2\text{O}_5$ .

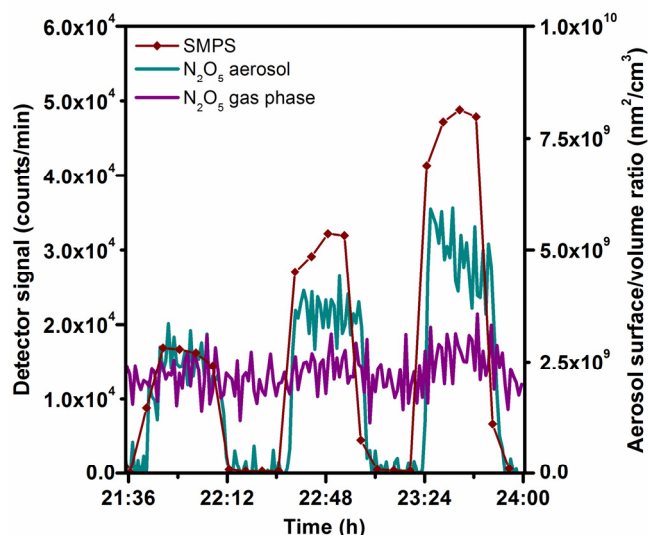


**Fig. 2.6.**  $\text{N}_2\text{O}_5$  interacting with ammonium sulphate particles at different aerosol S/V ratios (295 K, 52% RH): purple: first citric acid denuder signal (gas phase  $\text{N}_2\text{O}_5$ ); dark yellow: signal from particle filter (particle phase  $\text{N}_2\text{O}_5$  or nitrate); dark red: SMPS signal (aerosol surface/volume ratio)

Using the data obtained we calculated the uptake coefficient for ammonium sulphate at 52% RH, which is equal to  $1.45 \pm 0.35 \times 10^{-2}$ . This is in excellent agreement with previously reported results (Ammann et al., 2013).

As can be seen in Fig. 2.6, the particle signal in the case of ammonium sulphate is stronger than in the case of citric acid. This is consistent with the increased water content in ammonium sulphate vs. citric acid aerosol (40 vs. 10 M) as calculated using the Extended AIM Aerosol Thermodynamics Model (Clegg et al., 1998) and a parameterization of the hygroscopic studies of citric acid (Zardini et al., 2008). Assuming that the Henry's Law coefficient ( $H$ ) does not change with the ionic strength of the solution, the increased water content increases the amount of dissolved  $\text{N}_2\text{O}_5$ , and thus also the extent of the reversible disproportionation reaction of dissolved  $\text{N}_2\text{O}_5$  with water to give  $\text{NO}_2^+$  and  $\text{NO}_3^-$  in the aerosol phase. In turn, this leads to an increased extent of reaction of  $\text{NO}_2^+$  with water and thus increased net uptake of  $\text{N}_2\text{O}_5$  from the gas phase.

## 2.4. Conclusions and Outlook

We have produced  $^{13}\text{N}$  labeled  $\text{N}_2\text{O}_5$  for the first time. An experimental setup has been assembled for the study of uptake kinetics of  $\text{N}_2\text{O}_5$  on aerosol particles and has been successfully tested. Gas phase  $\text{N}_2\text{O}_5$  production data has shown good agreement with results obtained with a kinetic model. Measured data has shown that the experimental method also gives insight into the dynamics of the gas phase system. Routine production of  $\text{N}_2\text{O}_5$  in the ppb range has been achieved, allowing for further studies involving  $^{13}\text{N}$  labeled  $\text{N}_2\text{O}_5$ .

Additionally, aerosol uptake experiments were conducted in order to test the experimental setup under realistic conditions. Uptake on citric acid aerosol has been observed and quantified. Uptake on ammonium sulphate aerosol has likewise been observed and an uptake coefficient has been measured that is consistent with that reported in the literature for deliquesced ammonium sulphate. Since the method allows tracing uptake in the particulate phase, this opens the way for further experiments with other types of aerosols at a wider range of humidities as well as temperatures. Of particular interest would be the possibility to monitor the exchange with the particulate nitrate pool in nitrate aerosols.

Overall the study has shown the viability of the proposed method to produce  $^{13}\text{N}$  labeled  $\text{N}_2\text{O}_5$  for atmospheric science related experimental studies, and in particular the assembled setup and the related operating procedures will be used in future studies of  $\text{N}_2\text{O}_5$  uptake kinetics on aerosol particles.

*Acknowledgements.* The authors would like to thank the staff of the PSI accelerator facilities and of the isotope production facility IP-2 for their invaluable help. This work is supported by the Swiss National Science Foundation (grant no. 130175).

## References

- Ammann, M.: Using  $^{13}\text{N}$  as tracer in heterogeneous atmospheric chemistry experiments, *Radiochim. Acta*, 89, 831-838, 2001.
- Ammann, M., Cox, R. A., Crowley, J. N., Jenkin, M. E., Mellouki, A., Rossi, M. J., Troe, J., and Wallington, T. J.: Evaluated kinetic and photochemical data for atmospheric chemistry: Volume VI - Heterogeneous reactions with liquid substrates, *Atmos. Chem. Phys.*, 13, 8045-8228, 2013.
- Atkinson, R., Baulch, D. L., Cox, R. A., Crowley, J. N., Hampson, R. F., Hynes, R. G., Jenkin, M. E., Rossi, M. J., and Troe, J.: Evaluated kinetic and photochemical data for atmospheric chemistry: Volume I - gas phase reactions of Ox, HOx, NOx and SOx species, *Atmos. Chem. Phys.*, 4, 1461-1738, 2004.
- Badger, C. L., Griffiths, P. T., George, I., Abbatt, J. P. D., and Cox, R. A.: Reactive uptake of  $\text{N}_2\text{O}_5$  by aerosol particles containing mixtures of humic acid and ammonium sulfate, *Journal of Physical Chemistry A*, 110, 6986-6994, 2006.
- Bartels-Rausch, T., Eichler, B., Zimmermann, P., Gaggeler, H. W., and Ammann, M.: The adsorption of nitrogen oxides on crystalline ice, *Atmos. Chem. Phys.*, 2, 235-247, 2002.
- Bartels-Rausch, T., Ulrich, T., Huthwelker, T., and Ammann, M.: A novel synthesis of the N-13 labeled atmospheric trace gas peroxyntic acid, *Radiochimica Acta*, 99, 285-292, 2011.
- Brown, S. S., Dube, W. P., Fuchs, H., Ryerson, T. B., Wollny, A. G., Brock, C. A., Bahreini, R., Middlebrook, A. M., Neuman, J. A., Atlas, E., Roberts, J. M., Osthoff, H. D., Trainer, M., Fehsenfeld, F. C., and Ravishankara, A. R.: Reactive uptake coefficients for  $\text{N}_2\text{O}_5$  determined from aircraft measurements during the Second Texas Air Quality Study: comparison to current model parameterizations, *J. Geophys. Res.-Atmos.*, 114, D00F10, 2009.
- Chang, W. L., Bhave, P. V., Brown, S. S., Riemer, N., Stutz, J., and Dabdub, D.: Heterogeneous Atmospheric Chemistry, Ambient Measurements, and Model Calculations of  $\text{N}(\text{2})\text{O}(\text{5})$ : A Review, *Aerosol Sci. Technol.*, 45, 665-695, 2011.
- Clegg, S. L., Brimblecombe, P., and Wexler, A. S.: Thermodynamic model of the system  $\text{H}^+ - \text{NH}_4^+ - \text{SO}_4^{2-} - \text{NO}_3^- - \text{H}_2\text{O}$  at tropospheric temperatures, *J. Phys. Chem. A*, 102, 2137-2154, 1998.
- Dentener, F. J. and Crutzen, P. J.: Reaction of  $\text{N}_2\text{O}_5$  on tropospheric aerosols: Impact on the global distributions of  $\text{NO}_x$ ,  $\text{O}_3$ , and OH, *Journal of Geophysical Research: Atmospheres*, 98, 7149-7163, 1993.
- Evans, M. J. and Jacob, D. J.: Impact of new laboratory studies of  $\text{N}_2\text{O}_5$  hydrolysis on global model budgets of tropospheric nitrogen oxides, ozone and OH, *Geophys. Res. Lett.*, 32, L09813, 2005.

Finlayson-Pitts, B. J. and Pitts, J. N., Jr.: Chemistry of the upper and lower atmosphere, Academic Press, San Diego, CA, 2000.

Griffiths, P. T., Badger, C. L., Cox, R. A., Folkers, M., Henk, H. H., and Mentel, T. F.: Reactive uptake of N<sub>2</sub>O<sub>5</sub> by aerosols containing dicarboxylic acids. effect of particle phase, composition, and nitrate content, *J. Phys. Chem. A*, 113, 5082-5090, 2009.

Gross, S., Iannone, R., Xiao, S., and Bertram, A. K.: Reactive uptake studies of NO<sub>3</sub> and N<sub>2</sub>O<sub>5</sub> on alkenoic acid, alkanolate, and polyalcohol substrates to probe nighttime aerosol chemistry, *Physical Chemistry Chemical Physics*, 11, 7792-7803, 2009.

Guimbaud, C., Arens, F., Gutzwiller, L., Gaggeler, H. W., and Ammann, M.: Uptake of HNO<sub>3</sub> to deliquescent sea-salt particles: a study using the short-lived radioactive isotope tracer N-13, *Atmospheric Chemistry and Physics*, 2, 249-257, 2002.

Kalberer, M., Tabor, K., Ammann, M., Parrat, Y., Weingartner, E., Piguet, D., Rössler, E., Jost, D. T., Turler, A., Gaggeler, H. W., and Baltensperger, U.: Heterogeneous chemical processing of (NO<sub>2</sub>)-N-13 by monodisperse carbon aerosols at very low concentrations, *J. Phys. Chem.*, 100, 15487-15493, 1996.

Karagulian, F. and Rossi, M. J.: Heterogeneous chemistry of the NO<sub>3</sub> free radical and N<sub>2</sub>O<sub>5</sub> on decane flame soot at ambient temperature: Reaction products and kinetics, *Journal of Physical Chemistry A*, 111, 1914-1926, 2007.

Mentel, T. F., Sohn, M., and Wahner, A.: Nitrate effect in the heterogeneous hydrolysis of dinitrogen pentoxide on aqueous aerosols, *Physical Chemistry Chemical Physics*, 1, 5451-5457, 1999.

Miller, P. W., Long, N. J., Vilar, R., and Gee, A. D.: Synthesis of C-11, F-18, O-15, and N-13 Radiolabels for Positron Emission Tomography, *Angew. Chem.-Int. Edit.*, 47, 8998-9033, 2008.

Murphy, D. M. and Fahey, D. W.: Mathematical treatment of the wall loss of a trace species in denuder and catalytic-converter tubes, *Anal. Chem.*, 59, 2753-2759, 1987.

Peng, C., Chan, M. N., and Chan, C. K.: The hygroscopic properties of dicarboxylic and multifunctional acids: Measurements and UNIFAC predictions, *Environmental Science & Technology*, 35, 4495-4501, 2001.

Qaim, S. M.: Nuclear data relevant to the production and application of diagnostic radionuclides, *Radiochim. Acta*, 89, 223-232, 2001.

Sajjad, M., Lambrecht, R. M., and Wolf, A. P.: Cyclotron isotopes and radiopharmaceuticals .37. Excitation-functions for the O-16(p,α)N-13 and N-14(p,pn)N-13 reactions, *Radiochim. Acta*, 39, 165-168, 1986.

Sander, S. P., Abbatt, J., Barker, J. R., Burkholder, J. B., Friedl, R. R., Golden, D. M., Huie, R. E., Kolb, C. E., M. J. Kurylo, G., Moortgat, K., Orkin, V. L., and Wine, P. H.: Chemical kinetics and photochemical data for use in atmospheric studies, Evaluation no. 17, JPL Publication, Jet Propulsion Laboratory, Pasadena, USA, 10, 2011.

Sosedova, Y., Rouvière, A., Gäggeler, H. W., and Ammann, M.: Uptake of NO<sub>2</sub> to deliquesced dihydroxybenzoate aerosol particles, *The Journal of Physical Chemistry A*, 113, 10979–10987, 2009.

Tang, M. J., Thieser, J., Schuster, G., and Crowley, J. N.: Kinetics and mechanism of the heterogeneous reaction of N<sub>2</sub>O<sub>5</sub> with mineral dust particles, *Physical Chemistry Chemical Physics*, 14, 8551-8561, 2012.

Thornton, J. A. and Abbatt, J. P. D.: N<sub>2</sub>O<sub>5</sub> reaction on submicron sea salt aerosol: Kinetics, products, and the effect of surface active organics, *Journal of Physical Chemistry A*, 109, 10004-10012, 2005.

Ulrich, T., Ammann, M., Leutwyler, S., and Bartels-Rausch, T.: The adsorption of peroxyntic acid on ice between 230 K and 253 K, *Atmospheric Chemistry and Physics*, 12, 1833-1845, 2012.

Vlasenko, A., Sjogren, S., Weingartner, E., Stemmler, K., Gäggeler, H. W., and Ammann, M.: Effect of humidity on nitric acid uptake to mineral dust aerosol particles, *Atmospheric Chemistry and Physics*, 6, 2147-2160, 2006.

Wagner, C., Hanisch, F., Holmes, N., de Coninck, H., Schuster, G., and Crowley, J. N.: The interaction of N<sub>2</sub>O<sub>5</sub> with mineral dust: aerosol flow tube and Knudsen reactor studies, *Atmospheric Chemistry and Physics*, 8, 91-109, 2008.

Wagner, R., Naumann, K. H., Mangold, A., Mohler, O., Saathoff, H., and Schurath, U.: Aerosol chamber study of optical constants and N<sub>2</sub>O<sub>5</sub> uptake on supercooled H<sub>2</sub>SO<sub>4</sub>/H<sub>2</sub>O/HNO<sub>3</sub> solution droplets at polar stratospheric cloud temperatures, *J. Phys. Chem. A*, 109, 8140-8148, 2005.

Wahner, A., Mentel, T. F., Sohn, M., and Stier, J.: Heterogeneous reaction of N<sub>2</sub>O<sub>5</sub> on sodium nitrate aerosol, *Journal of Geophysical Research-Atmospheres*, 103, 31103-31112, 1998.

Zardini, A. A., Sjogren, S., Marcolli, C., Krieger, U. K., Gysel, M., Weingartner, E., Baltensperger, U., and Peter, T.: A combined particle trap/HTDMA hygroscopicity study of mixed inorganic/organic aerosol particles, *Atmospheric Chemistry and Physics*, 8, 5589-5601, 2008.



## Chapter 3

### 3. Humidity Dependence of N<sub>2</sub>O<sub>5</sub> Uptake on Citric Acid Aerosol

Goran Gržinić<sup>1,2</sup>, Thorsten Bartels-Rausch<sup>1</sup>, Andreas Türler<sup>1,2</sup> and Markus Ammann<sup>2</sup>

To be submitted to *Atmospheric Chemistry and Physics*

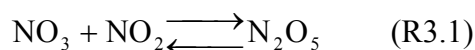
---

<sup>1</sup> Laboratory of Radiochemistry and Environmental Chemistry, Paul Scherrer Institute, 5232 Villigen, Switzerland

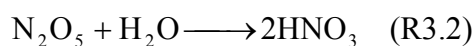
<sup>2</sup> Department of Chemistry and Biochemistry, University of Bern, 3012 Bern, Switzerland

### 3.1. Introduction

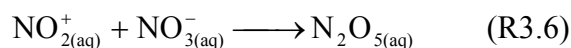
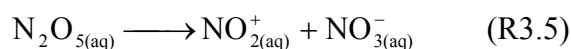
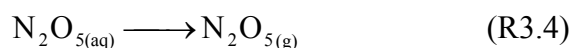
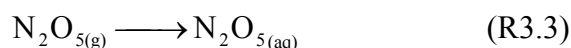
Nitrogen oxides play an important role in the chemistry of the troposphere. Together with methane, carbon monoxide and volatile organic compounds (VOCs) they drive the photochemistry of OH radicals and O<sub>3</sub> production. Besides their daytime activity, nitrogen oxides are also a major part of nighttime oxidation chemistry. In particular, dinitrogen pentoxide has been recognized as a topic of considerable interest (Abbatt et al., 2012; Chang et al., 2011). NO<sub>2</sub> reacts with O<sub>3</sub> to give NO<sub>3</sub>. N<sub>2</sub>O<sub>5</sub> is formed via reaction (R3.1).



The concentrations of N<sub>2</sub>O<sub>5</sub>, NO<sub>3</sub> and NO<sub>2</sub> are controlled by the rapid equilibrium established between the reactions of N<sub>2</sub>O<sub>5</sub> formation and N<sub>2</sub>O<sub>5</sub> loss due to thermal decomposition. N<sub>2</sub>O<sub>5</sub> hydrolyzes readily on aerosol surfaces, to give HNO<sub>3</sub> (R3.2).



The detailed reaction mechanism of heterogeneous uptake of N<sub>2</sub>O<sub>5</sub> on aerosol particles is complex and has been a topic of increasing interest (Hallquist et al., 2003; Mozurkewich and Calvert, 1988; Wahner et al., 1998). The suggested elementary steps of the mechanism are:





An essential aspect of the mechanism is that a reversible disproportionation (R3.5/R3.6) precedes the actual reaction of the nitronium ion  $\text{NO}_2^+$  with water (R3.7). In case of nitrate being present in the particle phase there is a considerable reduction of the uptake thanks to reaction R3.6 (Mentel et al., 1999). The aqueous  $\text{HNO}_3$  formed in reaction R3.7 can either deprotonate contributing additional nitrate to the particle pool or evaporate from the particle, according to its volatility and acid-base chemistry with other solutes in the system (Laskin et al., 2012). Water plays an important role in the mechanism, not only for solvation of  $\text{N}_2\text{O}_5$  and hydration of the nitronium ion, process but is also the main reaction partner of the nitronium ion in absence of other nucleophiles.

$\text{N}_2\text{O}_5$  acts as a sink for atmospheric  $\text{NO}_x$  species, removing them via heterogeneous hydrolysis on aerosols and therefore significantly impacting ozone production and in general the oxidative capacity of the atmosphere. Because of this,  $\text{N}_2\text{O}_5$  uptake kinetics on aerosols has been an important research topic. The loss of  $\text{N}_2\text{O}_5$  from the gas phase to aerosol particles is characterized by the uptake coefficient  $\gamma$ , which represents the probability that a gas kinetic collision of a  $\text{N}_2\text{O}_5$  molecule leads to its uptake at the interface compared to the overall collisional flux to the interface. Dentener and Crutzen, by taking an estimate of  $\gamma=0.1$  on sulfate aerosol (based on measurements by Hanson and Ravishankara (1991), Mozurkewich and Calvert (1988) and Vandoren et al. (1991)) demonstrated the impact of  $\text{N}_2\text{O}_5$  on  $\text{NO}_x$ , OH, and  $\text{O}_3$  global budgets (Dentener and Crutzen, 1993). These estimates have spurred further experimental studies to determine uptake coefficients for a wide variety of aerosols. Extensive studies on inorganic aerosols have shown that the primary factors influencing the uptake coefficient in the range of 0.0001 to 0.05 would be relative humidity (RH), phase, particle size and composition (Abbatt et al., 2012; Davis et al., 2008; George et al., 1994; Hallquist et al., 2003; Hu and Abbatt, 1997; Karagulian et al., 2006; Wahner et al., 1998). Additionally, supersaturated liquid particles have shown uptake coefficients up to 1-2 orders of magnitude higher than corresponding solid particles at the same RH, pointing to the importance of the hydrolysis reaction of  $\text{N}_2\text{O}_5$  with the water present in the aerosol (Hallquist et al., 2003; Thornton and Abbatt, 2005).

The more recent recognition of the importance and pervasiveness of organic materials in aerosols has prompted  $\text{N}_2\text{O}_5$  uptake studies on various types of organic and mixed inorganic and organic aerosol particles (Anttila et al., 2006; Gaston et al., 2014; Griffiths et al., 2009; Gross et al., 2009; Thornton et al., 2003). Hygroscopicity and thus the water content of the organic aerosol component is an important factor in the kinetics of  $\text{N}_2\text{O}_5$  uptake on organic aerosols. Hydrophobic organics do not necessarily deliquesce but may rather form organic surface films or phase separated liquid coatings and thereby may suppress  $\gamma$  for  $\text{N}_2\text{O}_5$  significantly compared to pure inorganic aerosols (Badger et al., 2006; Riemer et al., 2009; Thornton and Abbatt, 2005). Hygroscopic organics, due to their high water content, show values that in some cases approach those for inorganic aerosols (Griffiths et al., 2009; Thornton et al., 2003).

Several studies have been conducted analyzing the dependence of the uptake coefficient of  $\text{N}_2\text{O}_5$  on hygroscopic organic aerosols (in solid and deliquesced form) on the relative humidity (RH), mainly on polycarboxylic acids. Thornton et al. (2003) have analyzed the uptake of  $\text{N}_2\text{O}_5$  on deliquesced malonic acid aerosol in a range of 10-70% RH, noting that at RH below 50% the uptake seems to depend in an almost linear way on the water content, while at higher RH the dependence on water content is lost, probably due to bulk accommodation limitations. Griffiths et al. have studied the humidity dependence for several dicarboxylic acids (Griffiths et al., 2009). The observed uptake coefficients for malonic acid were lower than those from Thornton et al, which was attributed to the nitrate effect that suppresses uptake by increasing the rate of reaction (R6); nitrate in these experiments would come from  $\text{N}_2\text{O}_5$  being taken up into the particles during the residence time of the particles in the flow reactor used. The uptake rates for succinic and glutaric acid were about one order of magnitude lower than those for malonic acid. Both the data for malonic acid as well as those for other dicarboxylic acids show a dependence on the water content at RH <50%, indicating that uptake is limited by the rate of hydrolysis of  $\text{N}_2\text{O}_5$  in the bulk. Badger et al. (2006) have found similar behavior for humic acid aerosol, although with uptake coefficients significantly lower than for the previous compounds. Formation of a surface organic layer has been suggested as a possible explanation for this observation. In addition, the physical state of humic acid at low relative humidity is not well established.

Organic aerosols account for a significant fraction of atmospheric particulate mass (Kanakidou et al., 2005). However there are still significant gaps in our knowledge regarding the chemistry and physical state of organic aerosols, which leads to significant discrepancies between atmospheric model predictions and field results (De Gouw and Jimenez, 2009; Kanakidou et al., 2005; Zhang et al., 2007). Recent studies have shown that the previous assumptions of low-viscosity, well mixed aerosol phases are incorrect and that organic aerosols are frequently present in the semi-solid form, with high viscosity and corresponding low diffusivity (Abramson et al., 2013; Renbaum-Wolff et al., 2013; Vaden et al., 2011). Field measurements (Bertram et al., 2009; Brown et al., 2009) have shown that the observed reactivity of  $\text{N}_2\text{O}_5$  on organic containing aerosol particles can be up to a factor of 10 lower than the values predicted by model parameterizations, which are based on laboratory measurements on conventionally used organic compounds like malonic acid.

In this study we have investigated the uptake of  $\text{N}_2\text{O}_5$  on citric acid aerosol using the short-lived  $^{13}\text{N}$  radioactive tracer technique developed at the Paul Scherrer Institute (Ammann, 2001; Gržinić et al., 2014). This technique has been used to study the uptake of various types of nitrogen oxides, like  $\text{HNO}_3$  (Guimbaud et al., 2002; Vlasenko et al., 2009),  $\text{NO}_2$  (Sosedova et al., 2009) or HONO (Gutzwiller et al., 2002) on aerosol surfaces, or on ice (Bartels-Rausch et al., 2011). Citric acid was used as a proxy for highly oxidized organic species found in secondary organic aerosol (SOA). It has well-known thermodynamic properties and new studies on viscosity and water diffusivity in citric acid have recently become available (Lienhard et al., 2012; Lienhard et al., 2014). In our study, measurements were conducted over a wide range of RH and several parameterization methods have been used to describe the correlation between uptake and humidity.

### **3.2. Experimental**

The experimental method used in this study has been described in detail in our previous publication relating to the production and use of  $^{13}\text{N}$  labeled  $\text{N}_2\text{O}_5$  (Gržinić et al., 2014).  $\text{N}_2\text{O}_5$  labeled with the  $^{13}\text{N}$  short-lived radioactive isotope is mixed with citric acid aerosol in an aerosol flow tube. The resulting gas and aerosol phase products are selectively separated and trapped in a parallel plate diffusion denuder

system and a particle filter, respectively, situated downstream of the aerosol flow tube. The concentration of the various species can be measured simultaneously by monitoring the radioactive decay of the  $^{13}\text{N}$  labeled species on each trap over time. A schematic representation of our experimental setup can be seen found in Gržinić et al. (2014).

### 3.2.1. Production of $^{13}\text{N}$ labeled $\text{N}_2\text{O}_5$

A facility for the online production of  $^{13}\text{NO}$  has been operating at the Paul Scherrer Institute for many years. A detailed description of the facility and recent upgrades can be found elsewhere (Ammann, 2001; Gržinić et al., 2014). In short,  $^{13}\text{N}$  ( $T_{1/2} \approx 10$  min.) is produced in a gas-target via the  $^{16}\text{O}(p,\alpha)^{13}\text{N}$  reaction. The highly oxidized  $^{13}\text{N}$  labeled nitrogen species, along with non-labeled nitrogen oxides produced by the radiation chemistry from nitrogen impurities in the carrier gas ( $\sim 10$  ppbv), are reduced to  $^{13}\text{NO}$  over a Mo converter (at  $\sim 380$  °C) and transported from the production site to the laboratory through a 580 m long PVDF capillary tube. A small amount of the  $^{13}\text{NO}$  containing gas flow (50 ml/min) is mixed with nitrogen carrier gas and non-labeled NO ( $\sim 2$  ml/min) from a certified gas cylinder (10 ppm in  $\text{N}_2$ ). A  $\sim 8$  ppmv  $\text{O}_3$  containing gas flow (50 ml/min) is produced by irradiating a 10%  $\text{O}_2$  in  $\text{N}_2$  gas mixture with 185nm UV light in a cylindrical photolysis reactor. The  $^{13}\text{NO}$  and  $\text{O}_3$  flows are mixed in the  $\text{N}_2\text{O}_5$  synthesis reactor, where NO reacts with  $\text{O}_3$  to produce  $\text{NO}_2$  and  $\text{NO}_3$  which then react via reaction (R3.1) to form  $\text{N}_2\text{O}_5$ . The reactor is covered with a thin PTFE foil on the inside walls and is operated under dry conditions in order to minimize heterogeneous  $\text{N}_2\text{O}_5$  losses. Furthermore, the  $\text{N}_2\text{O}_5$  reactor is covered with a dark cloth shroud to prevent  $\text{NO}_3$  photolysis by laboratory room light which would lead to loss of  $\text{N}_2\text{O}_5$  because of the backwards reaction in (R3.1). The length of the synthesis reactor is 34 cm and the inner diameter is 4 cm, and the gas residence time (reaction time) is  $\sim 4$  min.

Design, performance and consistency of  $\text{N}_2\text{O}_5$  production with simulations obtained via a kinetic model has been described previously (Gržinić et al., 2014).

### 3.2.2. Aerosol production

An ultrasonic nebulizer was used to generate an aerosol suspension in a gas flow by nebulizing a 0.07% wt. solution of citric acid (HQ, Fluka, >99%) in MilliQ water. The resulting aerosol particles were dried over a Nafion membrane diffusion drier. To avoid efflorescence of the aerosol particles, the sheath gas used in the diffusion drier has been humidified. The resulting aerosol gas flow was passed through a homemade  $^{85}\text{Kr}$  bipolar ion source where an equilibrium charge distribution of the aerosol is attained, followed by an electrostatic precipitator to remove all charged particles. This was done to avoid uncontrollable wall losses of charged particles which are produced when nebulizing a solution. A homemade Gore-tex membrane humidifier was placed behind the precipitator for finer adjustments of the humidity in the gas flow and to bring it to the required experimental RH level, followed by an elution volume with a residence time of  $\sim 2$  min to facilitate equilibration between the gas and aerosol phases. In our case measurements were conducted from 17% to 70.3% RH. Finally the aerosol flow was directed into the aerosol flow tube.

A Scanning Mobility Particle Sizer (SMPS) was used to measure the aerosol surface to volume ratio. The SMPS system is made of an  $^{85}\text{Kr}$  ion source (to establish equilibrium charge distribution), a Differential Mobility Analyzer (DMA, TSI 3071) and a Condensation Particle Counter (CPC, TSI 3022). Filtered carrier gas was used as sheath gas for the DMA in order to keep the relative humidity of the two flows at the same level and thus maintain the water content of the particles during size separation. The SMPS was connected immediately after the aerosol flow tube via a T-connector. Alternatively a  $\text{NO}_x$  or  $\text{O}_3$  analyzer could be connected there instead for routine checks of the levels of these gases. A capacitance humidity sensor was placed in front of the SMPS to monitor humidity.

### 3.2.3. Aerosol flow tube

The gas flows containing aerosol and  $\text{N}_2\text{O}_5$ , respectively, were mixed in a cylindrical flow tube reactor consisting of a PFA tube with an inner diameter of 7 cm. The inlet and outlet, cylindrical in shape with an inverse cone projecting inside the cylinder, each have a pneumatic ring on the outer surface which when inflated seals the reactor. By deflating the pneumatic ring it is possible to move the inlet and outlet in order to

adjust the length of the reactor and thus the aerosol reaction time. The  $\text{N}_2\text{O}_5$  gas flow (102 ml/min) is introduced into the aerosol flow tube via a hole along the axis of the reactor. The aerosol feed (720 ml/min) is introduced via a stainless-steel tubular injector (6 mm in diameter) which protrudes from the inlet and is bent in such a way that the injector nozzle is equidistant from the walls of the flow tube. The aerosol flow is injected perpendicularly to the  $\text{N}_2\text{O}_5$  gas flow within the flow tube. Reaction times from 10 to 60 seconds were adjusted. For the flow rate used, a laminar flow profile is assumed to have been established within the flow tube a few cm downstream of the aerosol injector. As with the  $\text{N}_2\text{O}_5$  synthesis reactor, a black shroud is used to shield the aerosol flow tube from daylight in order to prevent  $\text{NO}_3$  photolysis and thus loss of  $\text{N}_2\text{O}_5$ . The overall system exhaust is pressure controlled and the pressure is set at slightly below ambient pressure (960-970 mbar).

#### **3.2.4. Separation and detection of $^{13}\text{N}$ labeled species**

The gas flow resulting from the aerosol flow tube is split with one fraction going to the SMPS system or alternatively a  $\text{NO}_x$  (Teledyne T200) or  $\text{O}_3$  analyzer (ML 9810) and the other being directed into the parallel plate diffusion denuder system. This system consists of a series of parallel plates placed within an aluminium housing. The plates, which are coated with specific coatings, trap the  $^{13}\text{N}$  containing gaseous species ( $\text{N}_2\text{O}_5$ ,  $\text{NO}_3$  and  $\text{NO}_2$ ) by lateral diffusion and chemical reaction. Meanwhile, the aerosol particles, which have small diffusivity, pass through the denuder without being trapped and are deposited on a glass fiber filter located at the exit of the denuder system. Citric acid has been used as a denuder coating for  $\text{N}_2\text{O}_5$ . It mixes well with water and has a well-known hygroscopic cycle (Peng et al., 2001; Zardini et al., 2008), facilitating coating preparation and use, while at the same time being only weakly affected by  $\text{NO}_2$  interference. Citric acid was used as a coating on the first two denuder plates, the first one capturing  $\text{N}_2\text{O}_5$  while the second one is used to quantify the  $\text{NO}_2$  interference.  $\text{NO}_3$ , which is present in small quantities in the gas phase, cannot be easily separated from  $\text{N}_2\text{O}_5$  and is likewise absorbed on the first denuder plate together with  $\text{N}_2\text{O}_5$ . The citric acid solution used was a 2 % (by wt) solution in a 50% mix of water/methanol. The following two denuders were coated with a 1% N-(1-naphthyl) ethylene diamine dihydrochloride (NDA) solution in 1% KOH and 10%



water in methanol. NDA absorbs NO<sub>2</sub> very well while at the same time the basic nature of the solution prevents the re-evaporation of nitrite. Since NDA is sensitive to O<sub>3</sub>, which is present in high concentrations in our system, two denuder plate sets were used to extend the operating life. Fresh coatings were prepared and applied every day. Since N<sub>2</sub>O<sub>5</sub> and NO<sub>3</sub> are quite sticky, absorption of these species was noticed on the aluminium inlet of the parallel plate diffusion denuder system. This inlet is 10 cm long, non-coated and triangular in shape and thus an additional gamma detector was added to measure the N<sub>2</sub>O<sub>5</sub> signal on the inlet.

The <sup>13</sup>N containing species that were trapped on the denuder plates and particle filter were measured by monitoring the radioactive decay of <sup>13</sup>N. A CsI scintillator crystal with integrated PIN diode detector (Carroll and Ramsey, USA) was placed on each of the traps. <sup>13</sup>N, a well-known β<sup>+</sup> emitter, decays with emission of a positron which, upon annihilation with an electron, emits two coincident γ-rays in opposite directions. These γ-rays are detected by the above mentioned gamma-ray detectors and the signal is converted to the flux of the <sup>13</sup>N containing gaseous species into the respective traps via the inversion procedure reported elsewhere (Kalberer et al., 1996). The flux into a trap can be calculated using Equation 3.1.

$$I_j = \frac{A_{j(i)} - A_{j(i-1)} \exp(-\lambda(t_{(i)} - t_{(i-1)}))}{1 - \exp(-\lambda(t_{(i)} - t_{(i-1)}))} \quad (\text{Eq. 3.1})$$

Where  $I_j$  is the flux into trap  $j$ ,  $A_{j(i-1)}$  and  $A_{j(i)}$  are two consecutive activity measurements performed at times  $t_{(i-1)}$  and  $t_{(i)}$  and  $\lambda$  is the decay constant for <sup>13</sup>N ( $\lambda=0.00116 \text{ s}^{-1}$ ). The measured flux is proportional to the gas phase concentration of the respective species, which can therefore be determined. By comparing the value of the gas phase NO<sub>2</sub> concentration measured with the NO<sub>x</sub> analyzer to the <sup>13</sup>NO<sub>2</sub> and <sup>13</sup>N<sub>2</sub>O<sub>5</sub> signals measured at the denuder traps and the particle filter it is possible to calculate the concentration of N<sub>2</sub>O<sub>5</sub> in the gas and particle phase.

Additional information on coating preparation, traps and measurement efficiencies can be found in our previous publications (Ammann, 2001; Gržinić et al., 2014; Guimbaud et al., 2002).

### 3.3. Results and discussion

#### 3.3.1. Measuring the uptake coefficient of $\text{N}_2\text{O}_5$ over a wider humidity range

Over the course of several experiments the uptake of  $\text{N}_2\text{O}_5$  to citric acid aerosol particles was measured at different RH values. The overall signal of  $\text{N}_2\text{O}_5$  in the gas phase was obtained by adding the inlet and first citric acid coated denuder plate signals and subtracting the second citric acid denuder signal ( $\text{NO}_2$  interference). To correct for the small amounts of  $\text{NO}_3$  present in the gas phase the signal was multiplied with the  $\text{NO}_3/(\text{NO}_3+\text{N}_2\text{O}_5)$  ratio obtained via our gas phase  $\text{N}_2\text{O}_5$  production model used in our previous study (Gržinić et al., 2014). A typical experiment was performed as follows: after a period of stabilization, during which all flows were on, but the nebulizer switched off the  $\text{NO}_2$  concentration was measured via the  $\text{NO}_x$  analyzer connected to the system (in place of the SMPS). Concentrations around 9-10 ppbv of  $\text{NO}_2$  were obtained in the aerosol flow tube reactor. From the measured gamma-ray detector signals of  $\text{N}_2\text{O}_5$  and  $\text{NO}_2$ , a maximum initial concentration of  $\sim 5$  ppbv of  $\text{N}_2\text{O}_5$  was calculated. Next, a wall loss measurement was performed by changing the length of the aerosol flow tube and thus the reaction time, which is shown in the first part of the exemplary record of an experiment in Figure 3.1. Typical pseudo-first order wall loss rate constants,  $k_w$ , were  $\sim 9 \times 10^{-3}$  and  $\sim 3 \times 10^{-2} \text{ s}^{-1}$  for low and high humidity, respectively, indicating strong wall loss of the labelled  $\text{N}_2\text{O}_5$  molecules. After the wall loss measurement was completed, the SMPS was connected to the system and the reactor length was adjusted to a 60 sec reaction time within the aerosol flow tube.

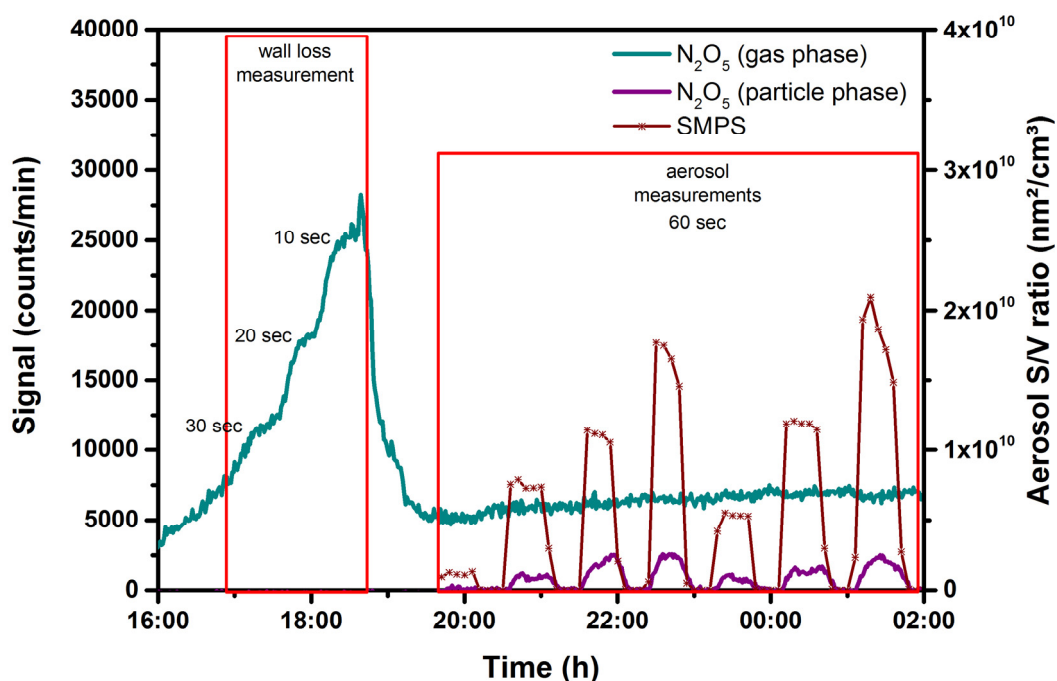


**Fig. 3.1.** Exemplary traces of inverted detector signals for an experiment: teal: gas-phase  $^{13}\text{N}_2\text{O}_5$  signal; purple: particle-phase  $^{13}\text{N}$  signal; red: SMPS signal (aerosol surface/volume ratio)

At this point the nebulizer was switched on to generate citric acid aerosol for 25-30 minutes and then switched off again for an interval of the same duration. By varying the vibration frequency of the piezoelectric membrane in the ultrasonic nebulizer it is possible to change the characteristics of the generated aerosol, in particular the aerosol surface to gas volume ratio. Figure 3.2 shows the resulting data for one such experiment.

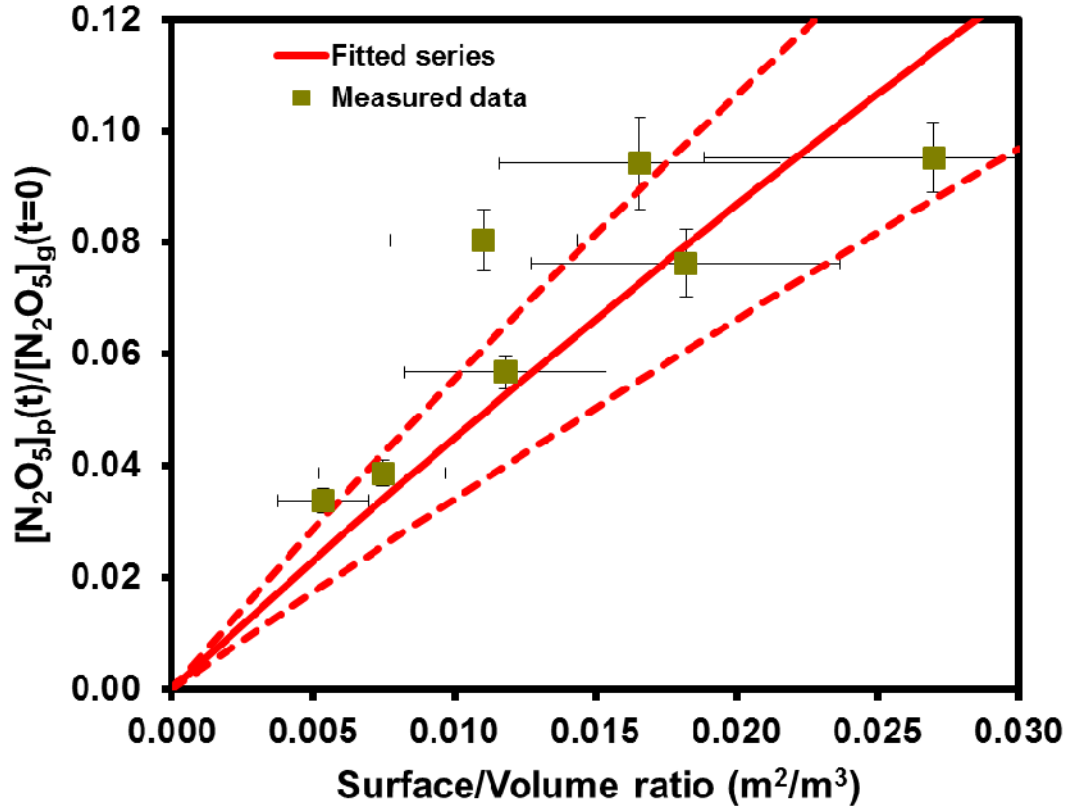


**Fig. 3.2.** Normalized particle-phase  $\text{N}_2\text{O}_5$  concentration vs. aerosol surface/volume ratio graph for the experiment from Fig 2. The data points represent experimental data; vertical error bars represent a 95% confidence interval, horizontal error bars represent the S/V measurement error (30%), the full red line is the fitted series determined by least-squares fitting of Eq. 2 to experimental data, the dashed red lines are 95% confidence intervals.

The gas-aerosol interaction kinetics can be described by Equation 3.2:

$$\frac{C_p^{(t)}}{C_g^{(t=0)}} = \frac{1 - e^{-(k_w + k_p)t}}{1 + \frac{k_w}{k_p}} \quad (\text{Eq. 3.2})$$

where  $C_g^{(t=0)}$  is the gas-phase  $\text{N}_2\text{O}_5$  concentration at time zero,  $C_p^{(t)}$  is the  $\text{N}_2\text{O}_5$  concentration in the particle phase,  $k_w$  is the wall loss constant, measured as described above, and  $k_p$  denotes the apparent first order rate coefficient for loss of  $\text{N}_2\text{O}_5$  from

the gas phase due to its heterogeneous reaction with the aerosol phase. Equation 3.3 relates  $k_p$  to the uptake coefficient  $\gamma$ :

$$\gamma = \frac{4k_p}{S_p \omega} \quad \omega = \sqrt{\frac{8RT}{\pi M}} \quad (\text{Eq. 3.3})$$

where  $S_p$  is the total aerosol surface area to gas volume ratio obtained with the SMPS,  $\omega$  is the mean thermal velocity of  $\text{N}_2\text{O}_5$ ,  $R$  is the gas constant,  $T$  is the absolute temperature and  $M$  is the molar weight of  $\text{N}_2\text{O}_5$ . Eq. 3.2 was then used to fit the experimental data as shown in Figure 3.2 with  $\gamma$  being the only variable. The results are shown in Figure 3.3.

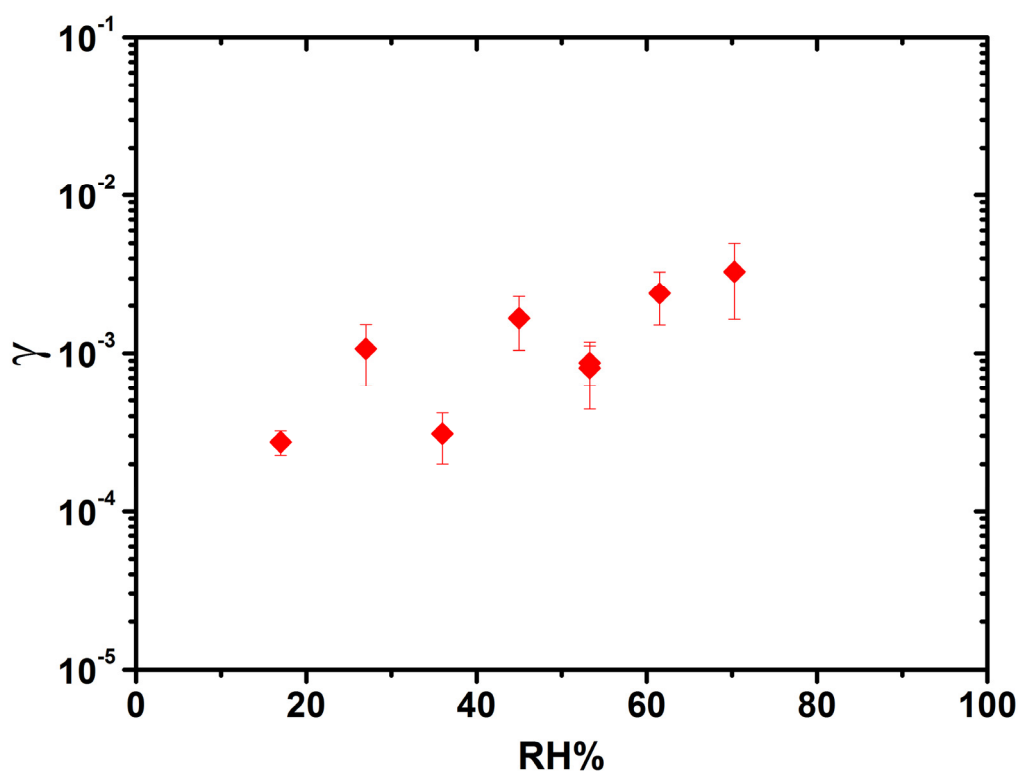


**Fig. 3.3.** Uptake coefficients obtained in this study at various RH values. Error bars represent 95% confidence bounds

A trend of increased uptake with increasing RH can be observed. This is consistent with the increasing water content of the aerosol at higher humidity. The uptake varies about one order of magnitude between the lowest and highest RH. Compared to some

other polycarboxylic acids (Griffiths et al., 2009; Thornton et al., 2003) citric acid is on the lower end of the scale as far as uptake of  $\text{N}_2\text{O}_5$  is concerned, being more than an order of magnitude lower than the uptake on malonic acid. The uncertainty in  $\gamma$  data arises primarily from the fact that aerosol uptake rates ( $k_p$ ) were smaller than wall loss rates ( $k_w$ ) as well as from the systematic error associated with the measurements of surface to volume ratio of the aerosol by the SMPS ( $S_p$ ), which amounts to  $\sim 30\%$ . The 95% confidence interval from replication (as can be seen in Fig. 3.2) does not overly influence the overall uncertainty for  $\gamma$ .

As mentioned in the experimental section, care was taken to avoid crystallization by not drying the particles to low RH, but rather to equilibrate the solution droplets from the nebulizer to the RH of the experiments. Therefore, the low uptake coefficients are unlikely to be caused by crystallization of the citric acid. With respect to the humidity range, the primary limitations were wall loss (at high RH) and potential efflorescence of the liquid aerosol (at low RH).

There are a few factors that could have influenced the scatter among the measurements at different RH. We have noticed that a small but variable number of very large particles fell outside the measurement range of the DMA (one of the components of the SMPS), which for our settings was limited to particle diameters up to 806 nm. Additionally, two separate batches of citric acid (from the same producer) have been used to prepare the solutions, and we cannot exclude possible contaminations, which could have altered the surface tension of the solution.

### 3.3.2. Physical state, reaction mechanism and parameterization

The question of the physical state of the citric acid aerosol at low humidity is complex. Literature data suggests (Peng et al., 2001; Zardini et al., 2008) that citric acid particles are always liquid at room temperature, equilibrating with RH changes down to very low RH values and retain 5% wt. of residual water even after efflorescence (Peng et al., 2001). This can be explained by the strong interactions of the polar functional groups with water molecules at high supersaturations. In this regard citric acid is similar to malonic acid, a C3 dicarboxylic acid, and both can maintain a solution at high supersaturation at very low RH. We can assume however that even though citric acid particles do not undergo efflorescence at low RH values, they are

likely to have high viscosity and possibly a semi-solid physical state. The uptake coefficient of  $\text{N}_2\text{O}_5$  at low humidity observed here, in the order of  $10^{-4}$ , is comparable to succinic acid or oxalic acid in their effloresced form (Thornton et al., 2003). Thus, the difference between low and high humidity is similar to that of solid (effloresced) vs. liquid (deliquesced) inorganic aerosol, where likewise the solid particles show uptake rates significantly lower than their liquid counterparts (Hallquist et al., 2003). We can notice, however, that our data shows a gradual increase of the uptake coefficient with increasing RH and therefore water content. This is in contrast with the results presented for effloresced malonic acid (Thornton et al., 2003), which do not show an increase of the uptake coefficient with increased humidity, unless the deliquescence RH is reached. Taking this into consideration together with literature data, we posit that in our experiment the citric acid aerosol is most probably in supersaturated form even at low RH values and that the continuous increase in the uptake coefficient  $\text{N}_2\text{O}_5$  is related to the increasing water content and/or the increasing diffusion coefficient.

For moderate uptake rates and submicron particles, where gas-phase diffusion constraints can be neglected, the  $\text{N}_2\text{O}_5$  uptake coefficient can be described according to the resistor model (Davidovits et al., 1995) with Equation 3.4:

$$\frac{1}{\gamma} = \frac{1}{\alpha_b} + \frac{1}{\Gamma_b} = \frac{1}{\alpha_b} + \frac{\omega}{4HRT\sqrt{D_l k^l}} \left( \coth q - \frac{1}{q} \right)^{-1} \quad (\text{Eq. 3.4})$$

where  $\alpha_b$  is the bulk accommodation coefficient,  $H$  is the Henry's law constant,  $R$  is the gas constant,  $T$  is the absolute temperature,  $D_l$  is the liquid-phase diffusion coefficient,  $k^l$  is the apparent first-order loss rate constant for  $\text{N}_2\text{O}_5$  in the liquid phase,  $\omega$  is the mean thermal velocity of  $\text{N}_2\text{O}_5$  molecules in the gas phase and  $q$  is the reacto-diffusive parameter which accounts for the competition between reaction and diffusion within the particle. The reacto-diffusive parameter is defined by Equation 5:

$$q = \frac{l}{r} \quad (\text{Eq. 3.5})$$

where  $r$  is the radius of the particle and  $l$  is the reacto-diffusive length, defined by Equation 3.6:

$$l = \sqrt{\frac{D_l}{k^I}} \quad (\text{Eq. 3.6})$$

The reacto-diffusive length is the characteristic distance that a molecule will diffuse within a particle before reacting. When  $l$  is small compared to the radius of the particle ( $q \ll 1$ ), the mechanism is dominated by reaction near the surface of the particle. On the other hand, when  $l$  is comparable or larger than the radius of the particle ( $q > 1$ ) the turnover of  $\text{N}_2\text{O}_5$  occurs throughout the volume of the particle and the process becomes volume-limited and the uptake coefficient dependent on size. Using Equation 3.4 as a starting point we have tried to parameterize the uptake of  $\text{N}_2\text{O}_5$  on citric acid vs RH. Within this treatment, the complex mechanism (R3.3-R3.7) is lumped into the net reaction (R3.2) by treating only one dissolved  $\text{N}_2\text{O}_5$  species, which undergoes a bimolecular reaction with liquid phase water. Therefore, this avoids a detailed treatment of the forward and backward reactions. So far, this has proved to be a reasonable parameterization to describe uptake of  $\text{N}_2\text{O}_5$  to laboratory generated aerosol particles. An analytical expression has been suggested to take into account the nitrate effect (Griffiths et al, 2009). But since we have worked at low enough  $\text{N}_2\text{O}_5$  concentrations, our experiments are not affected by the accumulation of nitrate within the residence time of particles in our flow tube. The calculated value for the maximum  $\text{HNO}_3$  concentration in the particle phase is  $\sim 10^{-3}$  M.

The Henry's law constant for  $\text{N}_2\text{O}_5$  on organic polycarboxylic aerosol particles is unknown, however in several studies (Badger et al., 2006; Robinson et al., 1997; Thornton et al., 2003) a generic value of  $H = 2 \text{ M atm}^{-1}$  has been suggested for liquid aerosol particle solutions. Recommended values (Ammann et al., 2013) for aqueous organic aerosols have been used for  $\alpha_b$  (0.035) and  $k^{\text{II}}$  ( $1.0 \times 10^5 \text{ M}^{-1} \text{ s}^{-1}$ ) which is the apparent second-order rate constant for the reaction of  $\text{N}_2\text{O}_5$  with water and  $k^{\text{I}} = k^{\text{II}}[\text{H}_2\text{O}]$ . These recommended values are based on several studies with dicarboxylic



and polycarboxylic acids (Badger et al., 2006; Griffiths et al., 2009; Thornton et al., 2003).

Since water is the main reactant, the parameterization relies heavily on the water concentration as a function of RH. Mass growth factor values (and consequently mass fractions) for citric acid and water were obtained from Zardini et al. (2008), while the citric acid solution densities have been obtained from several sources, each relating to the particular parameterization used for viscosity further below (Laguerie et al., 1976; Lienhard et al., 2012; Peng et al., 2001)

As far as the diffusion coefficient  $D_1$  is concerned, previous authors have used an estimate of  $1 \times 10^{-5} \text{ cm}^2 \text{ s}^{-1}$  (Badger et al., 2006; Griffiths et al., 2009; Hallquist et al., 2003; Thornton et al., 2003) for the diffusion coefficient of  $\text{N}_2\text{O}_5$  in an aqueous solution, independent of water activity. Together with the other parameters, this leads to a reasonable agreement of the parameterisation based on Equation 3.4 with the measured data for malonic acid. However, as it turns out, the parameterisation would largely overpredict the reactivity for citric acid. Citric acid solutions are substantially more viscous, i.e., for a solution of 1.04 M, the reported viscosity (Laguerie et al., 1976) of CA is  $1.49 \times 10^{-3} \text{ Pa s}$ , while for malonic acid it is  $1.09 \times 10^{-3} \text{ Pa s}$  (Chmielewska and Bald, 2008), close to that of water ( $0.91 \times 10^{-3} \text{ Pa s}$ ). It is therefore likely that the lower uptake coefficients of  $\text{N}_2\text{O}_5$  in citric acid compared to those for malonic acid are caused by lower diffusivity in the more viscous solution. Since the diffusivity of  $\text{N}_2\text{O}_5$  is not known in either medium, we used four methods to estimate it, summarized in Figure 3.4.

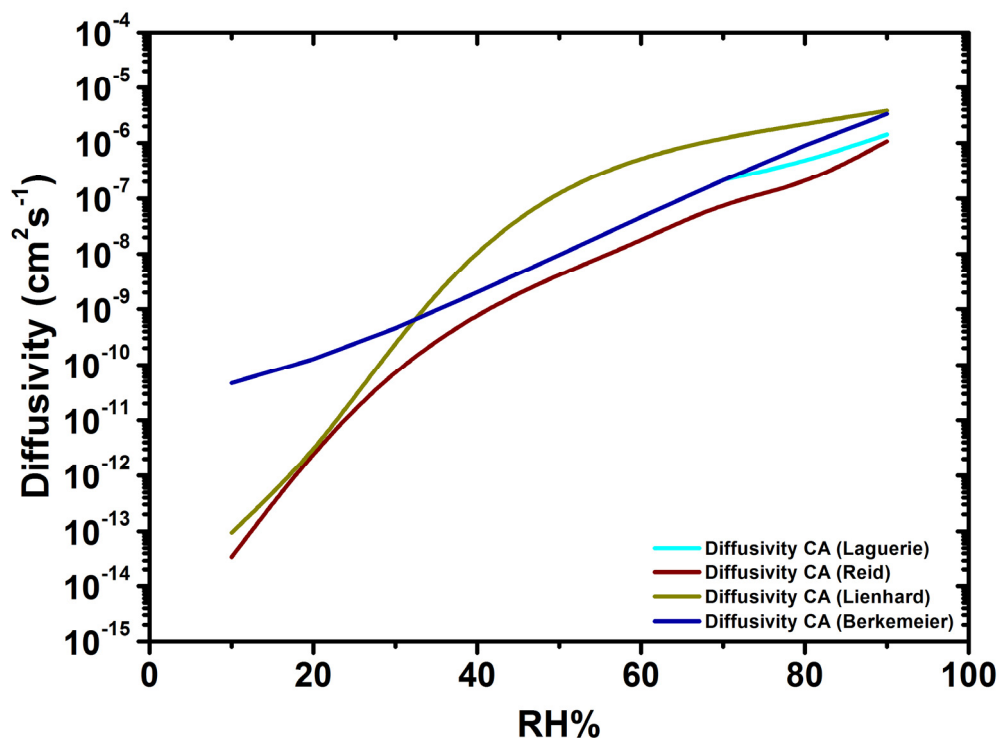


**Fig. 3.4.** Diffusivity of  $\text{N}_2\text{O}_5$  in citric acid solutions as calculated according to four parameterization methods: teal: Laguerie; red: Reid; green: Lienhard; blue: Berkemeier

The first one (Laguerie) is based on viscosity measurements by Laguerie et al. (1976), and within the range of solutions covered by their measurements,  $D_1$  for  $\text{N}_2\text{O}_5$  was calculated by applying the Stokes-Einstein relation (Equation 3.7).

$$D_l = \frac{k_B T}{6\pi\eta r} \quad (\text{Eq. 7})$$

Where  $k_B$  is the Boltzmann constant,  $T$  is the absolute temperature,  $\eta$  is the viscosity and  $r$  is the radius of the  $\text{N}_2\text{O}_5$  molecule assumed spherical ( $2.5 \text{ \AA}$ ). The viscosity parameterization in this case covers a range of citric acid concentrations up to  $\sim 4.3 \text{ M}$ , which in our case corresponds to RH values  $>70\%$ . While the viscosity in this range certainly allows using the Stokes-Einstein relation in principle, uncertainty remains with respect to the effective molecular radius to be used, since we don't know the identity of the solute for the rate limiting step (dissolved  $\text{N}_2\text{O}_5$  or  $\text{NO}_2^+$ ).

More recent measurements of viscosity of citric acid were provided by J. Reid (personal communication) from a combination of optical tweezers and electrodynamic balance (EDB) experiments that cover especially also the highly supersaturated solutions. The diffusion coefficients were again estimated via the Stokes-Einstein relation as before. A range of 3 to 73% RH was covered. For the humidity range above 50%, the same uncertainty applies with respect to the size of the diffusing species. At low RH, however, the use of the Stokes-Einstein relation may be questioned. Power et al. (2013) suggested that the diffusivity of water in sucrose droplets starts to decouple from the viscosity for viscosities around 1 Pa s, and at 10 Pa s the calculated diffusivity departs from measured values already by an order of magnitude, corresponding to ~40-50% RH in our citric acid solutions.

The third method is based on an estimate of the diffusivity of H<sub>2</sub>O in the organic matrix, which is in turn based on the principal parameterization for the one of H<sub>2</sub>O in sucrose from Zobrist et al. (2011). This method uses the measured glass transition and hygroscopicity data to infer diffusion properties of a target substance (e.g. citric acid) by extrapolation from a known reference substance (e.g. sucrose) (Berkemeier et al., 2014). The data was provided by T. Berkemeier (private communication). We have again used the Stokes-Einstein relation to estimate the diffusivity of N<sub>2</sub>O<sub>5</sub> based on that of H<sub>2</sub>O, i.e., assuming a molecular radius change only.

Finally, very recently, Lienhard et al. (2014), determined the diffusivity of H<sub>2</sub>O in citric acid solution droplets by measuring the kinetics of the size change in response to step changes in RH in an EDB. The data are parameterized via an empirical Vignes-type equation (Lienhard et al., 2012; Lienhard et al., 2014). The diffusivity of N<sub>2</sub>O<sub>5</sub> was again estimated from that of H<sub>2</sub>O using Equation 3.7.

The result of calculating the uptake coefficient according to Equation 3.4 and using diffusion coefficients estimated according to these four methods while keeping all other parameters constant, is presented in Figure 3.5. The solid lines cover the range of humidity where the Stokes-Einstein relation may likely be a good approximation for estimating the diffusivity based on either viscosity or the diffusivity of water, and the dashed lines for the range of humidity where usage of the latter is highly uncertain.

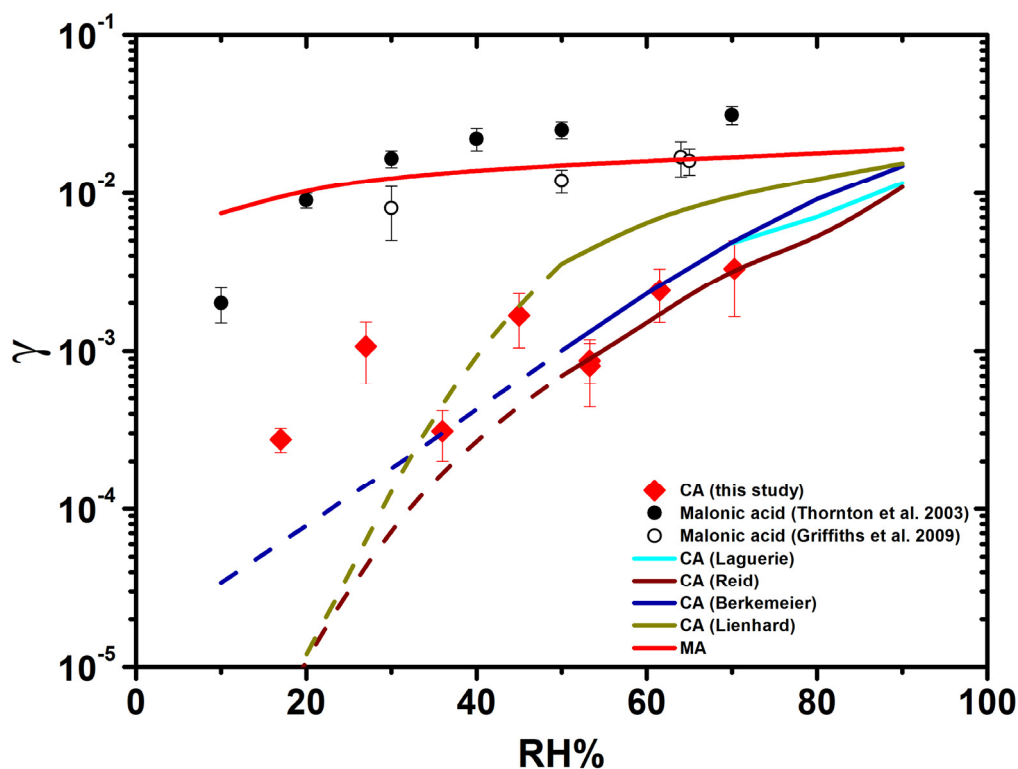


**Fig. 3.5.** Parameterization of  $\text{N}_2\text{O}_5$  uptake on citric acid aerosol based on diffusivities estimated by the four parameterization methods: teal: Laguerie; dark red: Reid; green: Lienhard; blue: Berkemeier; red: parameterization for malonic acid using the same kinetic parameters, but with  $D$  independent of  $\text{RH}$ ; red diamonds: uptake coefficients measured in this study; solid circles: uptake coefficients for malonic acid according to Thornton et al. (2003); open circles: uptake coefficients for malonic acid according to Griffiths et al. (2009)

We can notice that the uptake coefficient based on all of the diffusivity parameterizations show similar behavior at higher  $\text{RH}$  values ( $>70\%$ ), however the Lienhard one starts to deviate strongly from the rest as well as from the measured citric acid uptake coefficients fairly quickly, overestimating the uptake by about a factor 3-4. The Laguerie parameterization is limited by the small range of solution compositions covered by measurements ( $\text{RH} >70\%$ ). The other parameterizations (Berkemeier, Reid) follow the measured uptake values fairly well down to values of about 50-60%  $\text{RH}$ , where they start to diverge significantly from the measured data. This is not surprising due to the decoupling between viscosity and diffusivity at 10 Pa s (Debenedetti and Stillinger, 2001; Power et al., 2013) mentioned above. Unfortunately, the variability of the uptake data does not allow constraining the parameterizations further; however, we can conclude that variations in viscosity and

associated changes in diffusivity as a function of RH have a significant impact on the uptake of  $\text{N}_2\text{O}_5$ . The Stokes-Einstein relation underestimates the diffusivity at high viscosities, underestimating thus the uptake coefficient as well. Therefore, our inability to precisely predict the diffusivity of  $\text{N}_2\text{O}_5$  at lower humidity in spite of relatively well constrained estimates of  $\text{H}_2\text{O}$  diffusivity or viscosity, leaves room for interpretation of the difference between measured and predicted uptake coefficients.

The uptake, as described by Eq. 3.3, is likely not bulk accommodation limited; the measured uptakes as well as the predicted values for  $\Gamma_b$  are well below  $\alpha_b$  and do not show a plateau at high RH values. Based on the four different diffusivity estimates we can calculate the reacto-diffusive length (Table 1):

**Tab. 3.1.** Reacto-diffusive lengths calculated using diffusivity values obtained via the four above mentioned parameterizations.

RH [%]	Reacto-diffusive length [nm]			
	Laguerie	Reid	Berkemeier	Lienhard
30	-	0.09	0.21	0.16
50	-	0.49	0.74	2.88
70	3.03	1.83	2.96	7.21
90	6.33	5.26	9.63	10.29

As can be seen, even at very high RH values (90%) the maximum reacto-diffusive length obtained is equal to 10.29 nm, a value far short from the radius of our aerosol particles (100-150 nm) and at lower RH values (50-70%) the reacto-diffusive length is down to a few nanometers. Even considering a smaller  $k^{\text{II}}$  ( $1 \times 10^4 \text{ M}^{-1} \text{ s}^{-1}$ ), the reacto-diffusive length at moderate RH values is still fairly small ( $\sim 5$ -20 nm at 70% RH). This is in contrast with the values obtained for other polycarboxylic acids like maleic acid (Thornton et al., 2003) (48 nm at 50% RH) or humic acid (Badger et al., 2006) (30-50 nm at different RH), and points to the fact that the reaction is not volume limited. The reacto-diffusive length itself indicates that reaction is faster than diffusion into the bulk. However, as can be seen in our data, the reacto-diffusive

length decreases with decreasing uptake. The reduction in diffusivity is the driving factor behind this.

In turn, Equation 4 assumes that water, the reactant for  $\text{N}_2\text{O}_5$ , remains well mixed. Even for 15 % RH, using the diffusivity parameterization closest to our measured results (Berkemeier), the diffusivity of  $\text{H}_2\text{O}$  is about  $1.34 \times 10^{-10} \text{ cm}^2 \text{ s}^{-1}$ , for which across particle diffusion times  $t = d_p^2 / D_{\text{H}_2\text{O}}$  are about 0.75 s, significantly shorter than the time-scale of our uptake experiment. Therefore, Equation 4 can be safely used for the analysis of the data.

The parameterization given by Equation 4 is only considering the reacto-diffusive regime of loss of  $\text{N}_2\text{O}_5$  within the bulk of the particles. However, the reduction in the reactivity brought about by the significant increase in viscosity, would allow uptake to become significantly affected by a surface reaction (Ammann et al., 2003). Therefore, apart from diffusivities being higher than estimated, the deviation of the predicted uptake coefficients from the measured ones at low RH could also be due to a surface reaction becoming rate limiting. Other effects, such as salting in of  $\text{N}_2\text{O}_5$  or an increase in the apparent rate constant  $k^{\text{II}}$  are probably less likely. Effloresced polycarboxylic acid particles that might serve as a first model for an assessment of surface hydrolysis of  $\text{N}_2\text{O}_5$  have shown uptake coefficients similar to the ones measured with citric acid at low humidity, roughly in the  $10^{-4}$  range. While some, like malonic acid (Thornton et al., 2003), do not show noticeable dependence on water content, others like succinic or oxalic acid (Griffiths et al., 2009) seem to be influenced by RH, possibly driven by increasing amounts of surface adsorbed  $\text{H}_2\text{O}$  with increasing RH. Also mineral oxides that expose hydroxylated surface sites to the gas phase have shown similar behavior of  $\text{N}_2\text{O}_5$  uptake as a function of RH (though in the  $10^{-3}$ - $10^{-2}$  range). As surface reactive sites are deactivated, a corresponding reduction in reactivity was noticed (Karagulian et al., 2006; Seisel et al., 2005). Discrepancies in uptake rates in dry and low RH conditions have been attributed to surface adsorbed  $\text{H}_2\text{O}$  (Wagner et al., 2008). Effloresced ammonium sulphate and bisulphate aerosols have shown similar behavior as well (Davis et al., 2008). Therefore, it is likely that surface hydrolysis of  $\text{N}_2\text{O}_5$  on high viscosity citric acid may indeed contribute to uptake at low RH.

### 3.4. Conclusions and atmospheric impact

We have conducted measurements of  $\text{N}_2\text{O}_5$  uptake to citric acid aerosol over an atmospherically relevant RH range at room temperature. Our results have shown that uptake coefficients change by roughly one order of magnitude ( $\sim 3 \times 10^{-4}$  -  $3 \times 10^{-3}$ ) between low (17%) and high (70%) RH. The results are in line with citric acid being present as a supersaturated liquid down to low RH values. As recent studies have shown, citric acid particle viscosity is higher than that of similar di- and polycarboxylic acids, which have been studied so far and diffusivity is lower. We have calculated that the reacto-diffusive length, according to the diffusivity parameterizations presented in this study, is down to a few nm. The reacto-diffusive length decreases with decreasing uptake coefficient, apparently under the influence of increased viscosity (and thus decreased diffusivity). However the uptake of  $\text{N}_2\text{O}_5$ , driven by the bulk reaction of  $\text{N}_2\text{O}_5$  with water, remains in the reacto-diffusive kinetic regime. Thus, the decreasing uptake coefficients with decreasing RH are well explained by the decreasing diffusivity of  $\text{N}_2\text{O}_5$ . However, because estimating the diffusivity of  $\text{N}_2\text{O}_5$  from measured diffusivity of  $\text{H}_2\text{O}$  or measured viscosity is problematic due to the decoupling between viscosity and diffusivity at high viscosity, the parameterization of  $\text{N}_2\text{O}_5$  uptake by the traditional bulk reacto-diffusive uptake regime alone becomes uncertain at low RH. It cannot be ruled out that a surface reaction contributes significantly to uptake at low relative humidity.

Nevertheless, diffusivity seems to play a very important role in the reactivity of citric acid and is the decisive parameter to describe the difference in reactivity to other simple carboxylic acid forming lower viscosity aqueous solutions. The range of viscosity of citric acid solutions is likely similar or even still at the lower end of realistic secondary organic aerosol (SOA) components. Higher viscosity could also explain the previously mentioned discrepancy between  $\text{N}_2\text{O}_5$  reactivity in field measurements and model predictions based on laboratory measurements, in particular those of malonic acid. This could also explain the behavior of citric acid described in a recent study which suggested that the organic O:C ratio in mixed inorganic-organic aerosols may be used as an indicator of  $\text{N}_2\text{O}_5$  reactivity (Gaston et al., 2014), based on a trend of increasing uptake coefficient with increasing O:C ratio. However, citric acid and some high O:C mixtures containing citric acid and other highly functionalized oxidized organic compounds are an exception to this trend, showing

reactivity which is noticeably below expected values. O:C might indeed serve as an indicator, but it should be convoluted with viscosity, which might be related to the O:C ratio as well. This could provide a way to a better representation of  $\text{N}_2\text{O}_5$  reactivity in atmospheric models.



## References

- Abbatt, J. P. D., Lee, A. K. Y., and Thornton, J. A.: Quantifying trace gas uptake to tropospheric aerosol: recent advances and remaining challenges, *Chemical Society Reviews*, 41, 6555-6581, 2012.
- Abramson, E., Imre, D., Beranek, J., Wilson, J., and Zelenyuk, A.: Experimental determination of chemical diffusion within secondary organic aerosol particles, *Physical Chemistry Chemical Physics*, 15, 2983-2991, 2013.
- Ammann, M.: Using  $^{13}\text{N}$  as tracer in heterogeneous atmospheric chemistry experiments, *Radiochim. Acta*, 89, 831-838, 2001.
- Ammann, M., Cox, R. A., Crowley, J. N., Jenkin, M. E., Mellouki, A., Rossi, M. J., Troe, J., and Wallington, T. J.: Evaluated kinetic and photochemical data for atmospheric chemistry: Volume VI - heterogeneous reactions with liquid substrates, *Atmospheric Chemistry and Physics*, 13, 8045-8228, 2013.
- Ammann, M., Poschl, U., and Rudich, Y.: Effects of reversible adsorption and Langmuir-Hinshelwood surface reactions on gas uptake by atmospheric particles, *Physical Chemistry Chemical Physics*, 5, 351-356, 2003.
- Anttila, T., Kiendler-Scharr, A., Tillmann, R., and Mentel, T. F.: On the reactive uptake of gaseous compounds by organic-coated aqueous aerosols: Theoretical analysis and application to the heterogeneous hydrolysis of  $\text{N}_2\text{O}_5$ , *Journal of Physical Chemistry A*, 110, 10435-10443, 2006.
- Badger, C. L., Griffiths, P. T., George, I., Abbatt, J. P. D., and Cox, R. A.: Reactive uptake of  $\text{N}_2\text{O}_5$  by aerosol particles containing mixtures of humic acid and ammonium sulfate, *Journal of Physical Chemistry A*, 110, 6986-6994, 2006.
- Bartels-Rausch, T., Ulrich, T., Huthwelker, T., and Ammann, M.: A novel synthesis of the N-13 labeled atmospheric trace gas peroxyxynitric acid, *Radiochimica Acta*, 99, 285-292, 2011.
- Berkemeier, T., Shiraiwa, M., Pöschl, U., and Koop, T.: Competition between water uptake and ice nucleation by glassy organic aerosol particles, *Atmos. Chem. Phys. Discuss.*, 14, 16451-16492, 2014.
- Bertram, T. H., Thornton, J. A., Riedel, T. P., Middlebrook, A. M., Bahreini, R., Bates, T. S., Quinn, P. K., and Coffman, D. J.: Direct observations of  $\text{N}_2\text{O}_5$  reactivity on ambient aerosol particles, *Geophysical Research Letters*, 36, 5, 2009.
- Brown, S. S., Dube, W. P., Fuchs, H., Ryerson, T. B., Wollny, A. G., Brock, C. A., Bahreini, R., Middlebrook, A. M., Neuman, J. A., Atlas, E., Roberts, J. M., Osthoff, H. D., Trainer, M., Fehsenfeld, F. C., and Ravishankara, A. R.: Reactive uptake coefficients for  $\text{N}_2\text{O}_5$  determined from aircraft measurements during the Second Texas Air Quality Study: Comparison to current model parameterizations, *Journal of Geophysical Research-Atmospheres*, 114, 2009.

- Chang, W. L., Bhave, P. V., Brown, S. S., Riemer, N., Stutz, J., and Dabdub, D.: Heterogeneous Atmospheric Chemistry, Ambient Measurements, and Model Calculations of N(2)O(5): A Review, *Aerosol Sci. Technol.*, 45, 665-695, 2011.
- Chmielewska, A. and Bald, A.: Viscosimetric studies of aqueous solutions of dicarboxylic acids, *Journal of Molecular Liquids*, 137, 116-121, 2008.
- Davidovits, P., Hu, J. H., Worsnop, D. R., Zahniser, M. S., and Kolb, C. E.: Entry of gas molecules into liquids, *Faraday Discussions*, 100, 65-81, 1995.
- Davis, J. M., Bhave, P. V., and Foley, K. M.: Parameterization of N<sub>2</sub>O<sub>5</sub> reaction probabilities on the surface of particles containing ammonium, sulfate, and nitrate, *Atmos. Chem. Phys.*, 8, 5295-5311, 2008.
- De Gouw, J. and Jimenez, J. L.: Organic Aerosols in the Earth's Atmosphere, *Environmental Science & Technology*, 43, 7614-7618, 2009.
- Debenedetti, P. G. and Stillinger, F. H.: Supercooled liquids and the glass transition, *Nature*, 410, 259-267, 2001.
- Dentener, F. J. and Crutzen, P. J.: Reaction of N<sub>2</sub>O<sub>5</sub> on tropospheric aerosols: Impact on the global distributions of NO<sub>x</sub>, O<sub>3</sub>, and OH, *Journal of Geophysical Research: Atmospheres*, 98, 7149-7163, 1993.
- Gaston, C. J., Thornton, J. A., and Ng, N. L.: Reactive uptake of N<sub>2</sub>O<sub>5</sub> to internally mixed inorganic and organic particles: the role of organic carbon oxidation state and inferred organic phase separations, *Atmos. Chem. Phys.*, 14, 5693-5707, 2014.
- George, C., Ponche, J. L., Mirabel, P., Behnke, W., Scheer, V., and Zetzsch, C.: Study of the Uptake of N<sub>2</sub>O<sub>5</sub> by Water and NaCl Solutions, *J. Phys. Chem.*, 98, 8780-8784, 1994.
- Griffiths, P. T., Badger, C. L., Cox, R. A., Folkers, M., Henk, H. H., and Mentel, T. F.: Reactive Uptake of N<sub>2</sub>O<sub>5</sub> by Aerosols Containing Dicarboxylic Acids. Effect of Particle Phase, Composition, and Nitrate Content, *Journal of Physical Chemistry A*, 113, 5082-5090, 2009.
- Gross, S., Iannone, R., Xiao, S., and Bertram, A. K.: Reactive uptake studies of NO<sub>3</sub> and N<sub>2</sub>O<sub>5</sub> on alkenoic acid, alkanolate, and polyalcohol substrates to probe nighttime aerosol chemistry, *Physical Chemistry Chemical Physics*, 11, 7792-7803, 2009.
- Gržinić, G., Bartels-Rausch, T., Birrer, M., Türler, A., and Ammann, M.: Production and use of <sup>13</sup>N labeled N<sub>2</sub>O<sub>5</sub> to determine gas-aerosol interaction kinetics, *Radiochim. Acta*, 102, 1025-1034, 2014.
- Guimbaud, C., Arens, F., Gutzwiller, L., Gaggeler, H. W., and Ammann, M.: Uptake of HNO<sub>3</sub> to deliquescent sea-salt particles: a study using the short-lived radioactive isotope tracer N-13, *Atmospheric Chemistry and Physics*, 2, 249-257, 2002.
- Gutzwiller, L., Arens, F., Baltensperger, U., Gaggeler, H. W., and Ammann, M.: Significance of Semivolatile Diesel Exhaust Organics for Secondary HONO Formation, *Environmental Science & Technology*, 36, 677-682, 2002.

- Hallquist, M., Stewart, D. J., Stephenson, S. K., and Cox, R. A.: Hydrolysis of N<sub>2</sub>O<sub>5</sub> on sub-micron sulfate aerosols, *Physical Chemistry Chemical Physics*, 5, 3453-3463, 2003.
- Hanson, D. R. and Ravishankara, A. R.: The reaction probabilities of ClONO<sub>2</sub> and N<sub>2</sub>O<sub>5</sub> on 40 to 75% sulfuric acid solutions, *Journal of Geophysical Research: Atmospheres*, 96, 17307-17314, 1991.
- Hu, J. H. and Abbatt, J. P. D.: Reaction probabilities for N<sub>2</sub>O<sub>5</sub> hydrolysis on sulfuric acid and ammonium sulfate aerosols at room temperature, *Journal of Physical Chemistry A*, 101, 871-878, 1997.
- Kalberer, M., Tabor, K., Ammann, M., Parrat, Y., Weingartner, E., Piguet, D., Rossler, E., Jost, D. T., Turler, A., Gaggeler, H. W., and Baltensperger, U.: Heterogeneous chemical processing of (NO<sub>2</sub>)-N-13 by monodisperse carbon aerosols at very low concentrations, *J. Phys. Chem.*, 100, 15487-15493, 1996.
- Kanakidou, M., Seinfeld, J. H., Pandis, S. N., Barnes, I., Dentener, F. J., Facchini, M. C., Van Dingenen, R., Ervens, B., Nenes, A., Nielsen, C. J., Swietlicki, E., Putaud, J. P., Balkanski, Y., Fuzzi, S., Horth, J., Moortgat, G. K., Winterhalter, R., Myhre, C. E. L., Tsigaridis, K., Vignati, E., Stephanou, E. G., and Wilson, J.: Organic aerosol and global climate modelling: a review, *Atmos. Chem. Phys.*, 5, 1053-1123, 2005.
- Karagulian, F., Santschi, C., and Rossi, M. J.: The heterogeneous chemical kinetics of N<sub>2</sub>O<sub>5</sub> on CaCO<sub>3</sub> and other atmospheric mineral dust surrogates, *Atmospheric Chemistry and Physics*, 6, 1373-1388, 2006.
- Laguerie, C., Aubry, M., and Couderc, J. P.: Some physicochemical data on monohydrate citric acid solutions in water: solubility, density, viscosity, diffusivity, pH of standard solution, and refractive index, *Journal of Chemical & Engineering Data*, 21, 85-87, 1976.
- Laskin, A., Moffet, R. C., Gilles, M. K., Fast, J. D., Zaveri, R. A., Wang, B., Nigge, P., and Shutthanandan, J.: Tropospheric chemistry of internally mixed sea salt and organic particles: Surprising reactivity of NaCl with weak organic acids, *Journal of Geophysical Research: Atmospheres*, 117, D15302, 2012.
- Lienhard, D. M., Bones, D. L., Zuend, A., Krieger, U. K., Reid, J. P., and Peter, T.: Measurements of Thermodynamic and Optical Properties of Selected Aqueous Organic and Organic-Inorganic Mixtures of Atmospheric Relevance, *The Journal of Physical Chemistry A*, 116, 9954-9968, 2012.
- Lienhard, D. M., Huisman, A. J., Bones, D. L., Te, Y.-F., Luo, B. P., Krieger, U. K., and Reid, J. P.: Retrieving the translational diffusion coefficient of water from experiments on single levitated aerosol droplets, *Physical Chemistry Chemical Physics*, 16, 16677-16683, 2014.
- Mentel, T. F., Sohn, M., and Wahner, A.: Nitrate effect in the heterogeneous hydrolysis of dinitrogen pentoxide on aqueous aerosols, *Physical Chemistry Chemical Physics*, 1, 5451-5457, 1999.

Mozurkewich, M. and Calvert, J. G.: Reaction probability of N<sub>2</sub>O<sub>5</sub> on aqueous aerosols, *Journal of Geophysical Research: Atmospheres*, 93, 15889-15896, 1988.

Peng, C., Chan, M. N., and Chan, C. K.: The hygroscopic properties of dicarboxylic and multifunctional acids: Measurements and UNIFAC predictions, *Environmental Science & Technology*, 35, 4495-4501, 2001.

Power, R. M., Simpson, S. H., Reid, J. P., and Hudson, A. J.: The transition from liquid to solid-like behaviour in ultrahigh viscosity aerosol particles, *Chemical Science*, 4, 2597-2604, 2013.

Renbaum-Wolff, L., Grayson, J. W., Bateman, A. P., Kuwata, M., Sellier, M., Murray, B. J., Shilling, J. E., Martin, S. T., and Bertram, A. K.: Viscosity of  $\alpha$ -pinene secondary organic material and implications for particle growth and reactivity, *Proceedings of the National Academy of Sciences*, 110, 8014-8019, 2013.

Riemer, N., Vogel, H., Vogel, B., Anttila, T., Kiendler-Scharr, A., and Mentel, T. F.: Relative importance of organic coatings for the heterogeneous hydrolysis of N<sub>2</sub>O<sub>5</sub> during summer in Europe, *Journal of Geophysical Research: Atmospheres*, 114, D17307, 2009.

Robinson, G. N., Worsnop, D. R., Jayne, J. T., Kolb, C. E., and Davidovits, P.: Heterogeneous uptake of ClONO<sub>2</sub> and N<sub>2</sub>O<sub>5</sub> by sulfuric acid solutions, *Journal of Geophysical Research-Atmospheres*, 102, 3583-3601, 1997.

Seisel, S., Borensen, C., Vogt, R., and Zellner, R.: Kinetics and mechanism of the uptake of N<sub>2</sub>O<sub>5</sub> on mineral dust at 298 K, *Atmospheric Chemistry and Physics*, 5, 3423-3432, 2005.

Sosedova, Y., Rouvière, A., Gäggeler, H. W., and Ammann, M.: Uptake of NO<sub>2</sub> to Deliquesced Dihydroxybenzoate Aerosol Particles, *The Journal of Physical Chemistry A*, 2009. 2009.

Thornton, J. A. and Abbatt, J. P. D.: N<sub>2</sub>O<sub>5</sub> reaction on submicron sea salt aerosol: Kinetics, products, and the effect of surface active organics, *Journal of Physical Chemistry A*, 109, 10004-10012, 2005.

Thornton, J. A., Braban, C. F., and Abbatt, J. P. D.: N<sub>2</sub>O<sub>5</sub> hydrolysis on sub-micron organic aerosols: the effect of relative humidity, particle phase, and particle size, *Physical Chemistry Chemical Physics*, 5, 4593-4603, 2003.

Vaden, T. D., Imre, D., Beránek, J., Shrivastava, M., and Zelenyuk, A.: Evaporation kinetics and phase of laboratory and ambient secondary organic aerosol, *Proceedings of the National Academy of Sciences*, 108, 2190-2195, 2011.

Vandoren, J. M., Watson, L. R., Davidovits, P., Worsnop, D. R., Zahniser, M. S., and Kolb, C. E.: Uptake of N<sub>2</sub>O<sub>5</sub> and HNO<sub>3</sub> by Aqueous Sulfuric-Acid Droplets, *J. Phys. Chem.*, 95, 1684-1689, 1991.

Vlasenko, A., Huthwelker, T., Gaggeler, H. W., and Ammann, M.: Kinetics of the heterogeneous reaction of nitric acid with mineral dust particles: an aerosol flowtube study, *Physical Chemistry Chemical Physics*, 11, 7921-7930, 2009.

Wagner, C., Hanisch, F., Holmes, N., de Coninck, H., Schuster, G., and Crowley, J. N.: The interaction of N<sub>2</sub>O<sub>5</sub> with mineral dust: aerosol flow tube and Knudsen reactor studies, *Atmospheric Chemistry and Physics*, 8, 91-109, 2008.

Wahner, A., Mentel, T. F., Sohn, M., and Stier, J.: Heterogeneous reaction of N<sub>2</sub>O<sub>5</sub> on sodium nitrate aerosol, *Journal of Geophysical Research-Atmospheres*, 103, 31103-31112, 1998.

Zardini, A. A., Sjogren, S., Marcolli, C., Krieger, U. K., Gysel, M., Weingartner, E., Baltensperger, U., and Peter, T.: A combined particle trap/HTDMA hygroscopicity study of mixed inorganic/organic aerosol particles, *Atmospheric Chemistry and Physics*, 8, 5589-5601, 2008.

Zhang, Q., Jimenez, J. L., Canagaratna, M. R., Allan, J. D., Coe, H., Ulbrich, I., Alfarra, M. R., Takami, A., Middlebrook, A. M., Sun, Y. L., Dzepina, K., Dunlea, E., Docherty, K., DeCarlo, P. F., Salcedo, D., Onasch, T., Jayne, J. T., Miyoshi, T., Shimojo, A., Hatakeyama, S., Takegawa, N., Kondo, Y., Schneider, J., Drewnick, F., Borrmann, S., Weimer, S., Demerjian, K., Williams, P., Bower, K., Bahreini, R., Cottrell, L., Griffin, R. J., Rautiainen, J., Sun, J. Y., Zhang, Y. M., and Worsnop, D. R.: Ubiquity and dominance of oxygenated species in organic aerosols in anthropogenically-influenced Northern Hemisphere midlatitudes, *Geophysical Research Letters*, 34, L13801, 2007.

Zobrist, B., Soonsin, V., Luo, B. P., Krieger, U. K., Marcolli, C., Peter, T., and Koop, T.: Ultra-slow water diffusion in aqueous sucrose glasses, *Physical Chemistry Chemical Physics*, 13, 3514-3526, 2011.



## Chapter 4

### 4. Uptake of $^{13}\text{N}$ -labelled $\text{N}_2\text{O}_5$ to Nitrate containing Aerosol

Goran Gržinić<sup>1,2</sup>, Thorsten Bartels-Rausch<sup>1</sup>, Andreas Türler<sup>1,2</sup> and Markus Ammann<sup>3</sup>

As a basis for a short paper in *Journal of Physical Chemistry Letters*

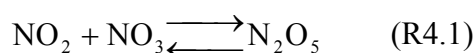
---

<sup>1</sup> Laboratory of Radiochemistry and Environmental Chemistry, Paul Scherrer Institute, 5232 Villigen, Switzerland

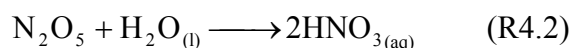
<sup>2</sup> Department of Chemistry and Biochemistry, University of Bern, 3012 Bern, Switzerland

## 4.1. Introduction

Because of the influence that the nitrogen oxide cycle has on tropospheric chemistry it has been the subject of intense interest ever since initial studies on photochemical smog identified  $\text{NO}_x$  ( $\text{NO} + \text{NO}_2$ ) and VOCs (volatile organic compounds) as its main ingredients and drivers of tropospheric  $\text{O}_3$  and  $\bullet\text{OH}$  production in polluted areas (Finlayson-Pitts and Pitts, 2000). Since then the central role of  $\text{NO}_x$  in the regulation of the oxidative capacity of the atmosphere has been established.  $\text{N}_2\text{O}_5$ , a reactive intermediate of the nighttime chemistry of nitrogen oxides, has been identified as one of the major reservoir species and potential sinks of  $\text{NO}_x$  (Abbatt et al., 2012; Chang et al., 2011).  $\text{NO}_2$  reacts with  $\text{O}_3$  to form  $\text{NO}_3$ , which then react together to form  $\text{N}_2\text{O}_5$  (R4.1).



Depending on location  $\text{N}_2\text{O}_5$  may be removed primarily by heterogeneous hydrolysis to nitric acid on aerosol surfaces, providing thus a nighttime sink for atmospheric  $\text{NO}_x$  atmospheric  $\text{NO}_x$  (R2) (Abbatt et al., 2012; Chang et al., 2011).



Removal of  $\text{N}_2\text{O}_5$  leads to a reduction of atmospheric  $\text{NO}_x$  and consequent reduction of tropospheric ozone and thus the oxidative capacity of the atmosphere (Dentener and Crutzen, 1993; Evans and Jacob, 2005). The reactivity of  $\text{N}_2\text{O}_5$  with aerosols has been of ongoing interest for the past two decades. Laboratory investigations have encompassed measurement of uptake kinetics to a wide array of inorganic aerosols, like  $\text{H}_2\text{SO}_4$ /sulphates (Hallquist et al., 2003; Hanson and Lovejoy, 1994),  $\text{NaCl}$ /marine aerosol (George et al., 1994; Thornton and Abbatt, 2005), nitrates (Hallquist et al., 2003; Wahner et al., 1998) and mineral dust (Karagulian et al., 2006; Wagner et al., 2008). The uptake coefficient  $\gamma$  (defined as the as the probability that a gas kinetic collision of a molecule leads to its uptake at the interface), on inorganic



aerosol is in the  $10^{-1}$ - $10^{-2}$  range. Organic aerosol on the other hand presents a wider range of reactivities, with values approaching those of inorganic aerosols in certain cases like with malonic acid (Griffiths et al., 2009; Thornton et al., 2003) at around  $10^{-2}$ , while in other cases the uptake coefficients go down to  $10^{-3}$ - $10^{-5}$ , like in the case of some polycarboxylic acids like citric acid (Chapter 2), succinic acid or humic acid (Badger et al., 2006; Griffiths et al., 2009), long chained fatty acids and polyalcohols (Gross et al., 2009). Additionally, coating particles with organic films has shown to have an inhibiting effect on  $N_2O_5$  uptake (Anttila et al., 2006; Folkers et al., 2003) by restricting transport from the gas phase to the aerosol phase, reduced solubility in the organic phase or limited water availability. The hydrolysis of  $N_2O_5(g)$  is believed to proceed through a multistep process (Behnke et al., 1997; Mozurkewich and Calvert, 1988): molecular solvation (R4.3) is followed by dissociation into nitronium and nitrate (R4.4). The fate of nitronium is governed by competition between the reaction with nitrate to yield molecular  $N_2O_5$  again (R4.5) and the reaction with  $H_2O(l)$  to yield  $HNO_3$  (R4.7).



As long as nitrate is a minority species in the aerosol phase, the overall uptake of  $N_2O_5$  is driven by reaction R4.7. Depending on the water content, either the transfer of  $N_2O_5$  into the aqueous phase, R4.3, also referred to as bulk accommodation, or R4.7 are rate limiting according to current understanding.

On the other hand, in presence of significant amounts of nitrate in the aqueous phase, the loss of nitronium ion by reaction with nitrate back to  $N_2O_5$ , R4.5, becomes

significant, and the uptake of  $\text{N}_2\text{O}_5$  becomes lower with increasing nitrate content in the aerosol phase, typically by an order of magnitude. This effect is referred to as the ‘nitrate effect’ (Hallquist et al., 2003; Mentel et al., 1999; Wahner et al., 1998). Most studies conducted so far were based on measuring the net gas-phase loss of  $\text{N}_2\text{O}_5$  due to uptake on an aerosol. Therefore, the actual size of the pool of dissolved  $\text{N}_2\text{O}_5$  (or its dissociated products  $\text{NO}_2^+$  and  $\text{NO}_3^-$ ), the true value of the bulk accommodation coefficient,  $\alpha_b$ , and the rate of dissociation remained obscured. In this study, we make specific use of the short-lived radioactive isotope  $^{13}\text{N}$  (Ammann, 2001; Gržinić et al., 2014) to trace the exchange of  $^{13}\text{N}$ -labelled nitrate resulting from uptake of labelled  $\text{N}_2\text{O}_5$  with the non-labelled nitrate pool in the aerosol phase. This allows to obtain a better estimate of  $\alpha_b$  and to obtain constraints of the  $\text{N}_2\text{O}_5$  dissociation (R4.4) and the recombination reaction (R4.5).

## 4.2. Experimental Section

A detailed description of the experimental method and setup can be found in our previous publications relating to the production of  $^{13}\text{N}$  labeled  $\text{N}_2\text{O}_5$  (Gržinić et al., 2014) and uptake of  $\text{N}_2\text{O}_5$  on citric acid aerosol (Chapter 3). Here we will present a very cursory description of the  $^{13}\text{N}$  production method and the changes that have been implemented to the experimental setup for the present uptake measurements.

The  $^{13}\text{N}$  short lived radioactive tracer ( $T_{1/2} \approx 10$  min.) is produced via the  $^{16}\text{O}(\text{p},\alpha)^{13}\text{N}$  reaction in a gas target by irradiating a 20%  $\text{O}_2$  in He flow with 11 MeV protons produced by the Injector II cyclotron at the Paul Scherrer Institute, Switzerland. The highly oxidized  $^{13}\text{N}$  labeled species are reduced to  $^{13}\text{NO}$  for transport via a 580 m long PVDF capillary tube to the laboratory.

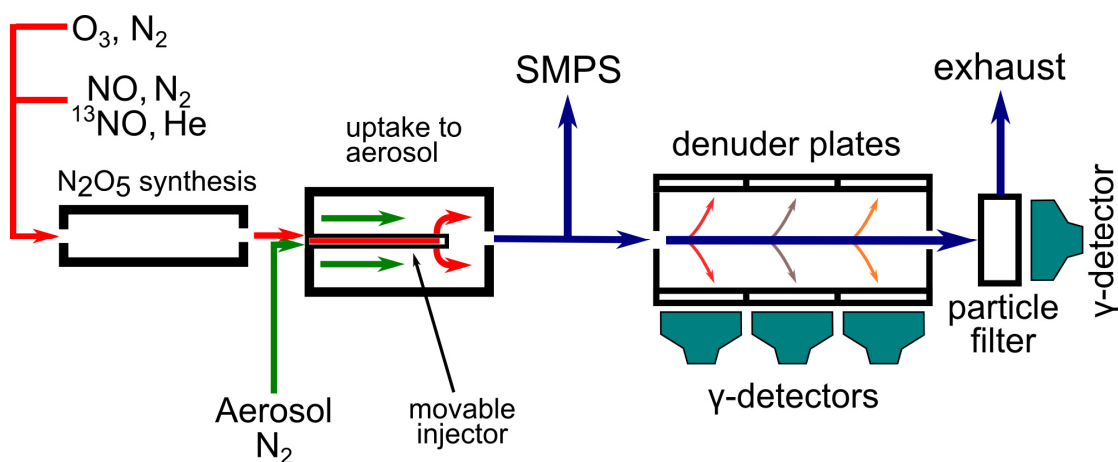


Fig. 4.1. Schematic of the modified experimental setup used in this study

Figure 4.1 shows a schematic of the experimental setup used in this study.  $^{13}\text{NO}$  containing gas originating from the accelerator facility (50 ml/min) is mixed with  $\sim 3$  ml/min of 10 ppmv non-labeled NO in  $\text{N}_2$  from a certified gas cylinder and nitrogen carrier gas (only a very small fraction of NO is labeled with  $^{13}\text{N}$ , about  $10^{-6}$  and lower). This gas flow is mixed in the  $\text{N}_2\text{O}_5$  synthesis reactor with a 50 ml/min flow containing  $\sim 8$  ppmv  $\text{O}_3$  produced by irradiating a 10%  $\text{O}_2$  in  $\text{N}_2$  gas mixture with 185nm UV light. The reactor is a glass tube of 34 cm length and 4 cm inner diameter, lined with PTFE foil and operated under dry conditions to minimize hydrolysis of  $\text{N}_2\text{O}_5$  on the walls. The gas phase chemistry of NO with  $\text{O}_3$  results in the formation of  $\text{NO}_2$ ,  $\text{NO}_3$  and finally  $\text{N}_2\text{O}_5$  (R4.1). The resulting gas flow is mixed with a secondary gas flow containing aerosol (720 ml/min) in an aerosol flow tube. This flow tube differs from the one that we used in previous studies in that it is optimized for measurement of uptake coefficients in the  $10^{-1}$ - $10^{-2}$  range. It consists of a glass tube 39.3 cm in length and 1.4 cm in diameter. The inside of the glass tube is coated with halocarbon wax to minimize  $\text{N}_2\text{O}_5$  losses to the wall by heterogeneous hydrolysis. A PTFE tube (6 mm diameter) is inserted coaxially into the flow tube to act as injector for the  $\text{N}_2\text{O}_5$  flow. The injector contains holes at the end which allow the  $\text{N}_2\text{O}_5$  flow to be injected perpendicularly to the aerosol flow. Mixing is assumed to be rapid and a laminar flow profile is assumed to have been established in the first few cm. A black shroud is used to cover the  $\text{N}_2\text{O}_5$  synthesis reactor and the aerosol flow tube in order to prevent  $\text{NO}_3$  photolysis and thus  $\text{N}_2\text{O}_5$  loss. Aerosol is produced by nebulizing 0.1% wt.  $\text{NaNO}_3$ ,  $\text{Na}_2\text{SO}_4$  and 1:1  $\text{NaNO}_3/\text{Na}_2\text{SO}_4$  solutions in MilliQ water. The resulting aerosol flow is dried over a Nafion membrane diffusion drier (RH of the drying gas outside is

adjusted to 40% RH to prevent efflorescence), passed through an  $^{85}\text{Kr}$  bipolar ion source and an electrostatic precipitator to equilibrate the charge distribution and remove the charged particles. A humidifier is placed after the ion source to adjust the humidity of the gas flow to the required experimental levels. The overall gas flow exiting from the aerosol fast-flow reactor is split into two flows via a T-connector, one to an SMPS (Scanning Mobility Particle Sizer) system used to characterize the aerosol, consisting of a differential mobility analyzer (DMA, TSI 3071) and a condensation particle counter (CPC, TSI 3022). The other part of the gas flow is directed into a parallel plate diffusion denuder system, where the various  $^{13}\text{N}$  containing gaseous species ( $\text{N}_2\text{O}_5$ ,  $\text{NO}_3$  and  $\text{NO}_2$ ) are trapped by lateral diffusion and chemical reaction on a series of parallel, selectively coated aluminium plates. The aerosol particles, which have small diffusivity, pass without loss through the denuder system and are trapped on a glass fiber filter placed at the exit. The radioactive decay of  $^{13}\text{N}$  is measured by placing a CsI scintillator crystal with PIN diode detectors (Carroll and Ramsey, USA) on each of the denuder traps and the particle filter.  $^{13}\text{N}$  decays by  $\beta^+$  decay and the resulting positron annihilates with an electron with emission of two coincident  $\gamma$ -rays in opposite directions. The resulting signal can be related to the concentration of the species in the gas and particle phase by comparing the  $\text{NO}_2$  concentration measured with a  $\text{NO}_x$  analyzer to the  $^{13}\text{NO}_2$  and  $^{13}\text{N}_2\text{O}_5$  signals on the denuder plates and particle filter, respectively. Unfortunately, due to experimental limitations, only a limited number of measurements have been performed. The  $^{13}\text{N}$  tracer technique is dependent on smooth operation of the accelerator facilities and constant online  $^{13}\text{N}$  production to be successful, which is not always the case.

### 4.3. Results and Discussion

The measurements were performed at 50% and 70% RH for all three of the solutions in question. The operating procedure is similar to the one reported in Gržinić et al. (2014) and (Chapter 3), although in this case the experiment was performed by measuring the change in signals under variation of the position of the injector (reaction time) and not aerosol surface to volume ratio. Appropriate corrections have been applied to the  $\text{N}_2\text{O}_5$  signal to account for  $\text{NO}_2$  interference on the denuder coating used for  $\text{N}_2\text{O}_5$  (citric acid) as well as for the small amounts of  $\text{NO}_3$  present in

the gas phase. Before each experimental run a wall loss measurement was performed without aerosol by moving the injector in 5-10 cm steps along the length of the aerosol flow tube and measuring the gas phase  $\text{N}_2\text{O}_5$  signal, in order to obtain the pseudo-first order wall loss rate constants ( $k_w$ ) for each experiment. These values varied between  $\sim 3 \times 10^{-2}$  and  $\sim 7 \times 10^{-2} \text{ s}^{-1}$ , depending on humidity. Because of the short residence time in the aerosol flow tube and its reduced surface area, losses to the wall were less pronounced than in our previous studies, and the overall signal strength was good.  $\text{NO}_2$  concentrations in the system were measured by switching a  $\text{NO}_x$  analyzer in place of the SMPS system at the beginning of the experiment. By comparing this result to the  $^{13}\text{N}_2\text{O}_5$  and  $^{13}\text{NO}_2$  signals, the concentration of non-labelled  $\text{N}_2\text{O}_5$  in the system was calculated. The uptake measurements were performed in a similar fashion to the wall loss measurements, although in this case aerosol was introduced at each step. By using Equation 4.1, which describes gas-aerosol phase interaction kinetics, we can estimate the uptake coefficient.

$$\frac{C_p^{(t)}}{C_g^{(t=0)}} = \frac{1 - e^{-(k_w + k_p)t}}{1 + \frac{k_w}{k_p}} \quad (\text{Eq. 4.1})$$

$$k_p = \frac{S_p \omega \gamma}{4} \quad (\text{Eq. 4.2})$$

where  $C_g^{(t=0)}$  is the gas-phase  $\text{N}_2\text{O}_5$  concentration at time zero,  $C_p^{(t)}$  is the  $\text{N}_2\text{O}_5$  concentration in the particle phase,  $k_w$  is the wall loss constant, measured as described above, and  $k_p$  denotes the apparent first order rate constant for gas-phase loss of  $\text{N}_2\text{O}_5$  to the aerosol phase, which can be related to the uptake coefficient ( $\gamma$ ) by Equation 4.2, where  $S_p$  is the total aerosol surface area to gas volume ratio and  $\omega$  is the mean thermal velocity of  $\text{N}_2\text{O}_5$ . Figure 2 shows the appearance of  $^{13}\text{N}$  in the aerosol phase as a function of time performed together with least-squares fits using Eq. 4.1 with  $\gamma$  as the only variable.

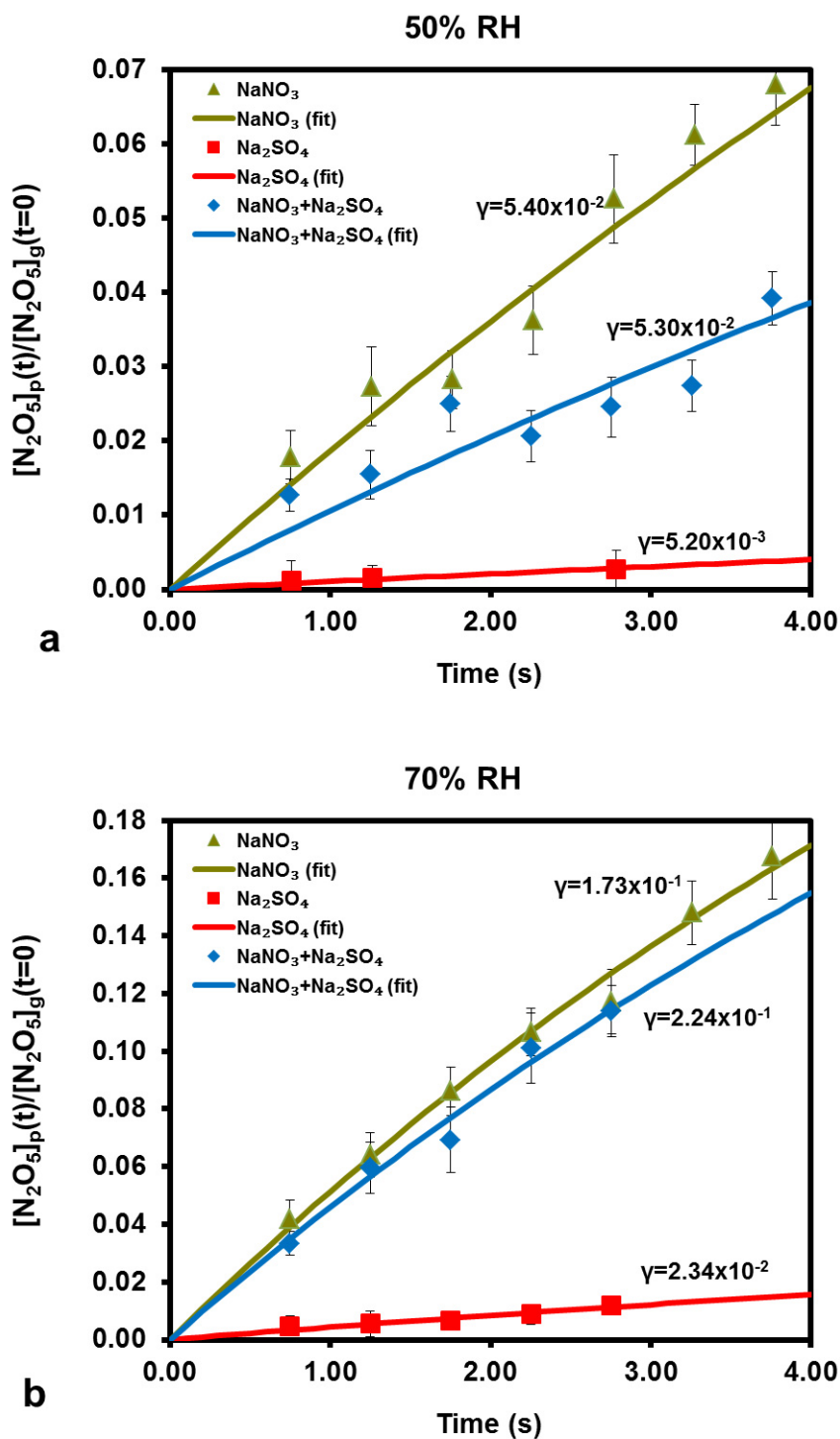


**Fig. 4.2.** Normalized particle-phase  $\text{N}_2\text{O}_5$  concentration vs. time graph for the experiments performed at 50% RH (a) and 70% RH (b). The data points represent the measurement data, the error bars represent the standard deviation of the measurements, the curves are a least-squares fit of Eq. 4.1 to the measured data.

Table 4.1 shows the results obtained for the various aerosols, with relative experimental parameters.

**Tab. 4.1.** Experimental parameters and results

Aerosol	NaNO <sub>3</sub>	NaNO <sub>3</sub>	NaNO <sub>3</sub> / Na <sub>2</sub> SO <sub>4</sub>	NaNO <sub>3</sub> / Na <sub>2</sub> SO <sub>4</sub>	Na <sub>2</sub> SO <sub>4</sub>	Na <sub>2</sub> SO <sub>4</sub>
Molar mixing ratio	-	-	1:1	1:1	-	-
Temperature (K)	295	295	295	295	295	295
RH (%)	50	70	51	70	51	70
Average S/V ratio (m <sub>2</sub> /m <sub>3</sub> )	5.92x10 <sup>-3</sup>	5.22x10 <sup>-3</sup>	3.40x10 <sup>-3</sup>	3.60x10 <sup>-3</sup>	3.42x10 <sup>-3</sup>	3.21x10 <sup>-3</sup>
γ (N <sub>2</sub> O <sub>5</sub> )	0.0540	0.173	0.0530	0.224	0.00520	0.0234
Error (95% confidence level)	±0.0040	±0.0007	±0.0080	±0.015	±0.0015	±0.0029

In absence of aerosol phase nitrate, the obtained results for Na<sub>2</sub>SO<sub>4</sub> are comparable to those reported by Mentel et al. (1999). In presence of aerosol phase nitrate, uptake of <sup>13</sup>N-labelled N<sub>2</sub>O<sub>5</sub> is drastically higher than the net uptake of non-labelled N<sub>2</sub>O<sub>5</sub> observed in earlier studies by Wahner et al. (1998), Mentel et al. (1999) and Hallquist et al. (2003). On mixed Na<sub>2</sub>SO<sub>4</sub> / NaNO<sub>3</sub> aerosol, the uptake is very close to that of NaNO<sub>3</sub>. Since the measured uptake coefficient for labelled <sup>13</sup>N into the nitrate containing aerosol is about an order of magnitude larger than previous estimates of the bulk accommodation coefficient, α<sub>b</sub>, our results provide a direct indication that gas – aqueous phase exchange of N<sub>2</sub>O<sub>5</sub> is considerably more efficient than previously thought and that limitations attributed in previous studies to α<sub>b</sub> might have been due to other processes.

More insight into the interpretation of the present experiments with <sup>13</sup>N labeled N<sub>2</sub>O<sub>5</sub> can be obtained by deconvoluting the chemical mechanism of N<sub>2</sub>O<sub>5</sub> hydrolysis (R4.3-4.7) to take into account the fate of the labelled species. Assuming that the labeled N<sub>2</sub>O<sub>5</sub> molecules contain only one <sup>13</sup>N atom (due to the very low labeled to non-labeled NO ratio) and under the assumption that no isotopic effects are in play, the chemical mechanism can be assumed to proceed as shown in Figure 4.3.

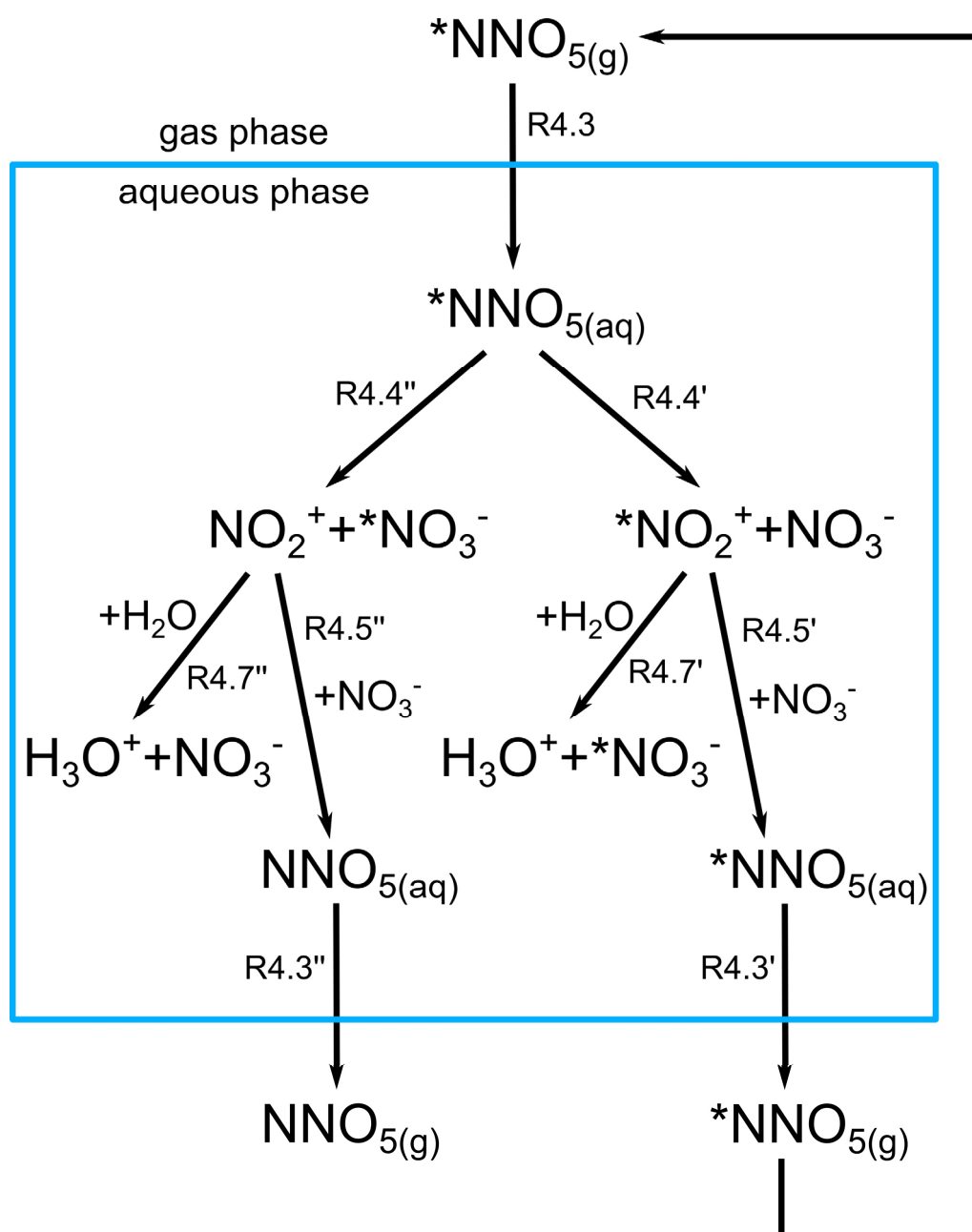


Fig. 4.3. The chemical mechanism of  $^{13}\text{N}$  labeled  $\text{N}_2\text{O}_5$  hydrolysis

We first assume that upon dissociation of  $^{13}\text{NNO}_5$ , there is an equal possibility that the  $^{13}\text{N}$  label will end up either in the nitronium ion ( $\text{NO}_2^+$ ) or in the nitrate ion ( $\text{NO}_3^-$ ). In the first scenario (left branch of the mechanism) the  $^{13}\text{N}$  label ends up on the nitrate ion (R4.4''). The corresponding non-labelled nitronium ion, if not reacting with  $\text{H}_2\text{O}$ , R4.7'', may react with nitrate to reform  $\text{N}_2\text{O}_5$ . This  $\text{N}_2\text{O}_5$  will predominantly be non-labeled, since the labeled  $^{13}\text{NO}_3^-$  ion is lost in the excess nitrate pool present in the aerosol and the likelihood of recombination of the non-labelled nitronium with the labeled nitrate is very small. Eventual  $\text{N}_2\text{O}_5$  that re-evaporates to the gas phase will



therefore be non-labeled. Thus, in this branch, all  $^{13}\text{N}$  labels will remain in the aqueous phase if evaporation as  $\text{HNO}_3$  does not occur, which is unlikely for our neutral aerosol. As evident from the experiments, the net rate of transfer of labelled  $\text{N}_2\text{O}_5$  into the aerosol nitrate pool is very high.

In the other scenario (right branch) of the mechanism,  $^{13}\text{N}$  ends up on the nitronium ion (R4.4'), and there are two possibilities for its further fate. The  $^{13}\text{NO}_2^+$  can react with water (R4.7'), bringing the label into the particulate nitrate pool. Alternatively  $^{13}\text{NO}_2^+$  can react with  $\text{NO}_3^-$  from the nitrate pool (R4.5') to reform  $^{13}\text{NNO}_5$  which can eventually re-evaporate. Obviously which of these two sub-channels will be prevalent depends on a series of factors, like water and nitrate concentrations as well as the rates of the two competing reactions. In presence of nitrate (R4.5') seems to be the dominant pathway, as suggested by Mentel et al. (1999) and Wahner et al. (1998), where  $k_{4.5}/k_{4.7}[\text{H}_2\text{O}]$  ratio values of  $35 \text{ kg mol}^{-1}$  and  $10 \text{ kg mol}^{-1}$  respectively have been used as fitting parameters to explain the entity of the nitrate effect. Such a conclusion is however self-evident since the difference in uptake measured with the  $^{13}\text{N}$  technique and that measured with traditional techniques is larger than an order of magnitude, so one can assume that the R4.5' sub-channel will be dominant.

Given that part of the  $^{13}\text{N}$  will find its way back to the gas phase (right branch), while the other part is trapped in the nitrate pool (left branch), it is obvious that the measured uptake will be higher than expected, since part of the  $^{13}\text{N}$  containing species will not be contributing to  $^{13}\text{N}_2\text{O}_5$  reformation, and therefore will not participate in re-evaporation to the gas phase.

The measured uptake increases with RH (water content) as the increase in water concentration drives  $^{13}\text{NO}_2^+$  reaction with water (R4.7') while at the same time a decrease in nitrate concentration suppresses the  $^{13}\text{NNO}_5$  reformation sub-channel (R4.5'). In the limiting case of total suppression of the  $^{13}\text{NNO}_5$  reformation sub-channel (all the  $^{13}\text{N}$  ending up in the nitrate pool), the measured uptake of  $^{13}\text{N}$ -labelled  $\text{N}_2\text{O}_5$  would tend to  $\alpha_b$ . However as has been mentioned, in presence of a nitrate pool the more likely fate of the label in the right branch of the mechanism is the reformation of labeled  $\text{N}_2\text{O}_5$ . In such a situation the measured uptake coefficient would be slightly larger than  $\alpha_b/2$ . Our results therefore strongly indicate that  $\alpha_b$  must

be at least twice as high as the uptake coefficient of  $^{13}\text{N}$ -labelled  $\text{N}_2\text{O}_5$  measured for  $\text{NaNO}_3$  and  $\text{NaNO}_3/\text{Na}_2\text{SO}_4$  aerosols and thus probably larger than 0.4, under the assumption that isotope effects do not influence the symmetry of the dissociation reaction.

Obviously for this technique to work a nitrate pool has to be available and it has to be substantial enough to 'trap' the  $^{13}\text{N}$  tracer and prevent its release. As can be seen, there is little difference in measured uptake between the pure  $\text{NaNO}_3$  and the 1:1  $\text{NaNO}_3/\text{Na}_2\text{SO}_4$  mix aerosol and we can assume that lower nitrate concentrations need to be probed to determine the limit at which the exchange with the nitrate pool becomes rate determining.

As has been shown, the particular properties of the  $^{13}\text{N}$  technique which lead to exchange of  $^{13}\text{N}$  labeled species with the nitrate pool allow obtaining a surprisingly large value for the bulk accommodation coefficient. This behavior is similar to that observed by Wachsmuth et al. (2002), where  $^{83-86}\text{Br}$  isotopes have been used to determine the bulk accommodation coefficient of  $\text{HOBr}$ . The dataset that we've obtained here is unfortunately relatively small, a larger dataset might help to further constrain the rate constants for dissociation and association of  $\text{N}_2\text{O}_5$  in the aqueous phase. The large value of  $\alpha_b$  obtained for  $\text{N}_2\text{O}_5$  implies that a revision of the mechanism and the parameterizations currently used to describe heterogeneous kinetics of  $\text{N}_2\text{O}_5$  are needed. Other limiting processes will need to be identified to explain results obtained in some studies (Griffiths et al., 2009; Thornton et al., 2003), where  $\gamma$  has plateaued to a constant level with increasing humidity (and thus water activity / concentration), which was interpreted as accommodation limitation. Such a large value of  $\alpha_b$  will probably also lead to a revision of the values for solubility and the net rate constant of the overall reaction in the aqueous phase. This study may help to explain results from field experiments (Wagner et al., 2013), where uptake coefficients constrained by combined  $\text{N}_2\text{O}_5$  and aerosol measurements are larger than those suggested by laboratory studies available to date.

## References

- Abbatt, J. P. D., Lee, A. K. Y., and Thornton, J. A.: Quantifying trace gas uptake to tropospheric aerosol: recent advances and remaining challenges, *Chemical Society Reviews*, 41, 6555-6581, 2012.
- Ammann, M.: Using  $^{13}\text{N}$  as tracer in heterogeneous atmospheric chemistry experiments, *Radiochim. Acta*, 89, 831-838, 2001.
- Anttila, T., Kiendler-Scharr, A., Tillmann, R., and Mentel, T. F.: On the reactive uptake of gaseous compounds by organic-coated aqueous aerosols: Theoretical analysis and application to the heterogeneous hydrolysis of  $\text{N}_2\text{O}_5$ , *Journal of Physical Chemistry A*, 110, 10435-10443, 2006.
- Badger, C. L., Griffiths, P. T., George, I., Abbatt, J. P. D., and Cox, R. A.: Reactive uptake of  $\text{N}_2\text{O}_5$  by aerosol particles containing mixtures of humic acid and ammonium sulfate, *Journal of Physical Chemistry A*, 110, 6986-6994, 2006.
- Behnke, W., George, C., Scheer, V., and Zetzsch, C.: Production and decay of  $\text{ClNO}_2$ , from the reaction of gaseous  $\text{N}_2\text{O}_5$  with  $\text{NaCl}$  solution: Bulk and aerosol experiments, *Journal of Geophysical Research-Atmospheres*, 102, 3795-3804, 1997.
- Chang, W. L., Bhave, P. V., Brown, S. S., Riemer, N., Stutz, J., and Dabdub, D.: Heterogeneous Atmospheric Chemistry, Ambient Measurements, and Model Calculations of  $\text{N}(2)\text{O}(5)$ : A Review, *Aerosol Sci. Technol.*, 45, 665-695, 2011.
- Dentener, F. J. and Crutzen, P. J.: Reaction of  $\text{N}_2\text{O}_5$  on tropospheric aerosols: Impact on the global distributions of  $\text{NO}_x$ ,  $\text{O}_3$ , and  $\text{OH}$ , *Journal of Geophysical Research: Atmospheres*, 98, 7149-7163, 1993.
- Evans, M. J. and Jacob, D. J.: Impact of new laboratory studies of  $\text{N}_2\text{O}_5$  hydrolysis on global model budgets of tropospheric nitrogen oxides, ozone, and  $\text{OH}$ , *Geophysical Research Letters*, 32, 2005.
- Finlayson-Pitts, B. J. and Pitts, J. N., Jr.: *Chemistry of the upper and lower atmosphere*, Academic Press, San Diego, CA, 2000.
- Folkers, M., Mentel, T. F., and Wahner, A.: Influence of an organic coating on the reactivity of aqueous aerosols probed by the heterogeneous hydrolysis of  $\text{N}_2\text{O}_5$ , *Geophysical Research Letters*, 30, 2003.
- George, C., Ponche, J. L., Mirabel, P., Behnke, W., Scheer, V., and Zetzsch, C.: Study of the Uptake of  $\text{N}_2\text{O}_5$  by Water and  $\text{NaCl}$  Solutions, *J. Phys. Chem.*, 98, 8780-8784, 1994.
- Griffiths, P. T., Badger, C. L., Cox, R. A., Folkers, M., Henk, H. H., and Mentel, T. F.: Reactive Uptake of  $\text{N}_2\text{O}_5$  by Aerosols Containing Dicarboxylic Acids. Effect of Particle Phase, Composition, and Nitrate Content, *Journal of Physical Chemistry A*, 113, 5082-5090, 2009.
- Gross, S., Iannone, R., Xiao, S., and Bertram, A. K.: Reactive uptake studies of  $\text{NO}_3$  and  $\text{N}_2\text{O}_5$  on alkenoic acid, alkanolate, and polyalcohol substrates to probe nighttime aerosol chemistry, *Physical Chemistry Chemical Physics*, 11, 7792-7803, 2009.

- Gržinić, G., Bartels-Rausch, T., Birrer, M., Türler, A., and Ammann, M.: Production and use of  $^{13}\text{N}$  labeled  $\text{N}_2\text{O}_5$  to determine gas–aerosol interaction kinetics, *Radiochimica Acta*, 102, 1025–1034, 2014.
- Hallquist, M., Stewart, D. J., Stephenson, S. K., and Cox, R. A.: Hydrolysis of  $\text{N}_2\text{O}_5$  on sub-micron sulfate aerosols, *Physical Chemistry Chemical Physics*, 5, 3453-3463, 2003.
- Hanson, D. R. and Lovejoy, E. R.: The Uptake of  $\text{N}_2\text{O}_5$  onto Small Sulfuric-Acid Particles, *Geophysical Research Letters*, 21, 2401-2404, 1994.
- Karagulian, F., Santschi, C., and Rossi, M. J.: The heterogeneous chemical kinetics of  $\text{N}_2\text{O}_5$  on  $\text{CaCO}_3$  and other atmospheric mineral dust surrogates, *Atmospheric Chemistry and Physics*, 6, 1373-1388, 2006.
- Mentel, T. F., Sohn, M., and Wahner, A.: Nitrate effect in the heterogeneous hydrolysis of dinitrogen pentoxide on aqueous aerosols, *Physical Chemistry Chemical Physics*, 1, 5451-5457, 1999.
- Mozurkewich, M. and Calvert, J. G.: Reaction probability of  $\text{N}_2\text{O}_5$  on aqueous aerosols, *Journal of Geophysical Research: Atmospheres*, 93, 15889-15896, 1988.
- Thornton, J. A. and Abbatt, J. P. D.:  $\text{N}_2\text{O}_5$  reaction on submicron sea salt aerosol: Kinetics, products, and the effect of surface active organics, *Journal of Physical Chemistry A*, 109, 10004-10012, 2005.
- Thornton, J. A., Braban, C. F., and Abbatt, J. P. D.:  $\text{N}_2\text{O}_5$  hydrolysis on sub-micron organic aerosols: the effect of relative humidity, particle phase, and particle size, *Physical Chemistry Chemical Physics*, 5, 4593-4603, 2003.
- Wachsmuth, M., Gäggeler, H. W., von Glasow, R., and Ammann, M.: Accommodation coefficient of  $\text{HOBr}$  on deliquescent sodium bromide aerosol particles, *Atmos. Chem. Phys.*, 2, 121-131, 2002.
- Wagner, C., Hanisch, F., Holmes, N., de Coninck, H., Schuster, G., and Crowley, J. N.: The interaction of  $\text{N}_2\text{O}_5$  with mineral dust: aerosol flow tube and Knudsen reactor studies, *Atmospheric Chemistry and Physics*, 8, 91-109, 2008.
- Wagner, N. L., Riedel, T. P., Young, C. J., Bahreini, R., Brock, C. A., Dubé, W. P., Kim, S., Middlebrook, A. M., Öztürk, F., Roberts, J. M., Russo, R., Sive, B., Swarthout, R., Thornton, J. A., VandenBoer, T. C., Zhou, Y., and Brown, S. S.:  $\text{N}_2\text{O}_5$  uptake coefficients and nocturnal  $\text{NO}_2$  removal rates determined from ambient wintertime measurements, *Journal of Geophysical Research: Atmospheres*, 118, 9331-9350, 2013.
- Wahner, A., Mentel, T. F., Sohn, M., and Stier, J.: Heterogeneous reaction of  $\text{N}_2\text{O}_5$  on sodium nitrate aerosol, *Journal of Geophysical Research-Atmospheres*, 103, 31103-31112, 1998.

## Chapter 5

### 5. Summary and Outlook

The main questions this work tried to answer are related to the gas-particle interaction kinetics of  $\text{N}_2\text{O}_5$ , and in particular to explore some of the discrepancies between predictions based on laboratory studies and results obtained in field studies, and what can be done in the laboratory setting to address this. Therefore the decision was to apply an experimental technique that allows tracing uptake in the particle phase and has some particular advantages in comparison to techniques that have been used thus far.

The first step in this work was to investigate the feasibility of  $^{13}\text{N}_2\text{O}_5$  production, keeping in mind that  $^{13}\text{N}$  is a short-lived radioisotope. This precluded the use of techniques like freeze crystallization of  $\text{N}_2\text{O}_5$  to be later released by sublimation, and restricted our choice to ambient condition gas phase production. A kinetic computer model of the gas-phase  $\text{N}_2\text{O}_5$  chemistry was created, starting from  $\text{NO}$  and  $\text{O}_3$ . This has allowed the design of an appropriate  $\text{N}_2\text{O}_5$  synthesis reactor to be used in the experimental setup used for the following experiments. Overall residence time in the experimental setup is a critical factor that has to be taken into account and an adequate equilibrium has to be achieved between time dedicated to the evolution of  $\text{N}_2\text{O}_5$  gas phase chemistry and lifetime of  $^{13}\text{N}$ . In that regard efforts have been successful and routine  $\text{N}_2\text{O}_5$  production in the ppb range was achieved. The experimental results obtained have shown good agreement with the kinetic model. Overall the instrumental design was successful. Awareness of the limitations of the  $^{13}\text{N}$  technique is needed

however. Operation must be planned ahead and the accelerator facilities are not always available. While it is possible to detect  $\text{N}_2\text{O}_5$  in the particle phase, the question of  $\text{HNO}_3$  evaporation remains open. Since the tracer method is not chemically selective, evaporated labeled  $\text{HNO}_3$  may be confused with evaporating  $\text{N}_2\text{O}_5$  and detected as unreacted  $\text{N}_2\text{O}_5$ .

Particles containing organic or mixed inorganic and organic compounds have been the topic of increasing interest in the last couple of years because of their ubiquitousness. Most of the early investigations have been based on the assumption that aerosol particles contain low-viscosity, well mixed aerosol phases; however, recent studies have shown that these assumptions are not correct and that particles containing organic material may have complex states, with imperfectly mixed bulks, encapsulated phases, homogeneous, but semi-solid forms and low viscosities (Renbaum-Wolff et al., 2013; Vaden et al., 2011). Citric acid, a polycarboxylic acid, has been used as a model compound and as a proxy for the highly oxidized species present in ambient organic aerosol. Citric acid is likewise fairly viscous and has been used to explore the influence that diffusivity of trace gases in aerosols can have on reactivity.  $\text{N}_2\text{O}_5$  uptake measurements on citric acid aerosol have been conducted over a wide humidity range (17-70% RH) and uptake coefficients ranging from  $\sim 3 \times 10^{-4}$  to  $\sim 3 \times 10^{-3}$  have been obtained. Available data on diffusivity of  $\text{H}_2\text{O}$  in citric acid and citric acid viscosity have been used to construct parameterizations that would describe the reactivity of citric acid over the humidity range in question. While the above mentioned parameterizations have not been able to fully describe the reactivity of  $\text{N}_2\text{O}_5$  on citric acid, the results nevertheless show that diffusivity (and by extension viscosity) play an important role in the behavior of citric acid and indeed organic aerosols.

The ‘nitrate effect’, which refers to the decrease of net  $\text{N}_2\text{O}_5$  uptake on nitrate containing aerosol, is generally explained in terms of the chemical reaction mechanism of  $\text{N}_2\text{O}_5$  heterogeneous hydrolysis on aerosols. The unique properties of the  $^{13}\text{N}$  radioisotope tracer have allowed probing the reaction mechanism in more detail, and in particular the exchange between absorbed  $\text{N}_2\text{O}_5$  and the nitrate pool present in the aerosol. Our measurements have shown that  $^{13}\text{N}$  labelled  $\text{N}_2\text{O}_5$  uptake

on nitrate containing aerosol is roughly an order of magnitude higher than values reported in previous studies on the subject. This has been explained by the fate of  $^{13}\text{N}$  labelled species in the chemical reaction mechanism, and in particular the sequestration of  $^{13}\text{NO}_3^-$  into the non-labeled aerosol nitrate pool. The obtained values for  $\gamma$  suggest that the bulk accommodation coefficient ( $\alpha_b$ ) is significantly higher than previously thought. The entity of the bulk accommodation coefficient, which is estimated to be higher than 0.4, implies that the gas-aerosol exchange of  $\text{N}_2\text{O}_5$  is considerably faster than expected. Such high  $\alpha_b$  values imply that other, yet unaccounted for, limiting processes need to be identified to explain some of the results obtained in previous studies, where limits to uptake at RH values higher than 50% (Griffiths et al., 2009; Thornton et al., 2003) were explained with bulk accommodation limitations. The current model predictions for  $\text{N}_2\text{O}_5$  heterogeneous kinetics will likely have to be revised to take into account the increased bulk accommodation estimates.

The influence of viscosity, and by extension diffusivity, on reactivity of organic aerosols has been recognized lately as an important factor (Abramson et al., 2013; Koop et al., 2011; Renbaum-Wolff et al., 2013). In that regard the use of citric acid as a model compound has proven to be an interesting choice. Its viscosity is above that of similar compounds (polycarboxylic acids) that have been used in previous studies and this has had a noticeable impact on the uptake of  $\text{N}_2\text{O}_5$ . Unfortunately the parameterizations that we have performed using the reacto-diffusive uptake regime, based on the resistor model, present significant discrepancies among each other. This can be explained by the heterogeneous sources of the diffusivity data used: measurements of viscosity of citric acid and diffusivity of  $\text{H}_2\text{O}$  in sucrose or citric acid. In both cases the diffusivity of  $\text{N}_2\text{O}_5$  in citric acid, the actual parameter used in the reacto-diffusive equation, has to be calculated using a relationship that describes the interdependence of viscosity, diffusivity, temperature and particle size. In our case we have used the Stokes-Einstein relation. Unfortunately, viscosity and diffusivity start to decouple at relatively modest values of viscosity ( $\sim 1$  Pa s), with significant deviations from expected values at RH <50-60% (Power et al., 2013). The ideal solution to this problem would be a technique that would enable measuring the diffusion of  $\text{N}_2\text{O}_5$  in citric acid directly.

The study of citric acid provides a possible explanation for the lower than expected uptake coefficients inferred from field aerosol measurements of particles containing significant amounts of organics. Viscosity (and therefore diffusivity) might be the determining factor that explains the discrepancies in reactivity between ambient aerosols and those observed in laboratory studies. It could likewise explain the behaviour of citric acid in the recent study by Gaston et al. (2014), where the increased O:C ratio of organic components in multicomponent inorganic-organic aerosol particles has been linked to an increase in their reactivity (Figure 5.1). Aerosol particles containing citric acid and other highly functionalized oxidized organic species do not follow this trend however. They present uncharacteristically low reactivity with relation to their O:C ratio. Therefore, use of more viscous and highly functionalized oxidized organic compounds like citric acid may provide a better insight into the reactivity of  $N_2O_5$  in atmospheric models and consequently help to bridge the gap between field measurements and model predictions.

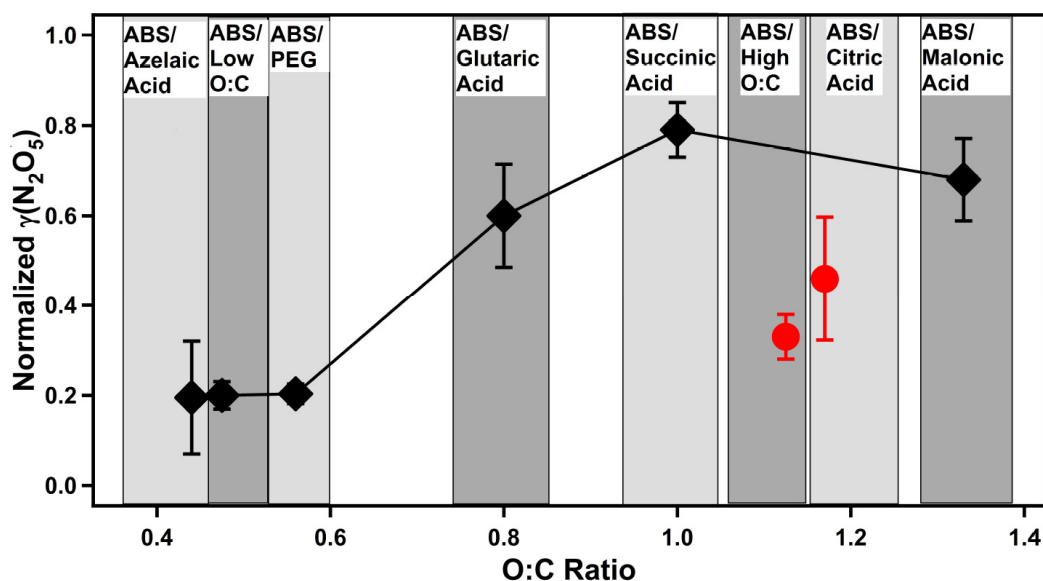


**Fig. 5.1.** Normalized  $\gamma(N_2O_5)$  values for mixtures of ammonium bisulfate and organics. Red markers denote values for mixtures with citric acid and a high O:C mixture respectively. Reproduced from Gaston et al. (2014)

As mentioned in Chapter 3, the presence of a surface reaction at low relative humidity could not be ruled out as a possible explanation for the discrepancy between measured uptake values and predictions based on the above mentioned parameterizations. In



such conditions the viscosity of the particle phase increases dramatically and this could drastically reduce diffusion into the bulk, making the surface reaction the rate determining step. A solution to this dilemma would be to study the system with a surface-sensitive technique, like X-ray photo emission spectroscopy (XPS) or Near Edge X-ray Absorption Fine Structure spectroscopy with electron yield (NEXAFS). Because these techniques rely on detection of electrons emitted upon core level excitation, which have very low inelastic mean free paths, the composition of the top most few nanometers can be assessed. A similar type of investigation has been tried by Steimer et al. (2014) for an ozone-shikimic acid aerosol system using a Scanning Transmission X-ray Microscope (STXM) in an attempt to observe a gradient of reacted shikimic acid within single aerosol particles. While a gradient has not been observed, there is a possibility that the gradient might simply be below detection limit, the resolution of the technique being around 20-40 nm.

The large bulk accommodation coefficient derived from the experiments with nitrate containing aerosols was quite unexpected. The list of laboratory experiments suggesting a lower value based on the saturating behavior of the uptake coefficient as a function of water content has been quite significant (Griffiths et al., 2009; Mozurkewich and Calvert, 1988; Thornton et al., 2003). However, since the net reactivity assessed in terms of loss of  $\text{N}_2\text{O}_5$  from the gas phase was not really sensitive to the elementary kinetic parameters such as the bulk accommodation coefficient and the forward and backward rate coefficient for  $\text{N}_2\text{O}_5$  dissociation into nitronium and nitrate ion, these were not accessible. In this context, the  $^{13}\text{N}$  tracer technique has been an unexpected advantage and provided a new estimate for  $\alpha_b$ . However, further experiments might be needed to corroborate these results, for example with aerosols containing different components, including among them chloride which can act as a competing reactant for the nitronium ion, as shown in Behnke et al. (1997). Temperature dependence of  $\alpha_b$  could be probed by conducting a set of measurements in bulk accommodation limitation regime over a wider temperature range. Previous studies using similar techniques have shown negative temperature dependence (Griffiths and Anthony Cox, 2009; Hallquist et al., 2003). In acid conditions, a secondary acid catalyzed hydrolysis channel becomes active (Robinson et al., 1997;

Talukdar et al., 2012). It might be worthwhile to explore the influence of acidity on the system.

The increased estimated value of  $\alpha_b$  might help to explain certain recent field data (Wagner et al., 2013) regarding uptake coefficients that sometimes are larger than expected (Figure 5.1).

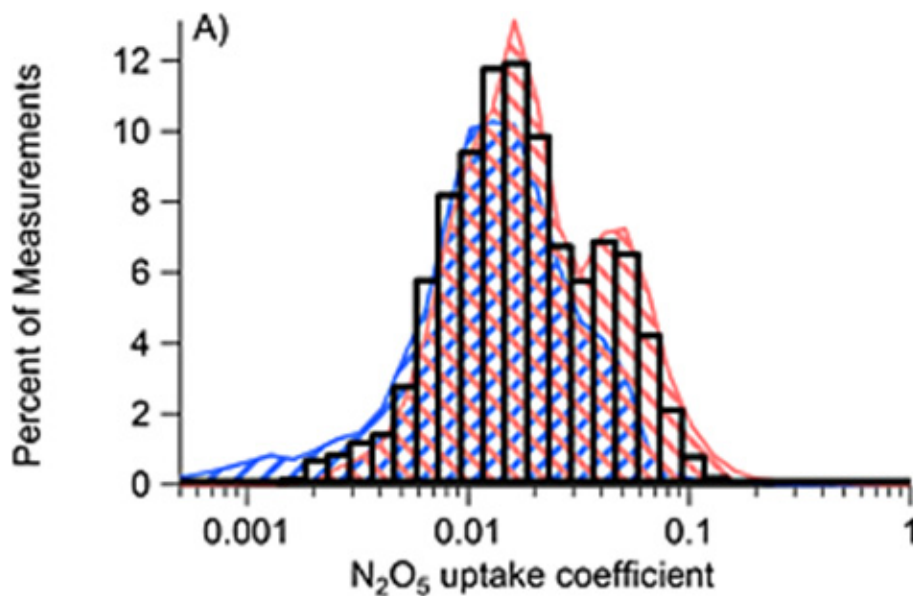


**Fig. 5.2.** A histogram of  $N_2O_5$  uptake coefficients determined using an iterative box model and determined from the NACHTT field study data set. The distribution ranges from 0.002 to 0.1. Adapted and reproduced from Wagner et al. (2013)

During the field study in question the average aerosol composition by mass was 19% sulfate, 39% nitrate, 14% ammonium, 27% organics, and < 1% chloride.

A larger  $\alpha_b$  value might likewise improve the parameterizations of  $N_2O_5$  uptake, as can be seen in Figure 5.2.

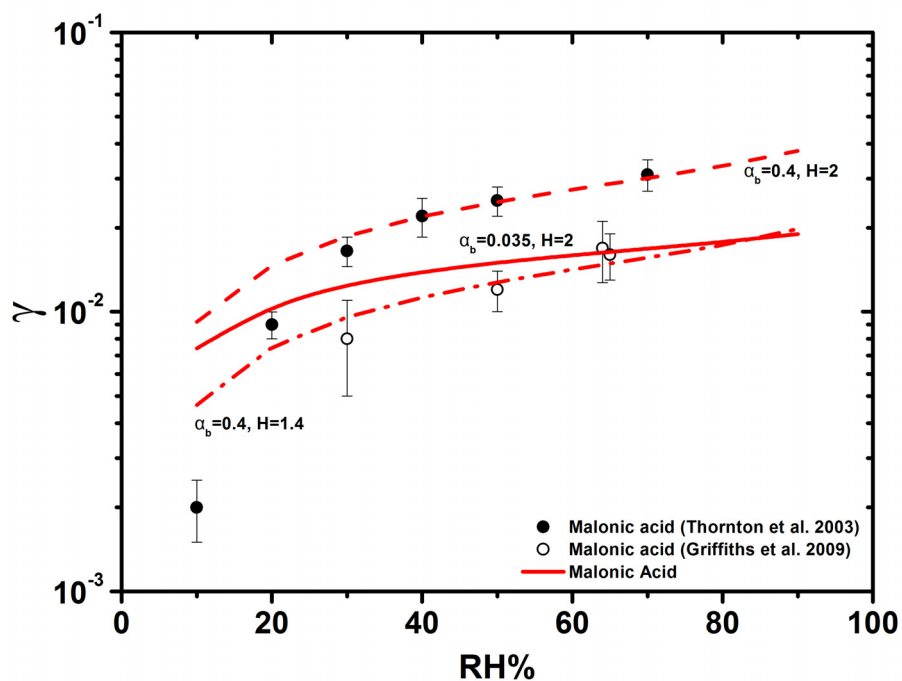


**Fig. 5.3.** Parameterizations of  $\text{N}_2\text{O}_5$  uptake on malonic acid, full line: according to IUPAC recommended parameter values (Ammann et al., 2013); dashed lines with  $\alpha_b = 0.4$  and variable Henry Law's constant H

As can be seen, within the uncertainty range of the model parameters, the parameterizations using  $\alpha_b = 0.4$  fit the measured values better than the one based on current IUPAC recommendations according to Ammann et al. (2013). We can therefore conclude that such a high  $\alpha_b$  value is compatible with currently available uptake data.

## References

- Abramson, E., Imre, D., Beranek, J., Wilson, J., and Zelenyuk, A.: Experimental determination of chemical diffusion within secondary organic aerosol particles, *Physical Chemistry Chemical Physics*, 15, 2983-2991, 2013.
- Ammann, M., Cox, R. A., Crowley, J. N., Jenkin, M. E., Mellouki, A., Rossi, M. J., Troe, J., and Wallington, T. J.: Evaluated kinetic and photochemical data for atmospheric chemistry: Volume VI - heterogeneous reactions with liquid substrates, *Atmospheric Chemistry and Physics*, 13, 8045-8228, 2013.
- Behnke, W., George, C., Scheer, V., and Zetzsch, C.: Production and decay of ClNO<sub>2</sub> from the reaction of gaseous N<sub>2</sub>O<sub>5</sub> with NaCl solution: Bulk and aerosol experiments, *Journal of Geophysical Research-Atmospheres*, 102, 3795-3804, 1997.
- Gaston, C. J., Thornton, J. A., and Ng, N. L.: Reactive uptake of N<sub>2</sub>O<sub>5</sub> to internally mixed inorganic and organic particles: the role of organic carbon oxidation state and inferred organic phase separations, *Atmos. Chem. Phys.*, 14, 5693-5707, 2014.
- Griffiths, P. T. and Anthony Cox, R.: Temperature dependence of heterogeneous uptake of N<sub>2</sub>O<sub>5</sub> by ammonium sulfate aerosol, *Atmospheric Science Letters*, 10, 159-163, 2009.
- Griffiths, P. T., Badger, C. L., Cox, R. A., Folkers, M., Henk, H. H., and Mentel, T. F.: Reactive Uptake of N<sub>2</sub>O<sub>5</sub> by Aerosols Containing Dicarboxylic Acids. Effect of Particle Phase, Composition, and Nitrate Content, *Journal of Physical Chemistry A*, 113, 5082-5090, 2009.
- Hallquist, M., Stewart, D. J., Stephenson, S. K., and Cox, R. A.: Hydrolysis of N<sub>2</sub>O<sub>5</sub> on sub-micron sulfate aerosols, *Physical Chemistry Chemical Physics*, 5, 3453-3463, 2003.
- Koop, T., Bookhold, J., Shiraiwa, M., and Pöschl, U.: Glass transition and phase state of organic compounds: dependency on molecular properties and implications for secondary organic aerosols in the atmosphere, *Physical Chemistry Chemical Physics*, 13, 19238-19255, 2011.
- Mozurkewich, M. and Calvert, J. G.: Reaction probability of N<sub>2</sub>O<sub>5</sub> on aqueous aerosols, *Journal of Geophysical Research: Atmospheres*, 93, 15889-15896, 1988.
- Power, R. M., Simpson, S. H., Reid, J. P., and Hudson, A. J.: The transition from liquid to solid-like behaviour in ultrahigh viscosity aerosol particles, *Chemical Science*, 4, 2597-2604, 2013.
- Renbaum-Wolff, L., Grayson, J. W., Bateman, A. P., Kuwata, M., Sellier, M., Murray, B. J., Shilling, J. E., Martin, S. T., and Bertram, A. K.: Viscosity of  $\alpha$ -pinene secondary organic material and implications for particle growth and reactivity, *Proceedings of the National Academy of Sciences*, 110, 8014-8019, 2013.

Robinson, G. N., Worsnop, D. R., Jayne, J. T., Kolb, C. E., and Davidovits, P.: Heterogeneous uptake of ClONO<sub>2</sub> and N<sub>2</sub>O<sub>5</sub> by sulfuric acid solutions, *Journal of Geophysical Research-Atmospheres*, 102, 3583-3601, 1997.

Steimer, S. S., Lampimäki, M., Coz, E., Grzanic, G., and Ammann, M.: The influence of physical state on shikimic acid ozonolysis: a case for in situ microspectroscopy, *Atmos. Chem. Phys.*, 14, 10761-10772, 2014.

Talukdar, R. K., Burkholder, J. B., Roberts, J. M., Portmann, R. W., and Ravishankara, A. R.: Heterogeneous Interaction of N<sub>2</sub>O<sub>5</sub> with HCl Doped H<sub>2</sub>SO<sub>4</sub> under Stratospheric Conditions: ClONO<sub>2</sub> and Cl<sub>2</sub> Yields, *The Journal of Physical Chemistry A*, 116, 6003-6014, 2012.

Thornton, J. A., Braban, C. F., and Abbatt, J. P. D.: N<sub>2</sub>O<sub>5</sub> hydrolysis on sub-micron organic aerosols: the effect of relative humidity, particle phase, and particle size, *Physical Chemistry Chemical Physics*, 5, 4593-4603, 2003.

Vaden, T. D., Imre, D., Beránek, J., Shrivastava, M., and Zelenyuk, A.: Evaporation kinetics and phase of laboratory and ambient secondary organic aerosol, *Proceedings of the National Academy of Sciences*, 108, 2190-2195, 2011.

Wagner, N. L., Riedel, T. P., Young, C. J., Bahreini, R., Brock, C. A., Dubé, W. P., Kim, S., Middlebrook, A. M., Öztürk, F., Roberts, J. M., Russo, R., Sive, B., Swarthout, R., Thornton, J. A., VandenBoer, T. C., Zhou, Y., and Brown, S. S.: N<sub>2</sub>O<sub>5</sub> uptake coefficients and nocturnal NO<sub>2</sub> removal rates determined from ambient wintertime measurements, *Journal of Geophysical Research: Atmospheres*, 118, 9331-9350, 2013.



## Acknowledgements

A Ph.D. Thesis is a complex task. Besides the author himself, a lot of people contribute to it with scientific input or friendly support. Without their contribution and encouragement this work would not have been completed. In light of this, I would like to thank the following people:

Andreas Türler for accepting me as a PhD student and contributing to this project with his valuable input.

Markus Ammann for offering me a position in the Surface Chemistry Group and for supervising my work on this project. I'm likewise very thankful for the support, the scientific discussions, the feedback and the encouragement even when my experiments didn't go as planned. I am very grateful and count myself lucky to have had such an outstanding group leader.

Christian George for accepting to be the external referee on this work.

Samuel Leutwyler for accepting to act as chairman of the thesis committee.

Mario Birrer, his technical expertise in fixing all that we use and break, and making sure PROTRAC works whenever things are not going according to plan.

All the members, past and present, of the Surface Chemistry Group. In particular Thorsten Bartels-Rausch and Sarah Steimer, who shared the office with me. Markus Lampimäki, for our talks and for being a member of the Brotherhood of the Flame Eternal. Sepp Schreiber for the long days and nights we spent together in the lab and for the scientific insight, discussions and help with both  $^{13}\text{N}$  use and Matlab. Ming-Tao Lee for being a very good friend and sharing his time with me. Thomas Ulrich for the great BBQs we had at his parent's house and the interests we've had in common.

Astrid, Fabrizio and Pablo, who I've had only a short time to work together with but became good friends notwithstanding.

All the members of the Laboratory of Radiochemistry and Environmental Chemistry, but in particular Isabella Mariani and Ilya Usoltsev for all the time we spent together at work and outside of it.

Thomas Berkemeier, for sharing labs with me and the discussions we've had.

My friends in Switzerland and in particular my ex flatmates, Sebastian Möllencamp, Ciprian Mieszczynski and Jan Girovsky, who I've spent a lot of fun times with.

All my friends at home and in BOPE. Far away but close in my heart.

My family, who have always supported me and been there for me when I most needed them.



## Curriculum Vitae

### Goran Gržinić

Born in Rijeka, Croatia on 03.02.1978.

## Education

- 2010 - 2014 **PhD Candidate** in Chemistry and Molecular Sciences  
University of Bern, Bern, Switzerland  
Paul Scherrer Institute, Switzerland  
Thesis: The Multiphase Chemical Kinetics of Dinitrogen Pentoxide with Aerosol Particles
- 1997 - 2008 **M.Sc.** in Chemistry  
Università degli Studi di Trieste, Trieste, Italy  
Thesis: Caratterizzazione di particolato atmosferico mediante micro fluorescenza a raggi X con luce di sincrotrone

## Conference Contributions

- Aug. 2014 **International Aerosol Conference 2014**  
Humidity dependence of  $\text{N}_2\text{O}_5$  uptake to citric acid Aerosol Particles, Poster presentation
- Dec. 2013 **American Geophysical Union Fall Meeting 2013**  
Humidity dependence of  $\text{N}_2\text{O}_5$  uptake to citric acid Aerosol Particles, Poster presentation
- Sept. 2013 **European Aerosol Conference 2013**  
Uptake of  $\text{N}_2\text{O}_5$  to citric acid aerosol particles, Poster presentation
- Apr. 2013 **European Geoscience Union General Assembly 2013**  
Uptake of  $^{13}\text{N}$ -labeled  $\text{N}_2\text{O}_5$  to citric acid aerosol particles, Poster presentation
- Sept. 2012 **University of Bern Graduate Student Symposium 2012**  
Kinetics of  $\text{N}_2\text{O}_5$  interaction with aerosols, Oral presentation

- Apr. 2012 **European Geoscience Union General Assembly 2012**  
Towards an experiment to investigate N<sub>2</sub>O<sub>5</sub> uptake to aerosol particles at ambient conditions using the radioactive tracer <sup>13</sup>N,  
Poster presentation
- Jan. 2012 **European Research Course on Atmospheres 2012**  
Towards an experiment to investigate N<sub>2</sub>O<sub>5</sub> uptake to aerosol particles at ambient conditions using the radioactive tracer <sup>13</sup>N

## **Publications**

Gržinić, G., Bartels-Rausch, T., Birrer, M., Türler, A., and Ammann, M.: Production and use of <sup>13</sup>N labeled N<sub>2</sub>O<sub>5</sub> to determine gas–aerosol interaction kinetics, *Radiochim. Acta*, **102**, 1025–1034, 2014.

# Erklärung

gemäss Art. 28 Abs. 2 RSL 05

Name/Vorname: Gržinić Goran

Matrikelnummer: 10-129-476

Studiengang: Chemie und Molekulare Wissenschaften

Bachelor       Master       Dissertation

Titel der Arbeit: The Multiphase Chemical Kinetics of Dinitrogen Pentoxide  
with Aerosol Particles

LeiterIn der Arbeit: Prof. Dr. Türlér, Andreas

Ich erkläre hiermit, dass ich diese Arbeit selbständig verfasst und keine anderen als die angegebenen Quellen benutzt habe. Alle Stellen, die wörtlich oder sinngemäss aus Quellen entnommen wurden, habe ich als solche gekennzeichnet. Mir ist bekannt, dass andernfalls der Senat gemäss Artikel 36 Absatz 1 Buchstabe r des Gesetzes vom 5. September 1996 über die Universität zum Entzug des auf Grund dieser Arbeit verliehenen Titels berechtigt ist. Ich gewähre hiermit Einsicht in diese Arbeit.

Villigen, 24.11.2014

.....  
Unterschrift

